

湖州师范学院原子核结构与中高能重离子碰撞交叉学科理论讲习班 (2021.07)

相对论重离子碰撞中 α - cluster效应

张松

复旦大学现代物理研究所



合作者：马余刚，何俊杰，程艺琳，王东方，李逸安，王远哲，马龙



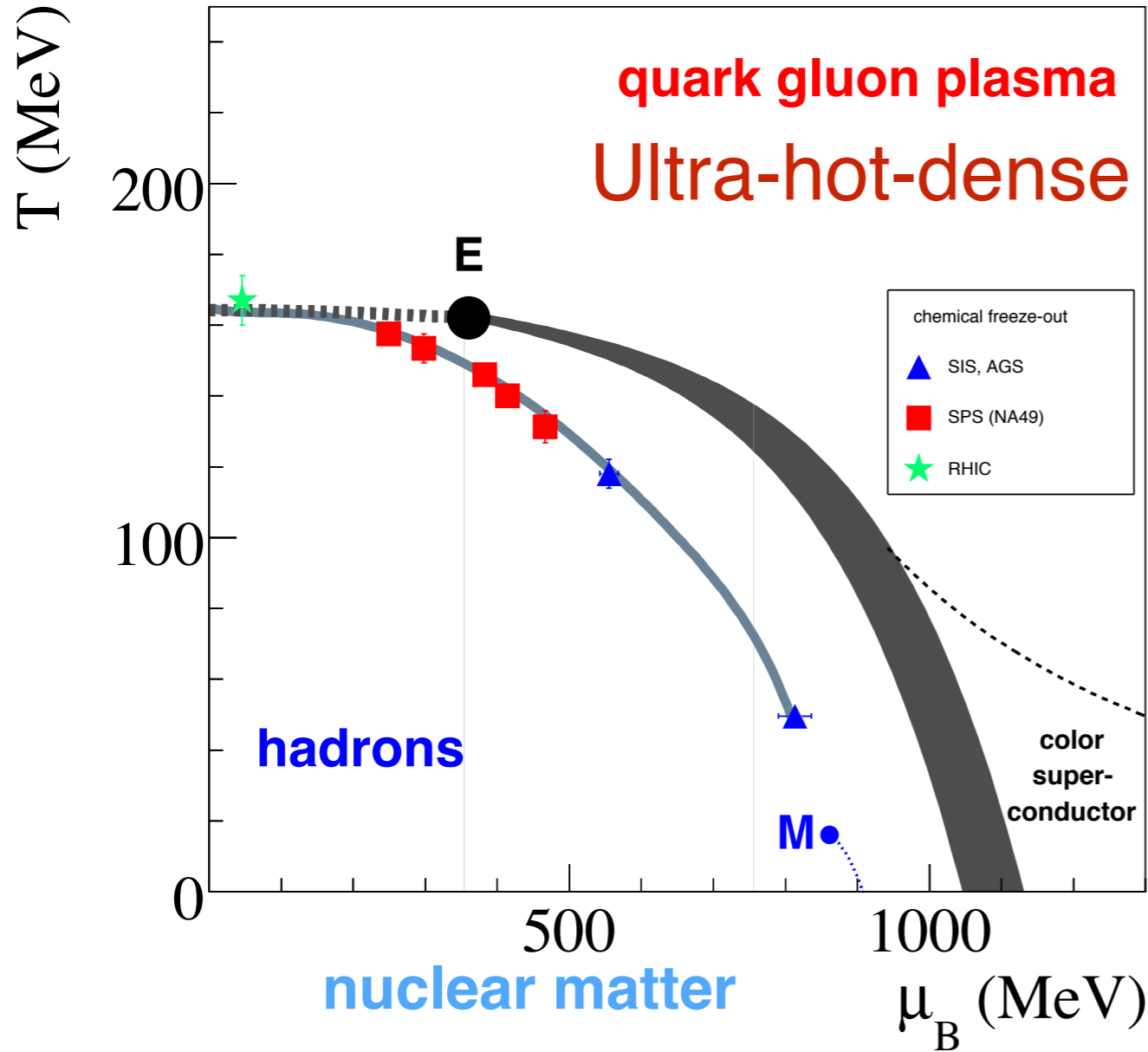
提纲

- 相对论重离子碰撞简介
- 碰撞初态对集体流的影响
- α -cluster结构核简介
- α -cluster结构在相对论重离子碰撞中的效应
- 总结



相对论重子碰撞简介

核物质与宇宙的历史



横四维而含阴阳，统宇宙而章三光——《淮南子》
汉·高诱。注：四方上下曰宇，古往今来曰宙



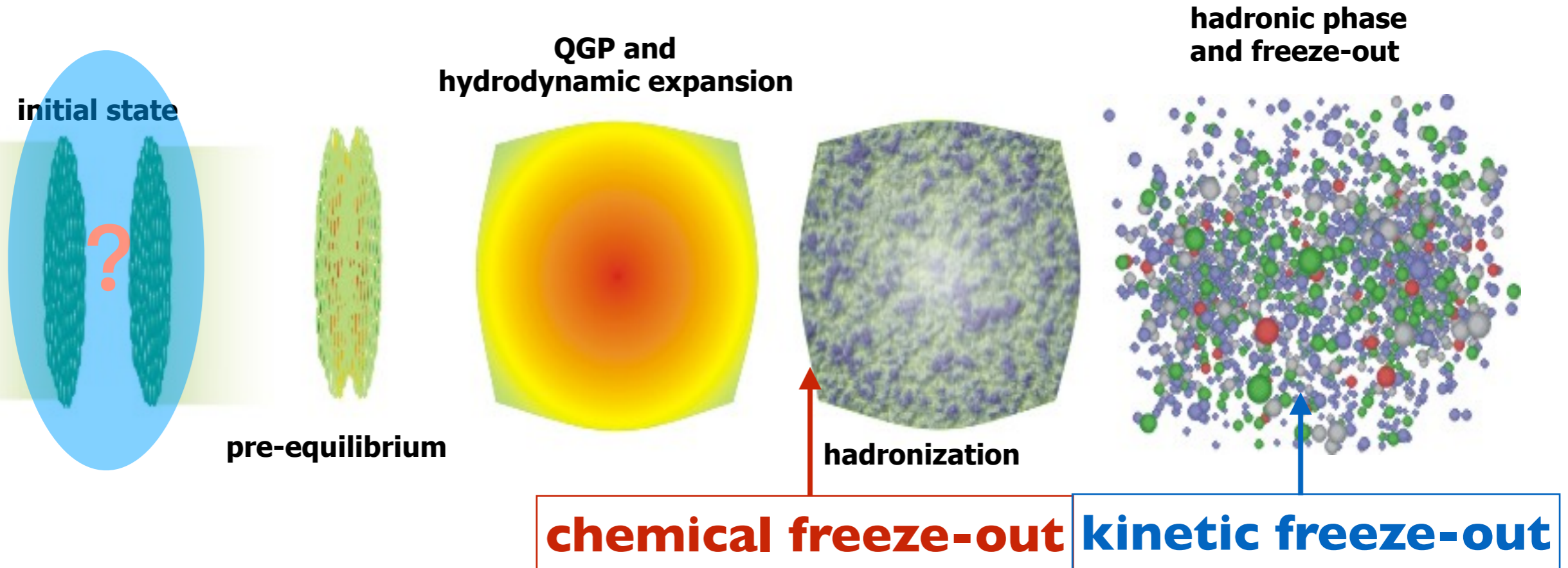
history of universe

✓ QCD, quark-gluon plasma (QGP)

✓ Early stage of universe, relativistic heavy-ion collisions at laboratory

高能重离子碰撞

Micro-bangs in A+A collisions at laboratory

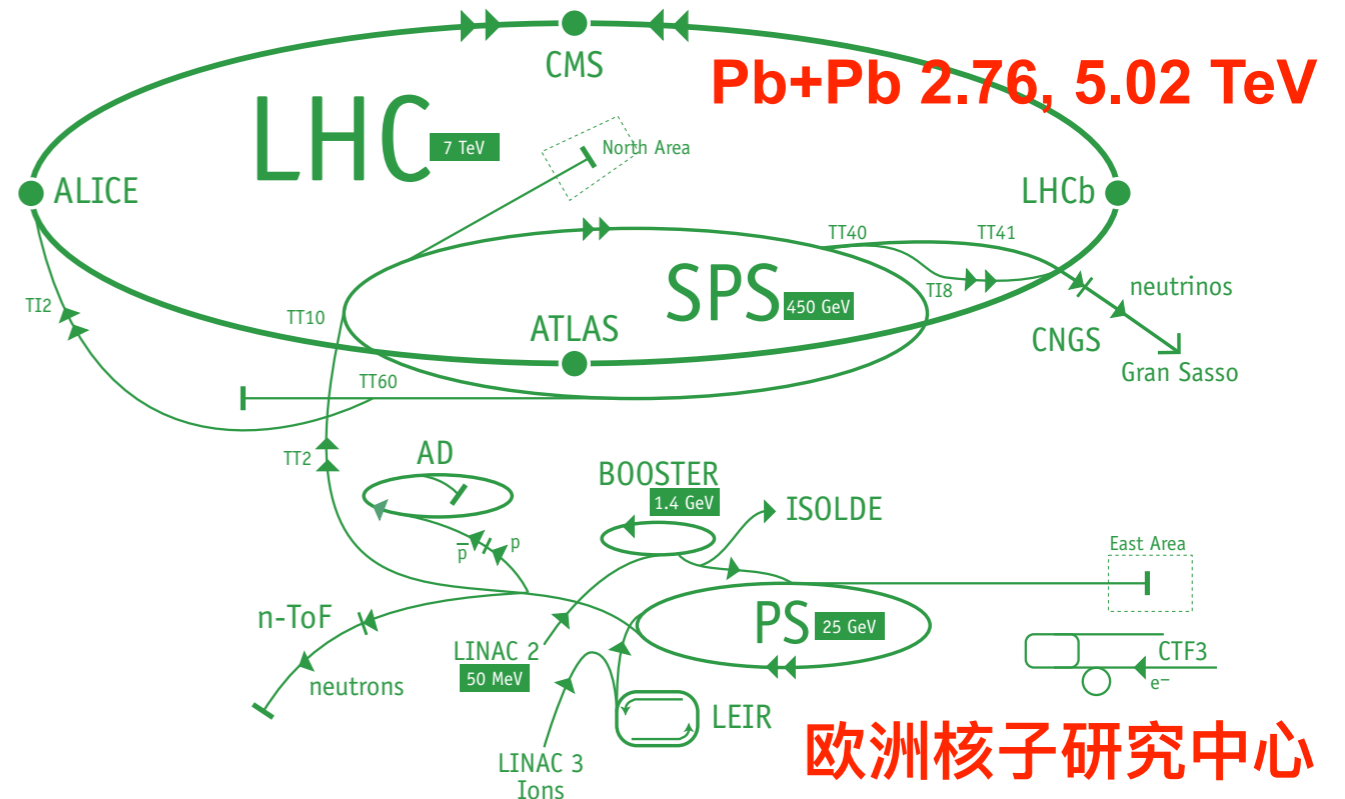
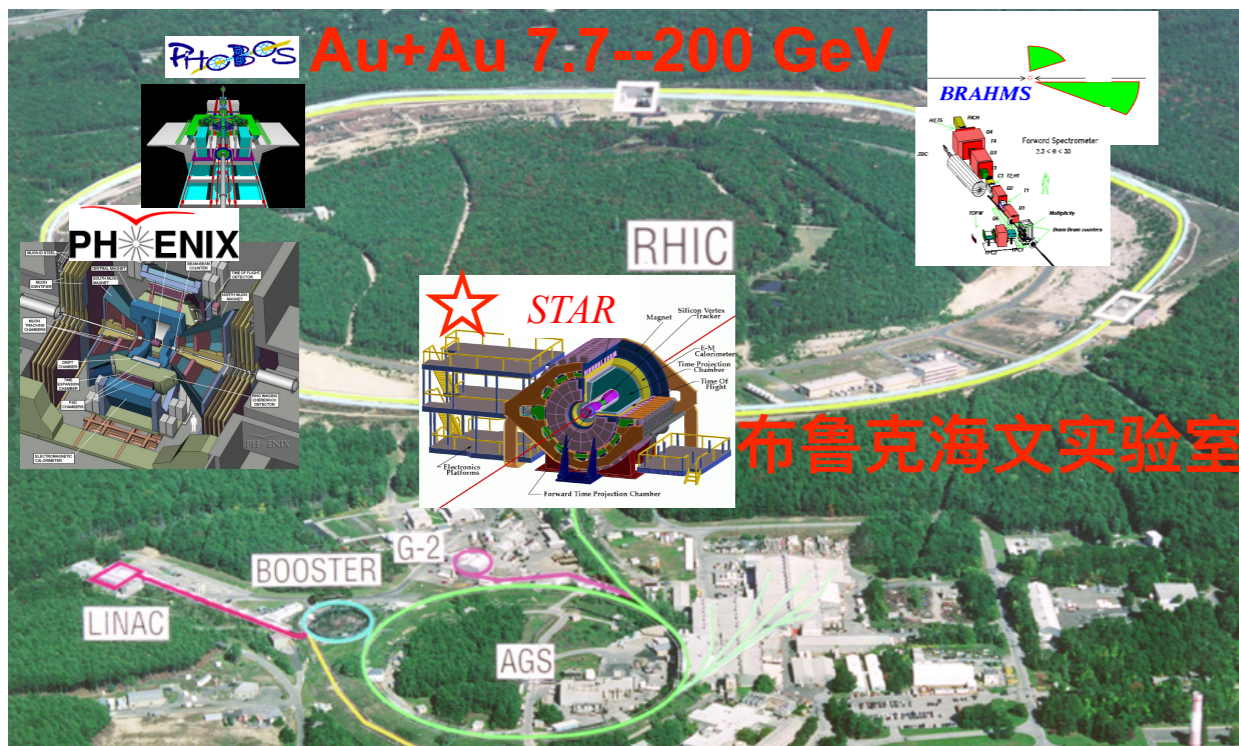
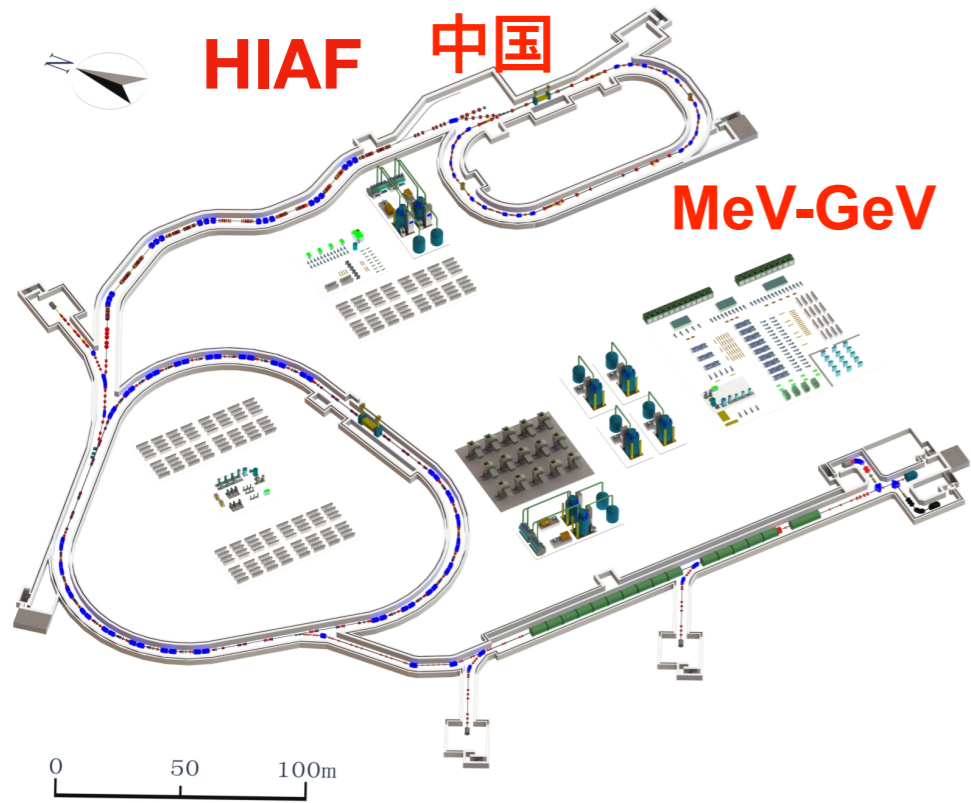


Physics:

- 1) Parton distributions in nuclei
- 2) Initial conditions of the collision
- 3) a new state of matter – Quark-Gluon Plasma and its properties
- 4) hadronization

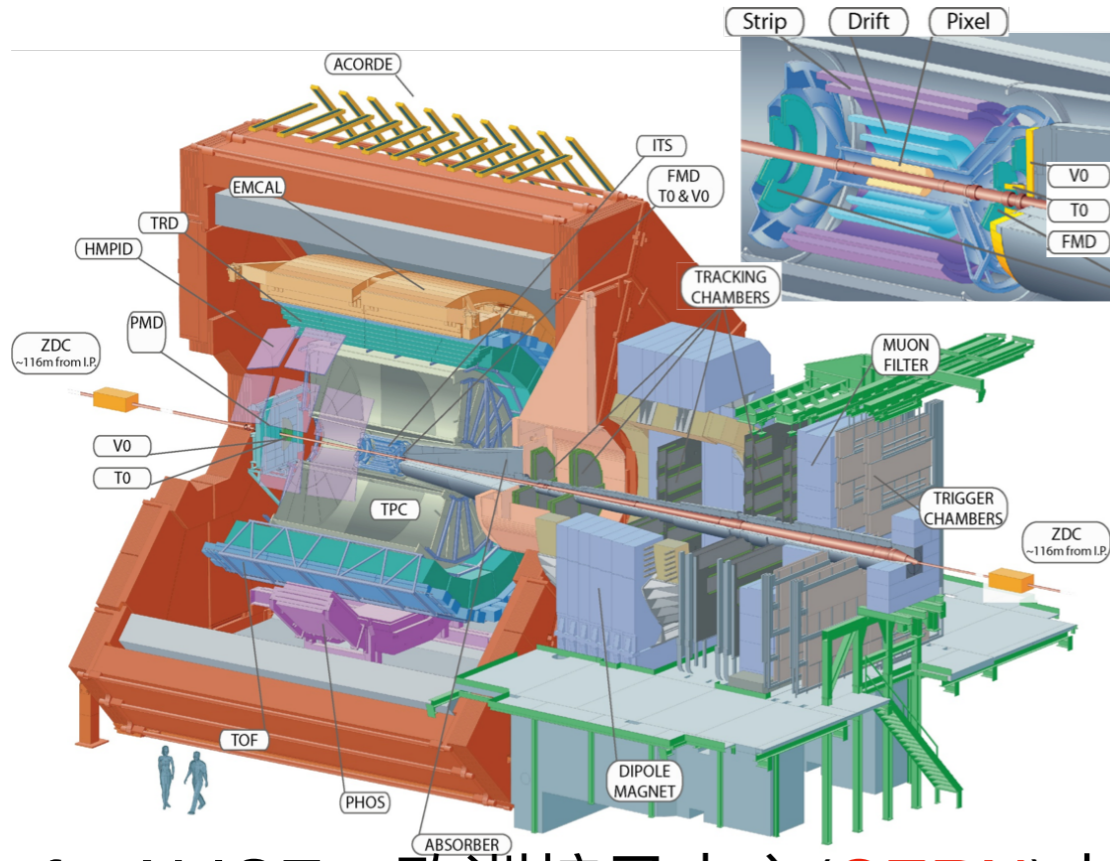


相对论重离子对撞机



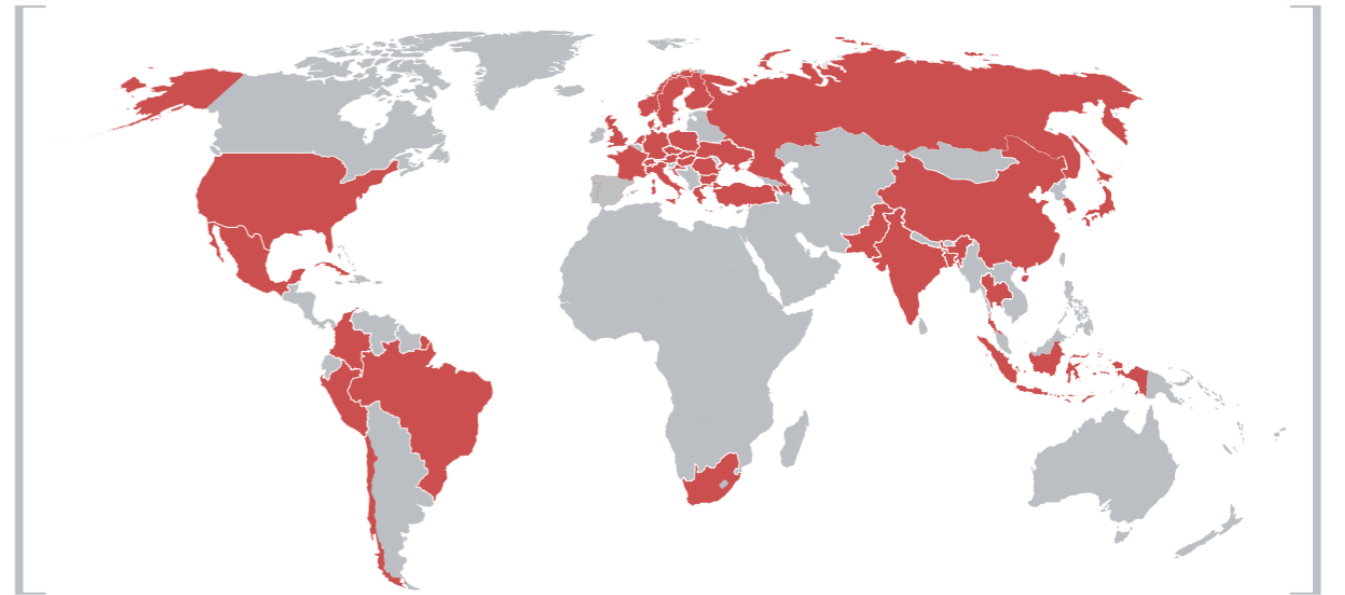


LHC-ALICE物理与合作



A Large Ion Collider Experiment

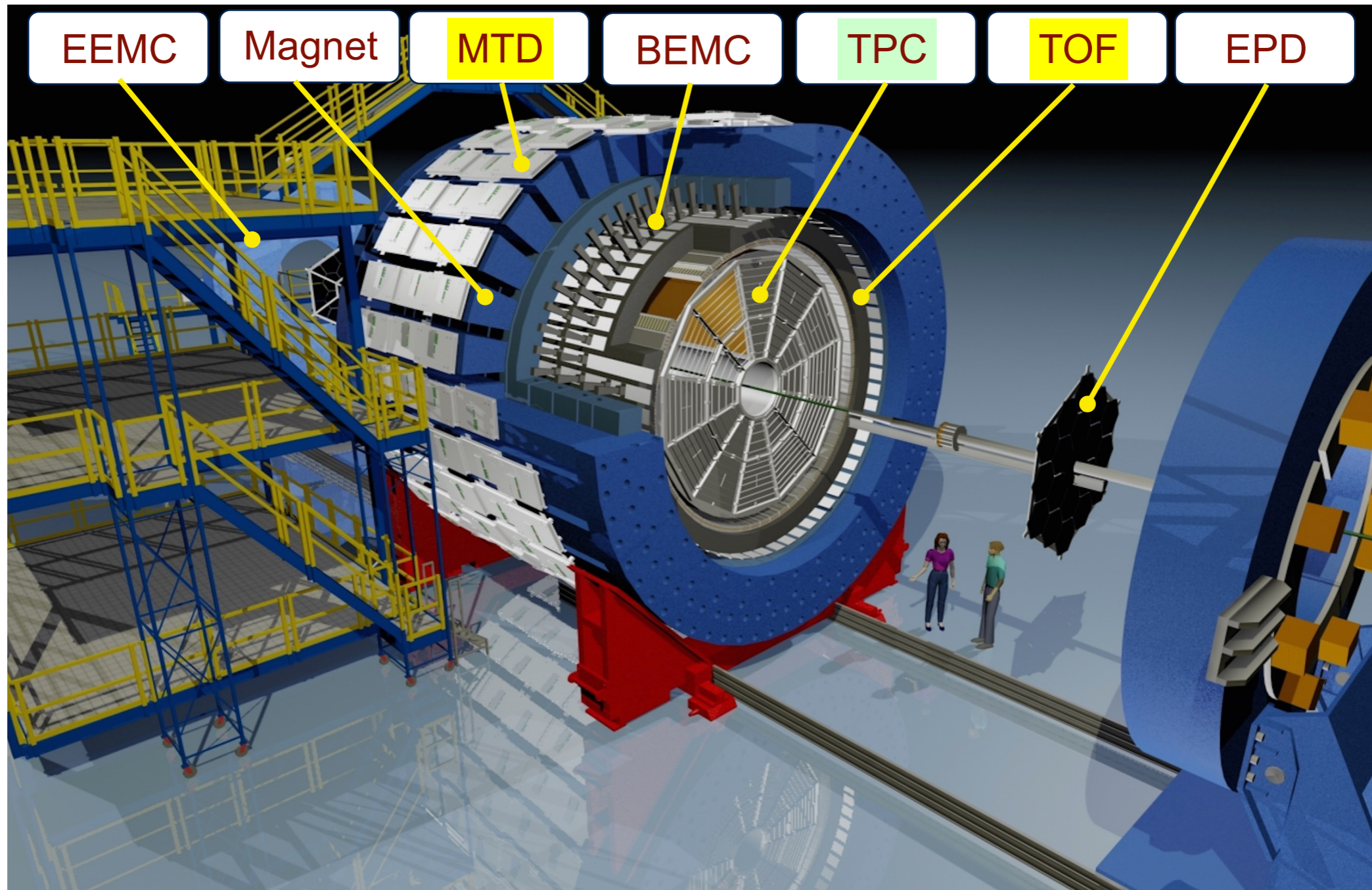
ALICE COLLABORATION
AS JANUARY 2018



- ✓ ALICE: 欧洲核子中心(CERN)大强子对撞机(LHC)上针对重离子对撞的探测装置
- ✓ 每核子对质心能量达TeV的重离子对撞物理
- ✓ 量子色动力学(QCD)特性研究
- ✓ 夸克-胶子等离子体(QGP)性质研究
- ✓ 宇宙早期演化规律, 核天体物理微观性质
- ✓ 双重子态、重超核、手征反常效应
- ✓



RHIC-STAR国际合作



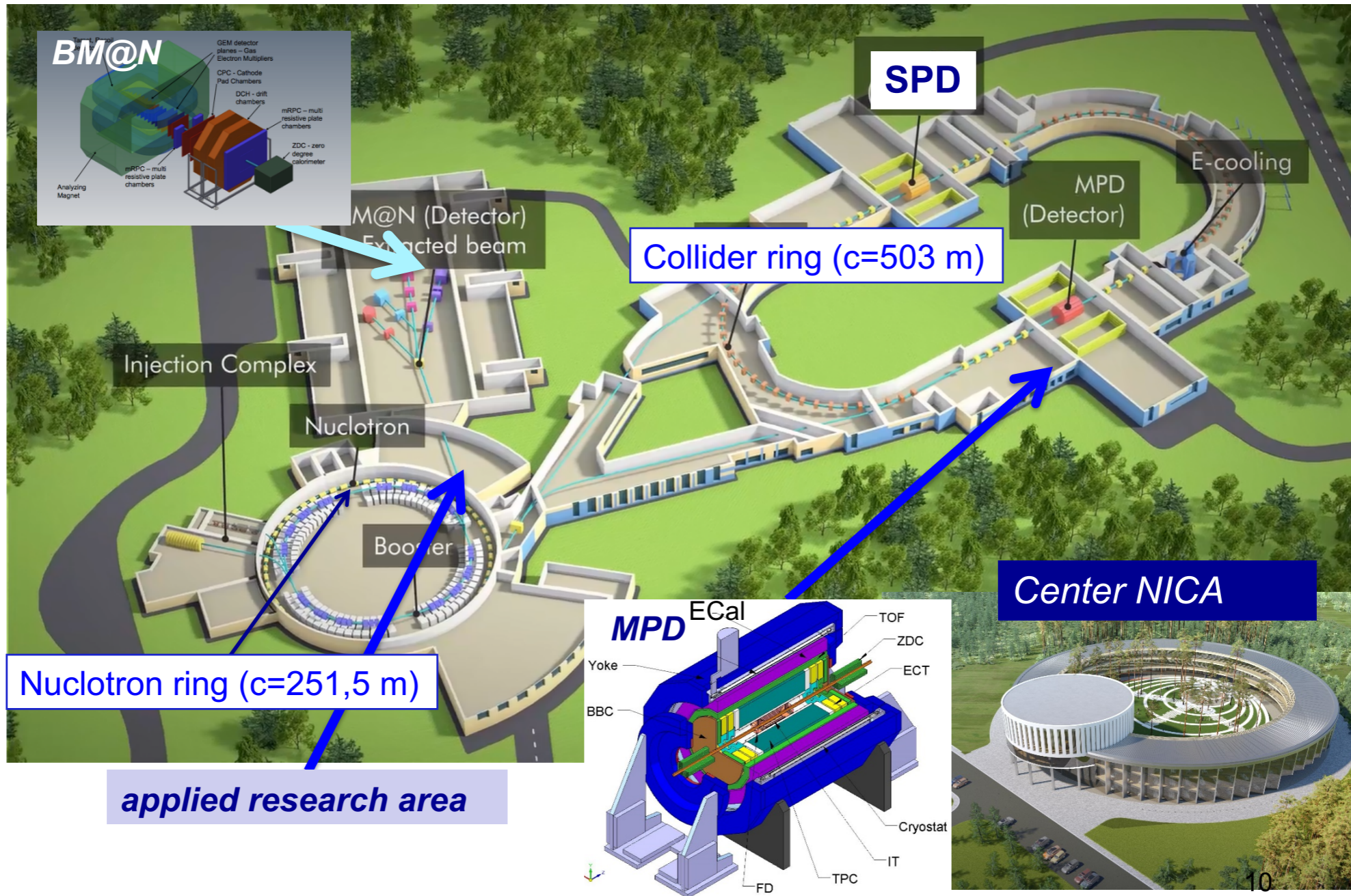
- ✓ QGP相变, 二期能量扫描
- ✓ 手征效应, isobar实验计划



NICA国际合作

basic facility

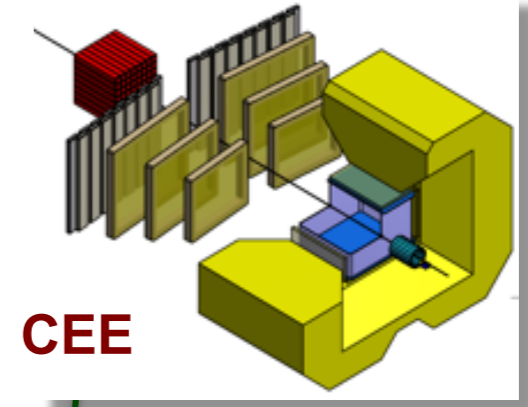
高重子数密度, 核物质状态方程



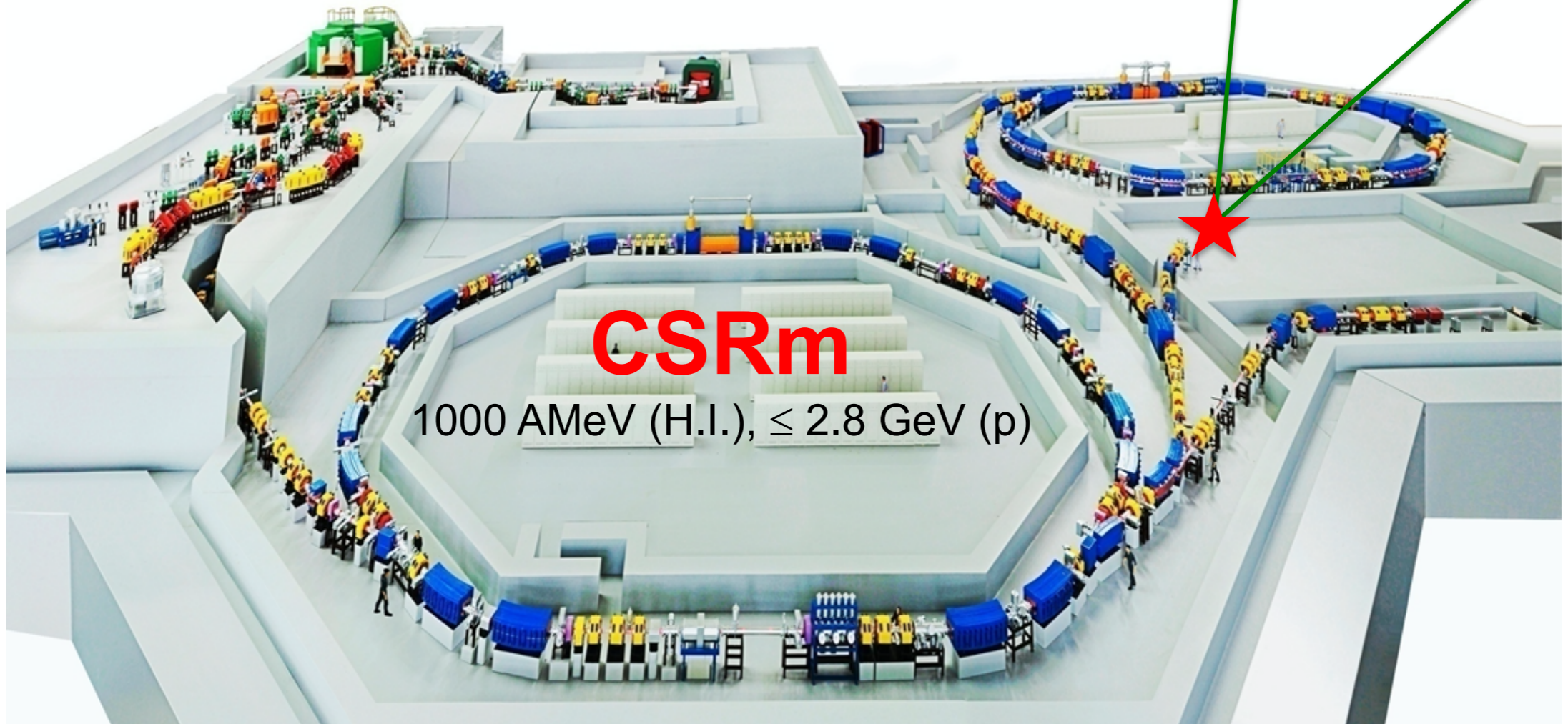


CEE合作

高重子数密度 (HIAF), 核物质状态方程, 超核



CEE



CSRm

1000 AMeV (H.I.), ≤ 2.8 GeV (p)



碰撞初态对集体流的影响



集体流研究中的几个标志性问题

- 在平面椭圆流的出现 (in-plane elliptic flow)
- 部分子标度 (NCQ-scaling)
- 初始状态涨落, 三角流的测量

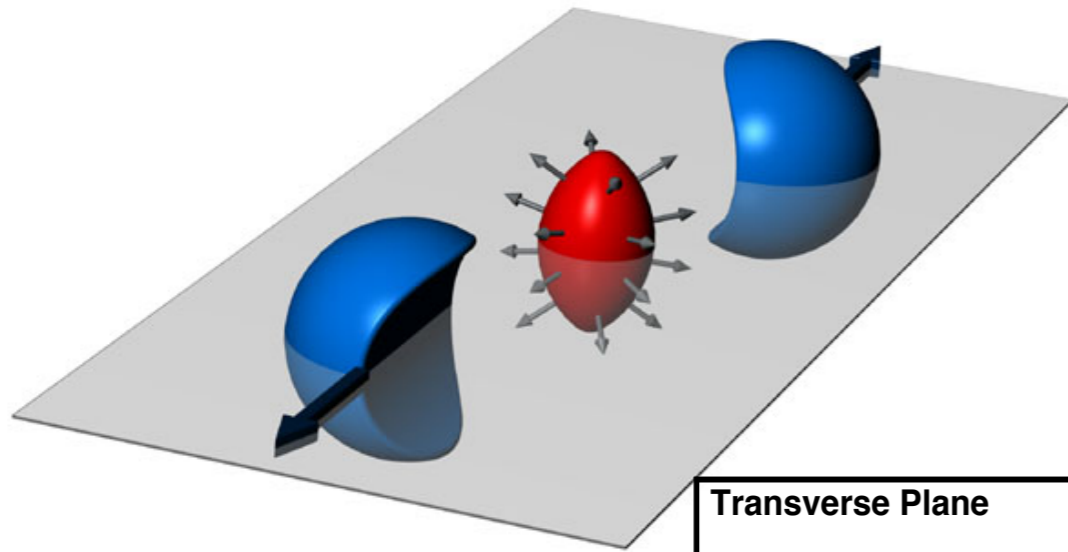


集体流的一般定义

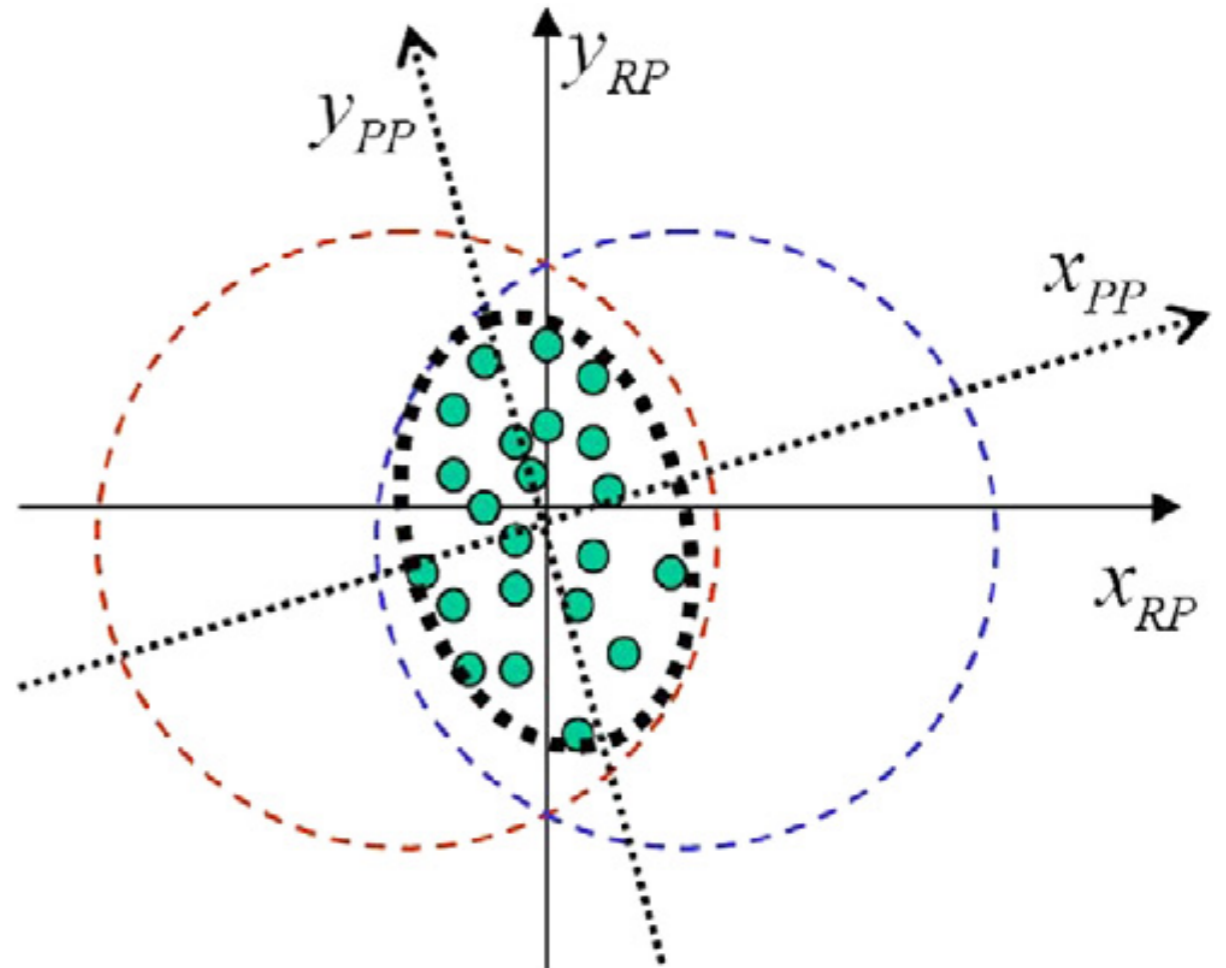
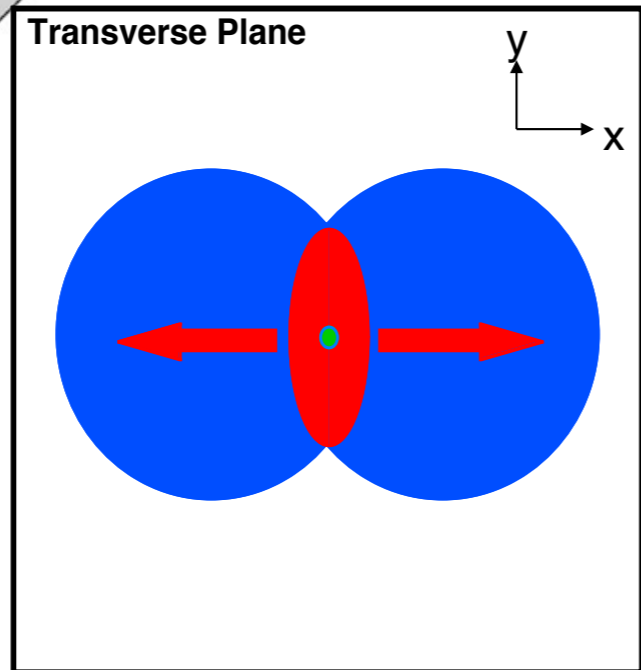
A. M. Poskanzer, S. A. Voloshin, Phys. Rev. C 58 (1998) 1671

$$E \frac{d^3 N}{d^3 p} = \frac{1}{2\pi} \frac{d^2 N}{p_T dp_T dy} \left(1 + \sum_{n=1}^{\infty} 2v_n \cos[n(\phi - \Psi_r)] \right)$$

$$v_n = \langle \cos[n(\phi - \Psi_r)] \rangle$$



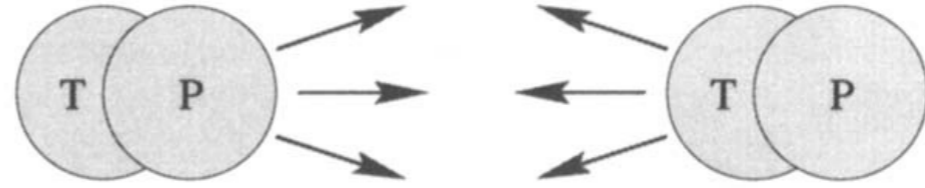
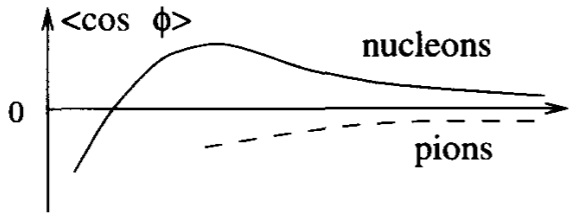
S.A. Voloshin et al. / Physics Letters B 659 (2008) 537–541



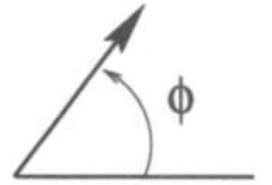
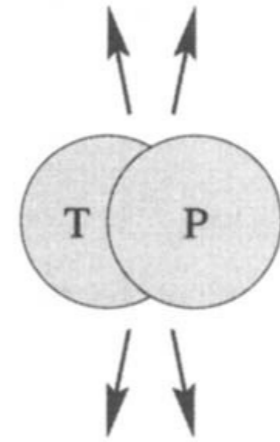
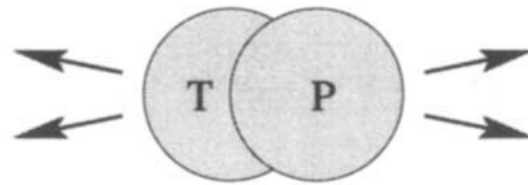
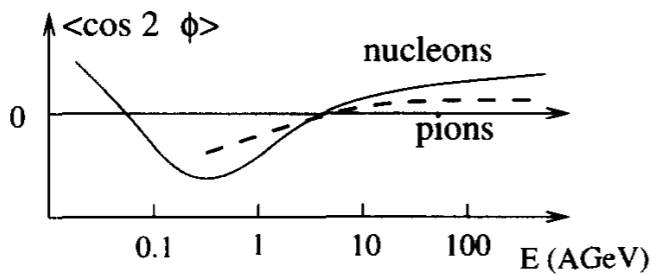


在平面椭圆流的出现

Directed flow

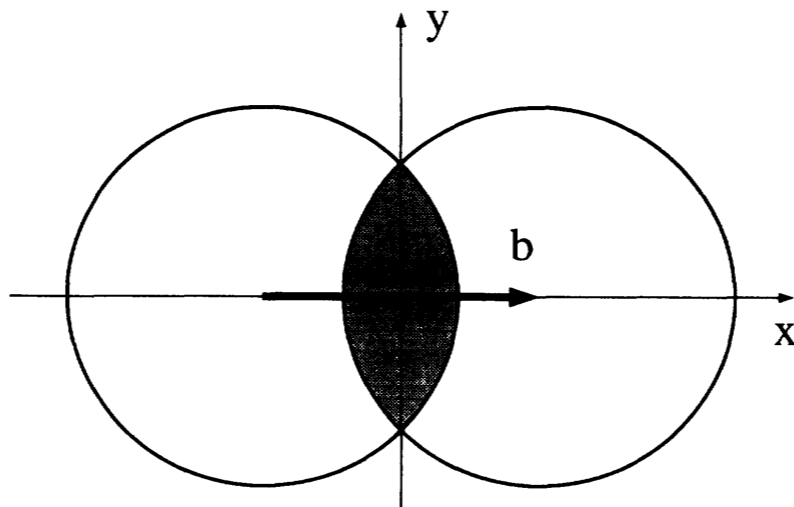


Elliptic flow



SIS Bevalac AGS SPS

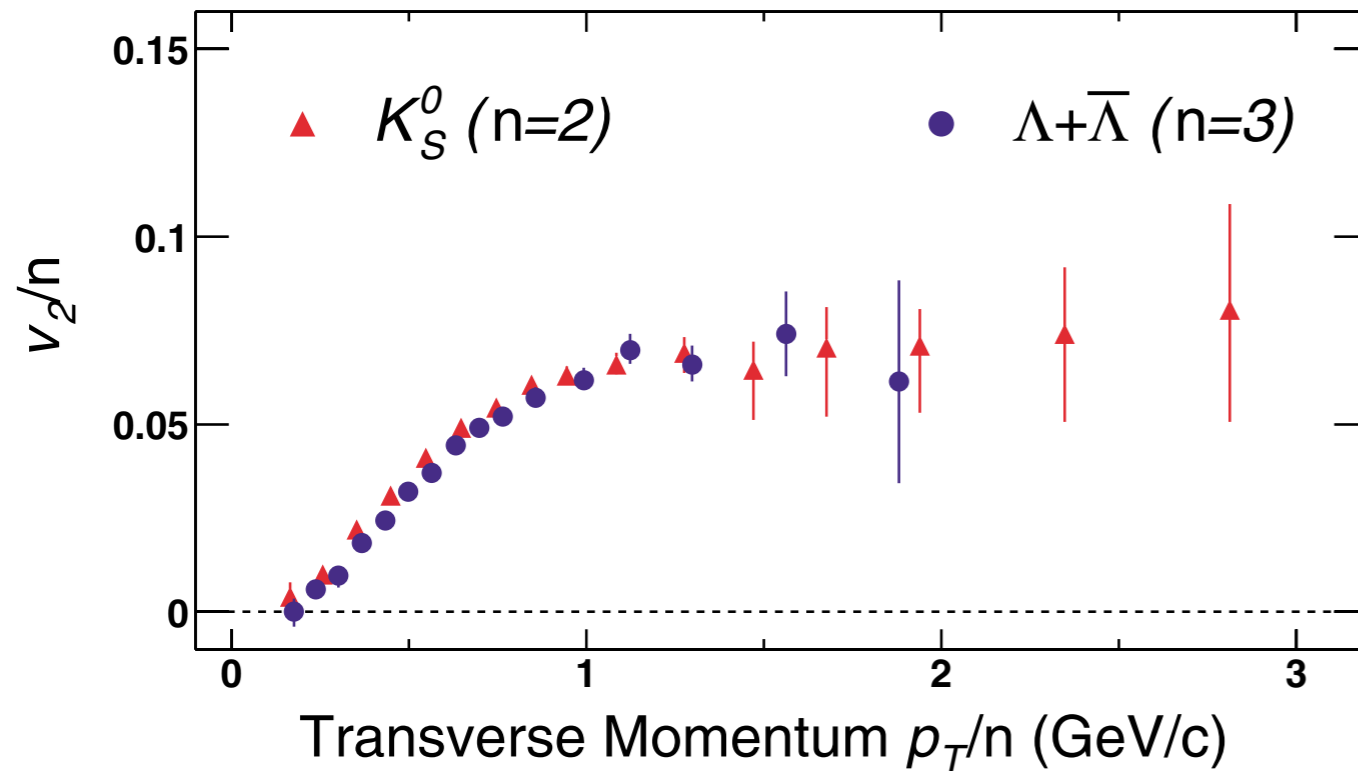
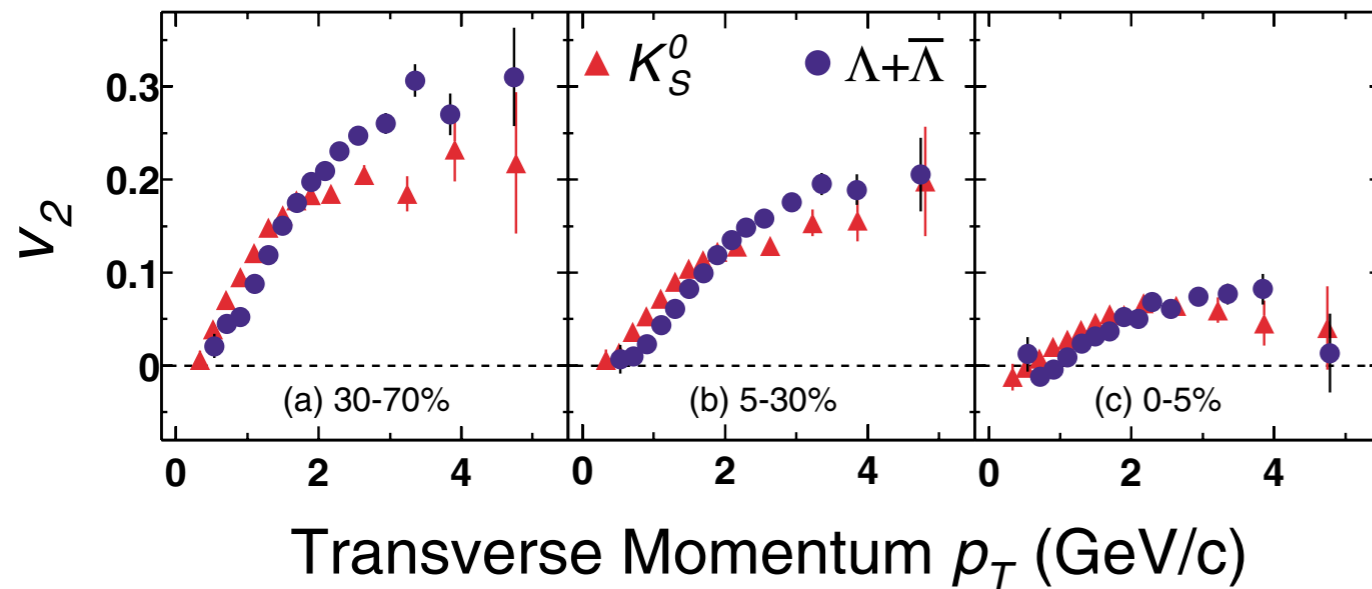
J-Y. Ollitrault, Nuclear Physics A638 (1998) 195c; Phys. Rev. D 46 (1992) 229





椭圆流的组分夸克标度 (NCQ-Scaling)

STAR, Phys. Rev. Lett. 92 (2004) 052302, 99 (2007) 112301

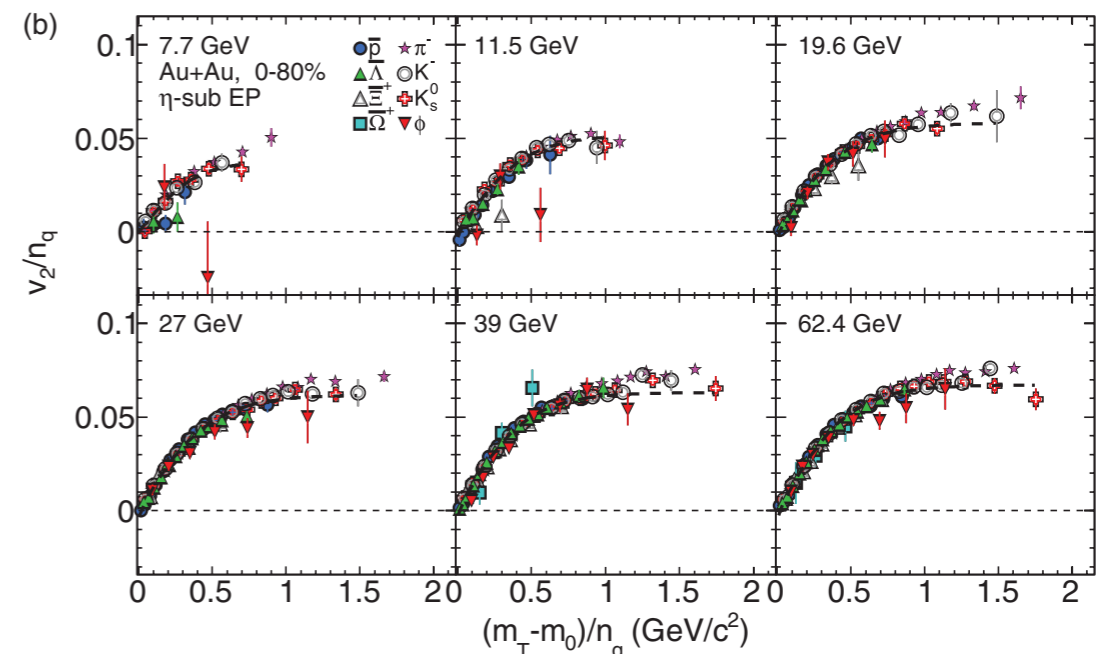
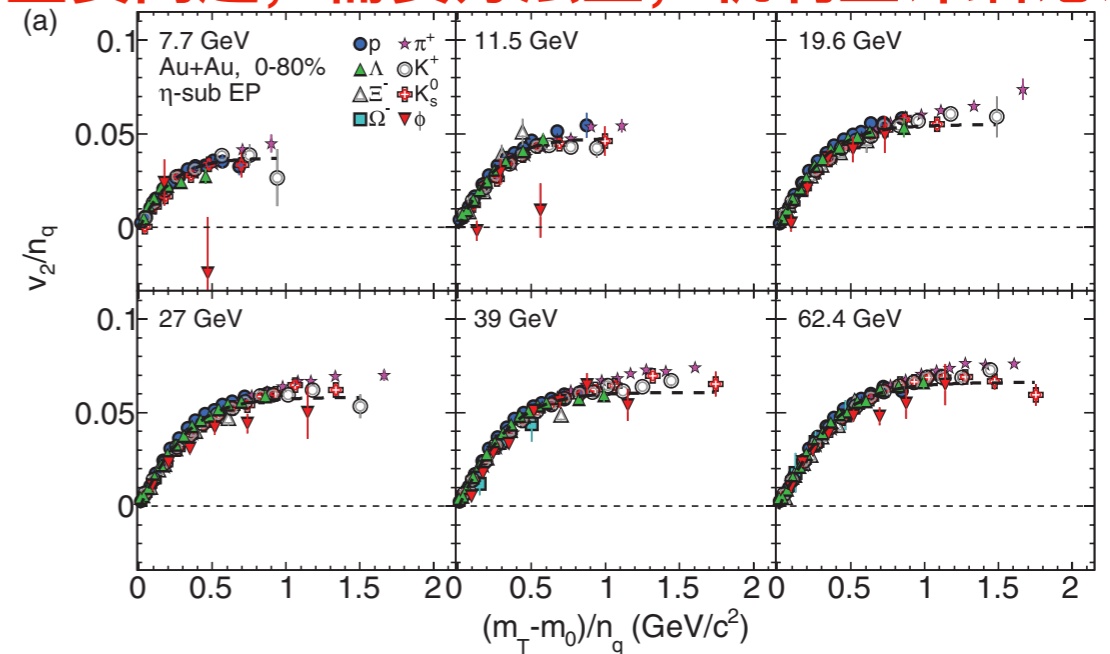


Similar measurement, PHENIX, Phys. Rev. Lett. 91 (2003) 182301

✓粒子形成机制

✓解紧闭相变

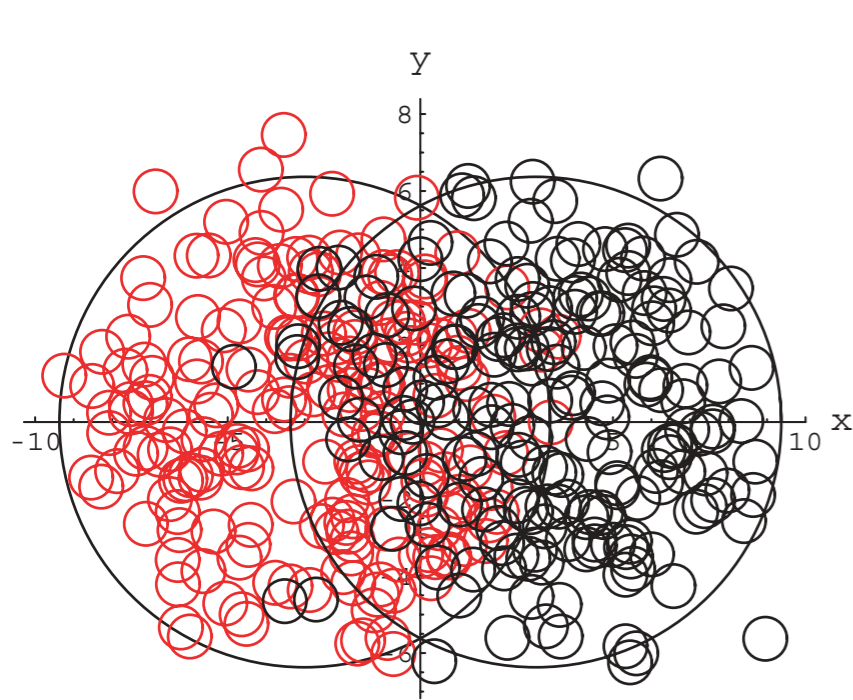
✓重要问题, 需要方法上, 机制上详细论证



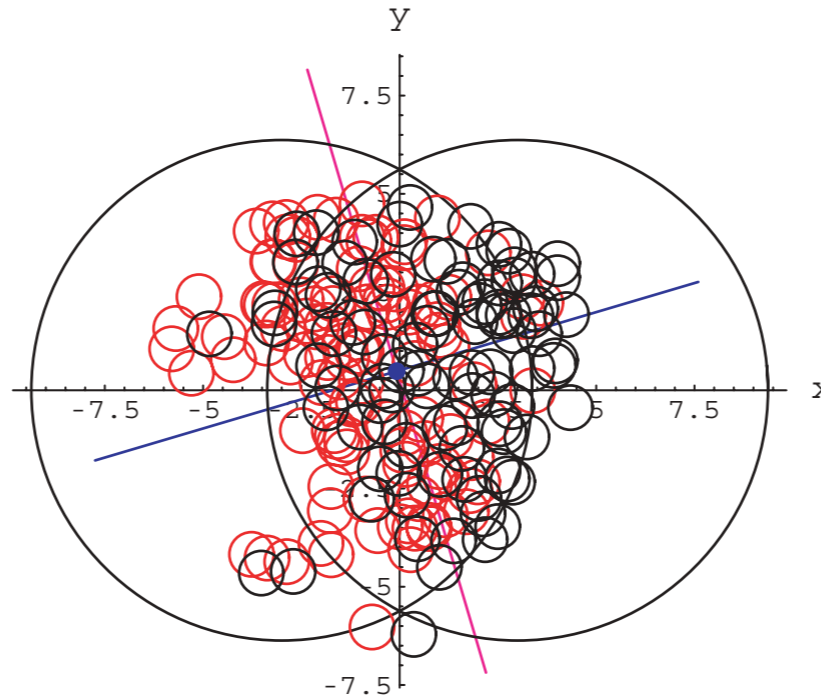
STAR, Phys. Rev. C 88 (2013) 014902

初始状态的几何涨落

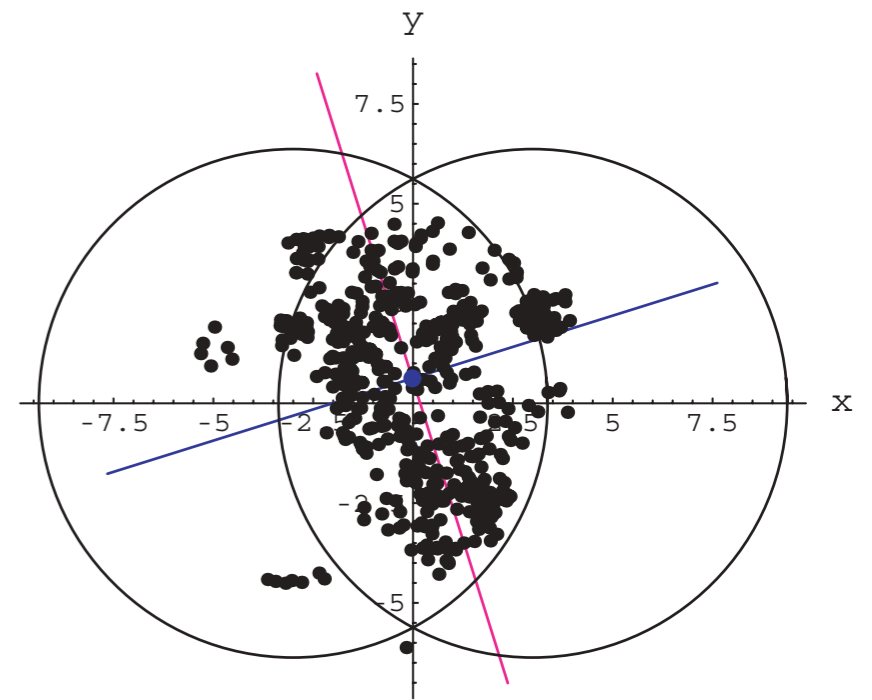
W. Broniowski et al., Phys. Rev. C 76 (2007) 054905



Nucleon from nuclei A and B



Participant initial coordinates



Participant in center of mass frame after binary collision

✓ Fluctuation, significant in small system



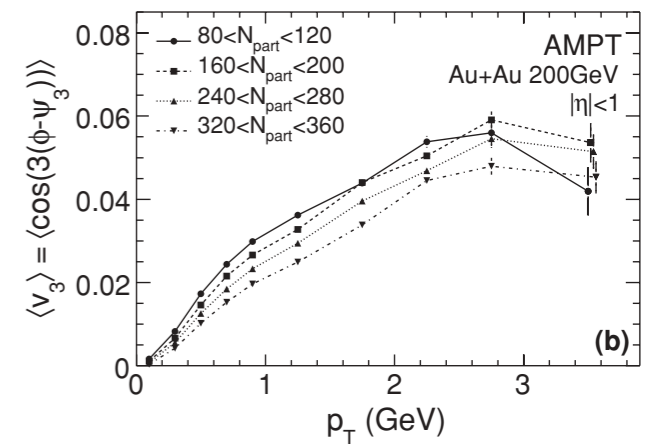
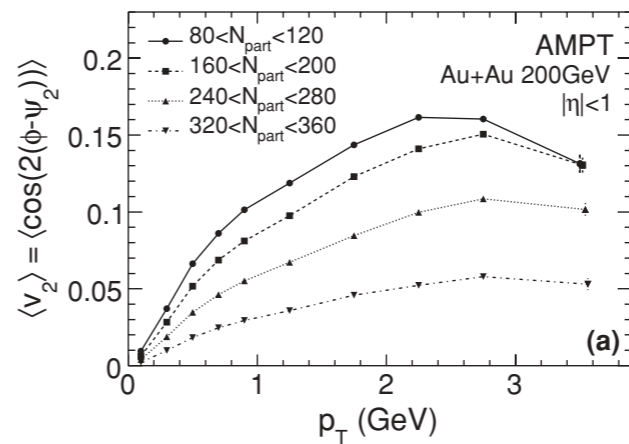
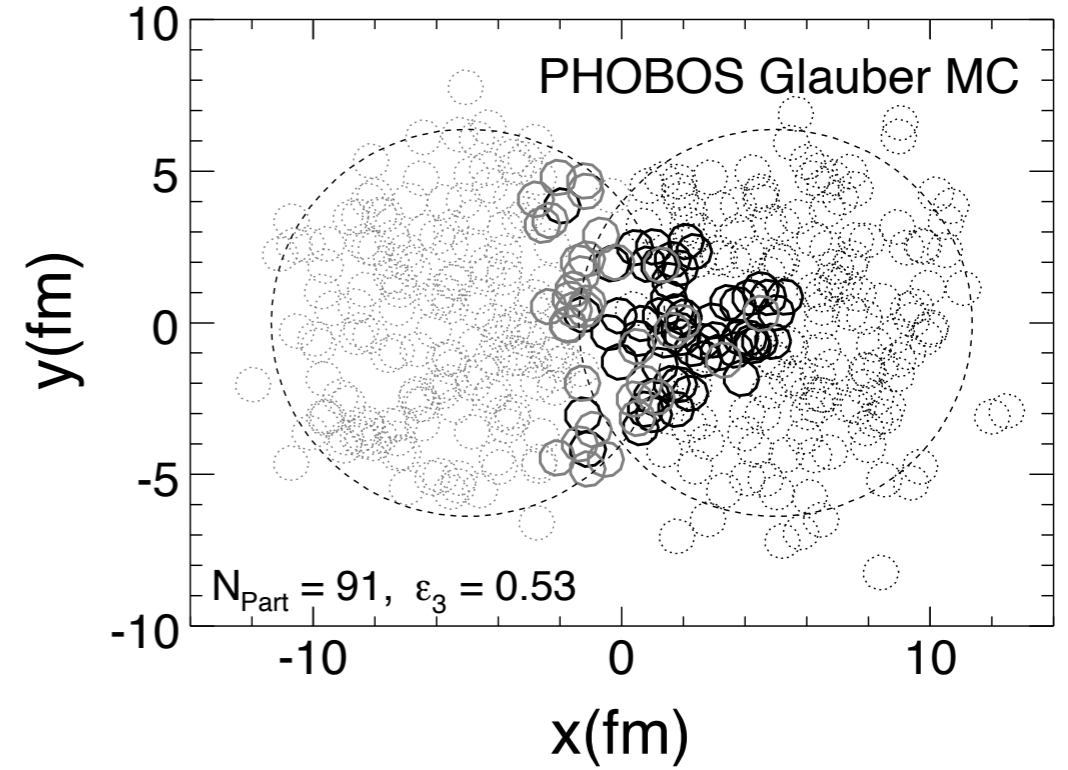
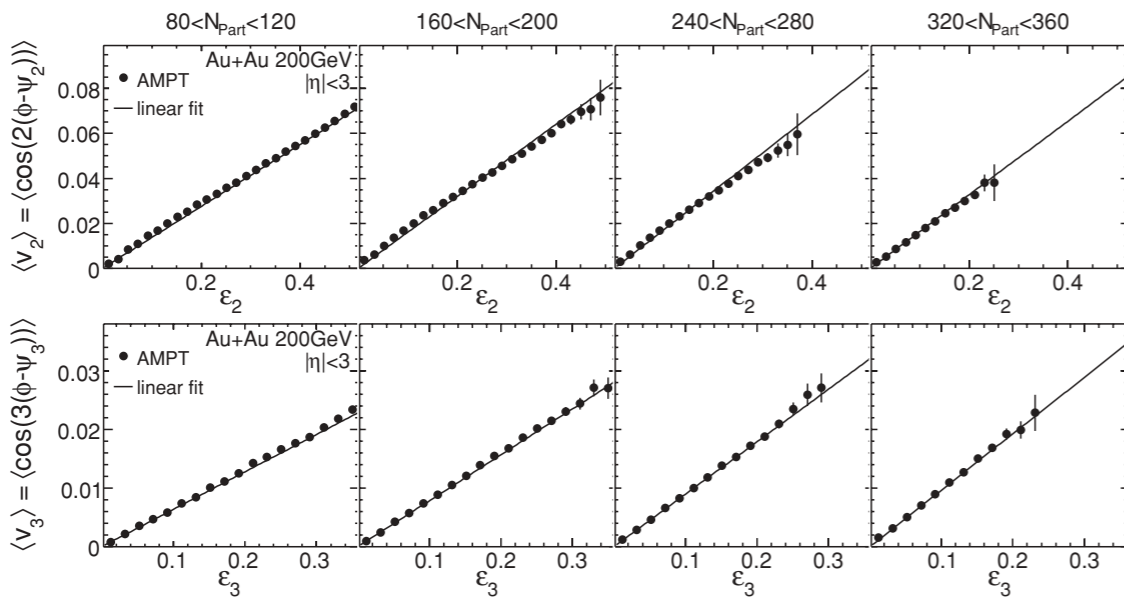
三阶流

B. Alver and G. Roland, Phys. Rev. C **81**, 054905 (2010)

$$\varepsilon_3 \equiv \frac{\sqrt{\langle r^2 \cos(3\phi_{\text{part}}) \rangle^2 + \langle r^2 \sin(3\phi_{\text{part}}) \rangle^2}}{\langle r^2 \rangle}$$

$$v_3 \equiv \langle \cos(3(\phi - \psi_3)) \rangle,$$

$$\psi_3 = \frac{\text{atan2}(\langle r^2 \sin(3\phi_{\text{part}}) \rangle, \langle r^2 \cos(3\phi_{\text{part}}) \rangle) + \pi}{3}$$



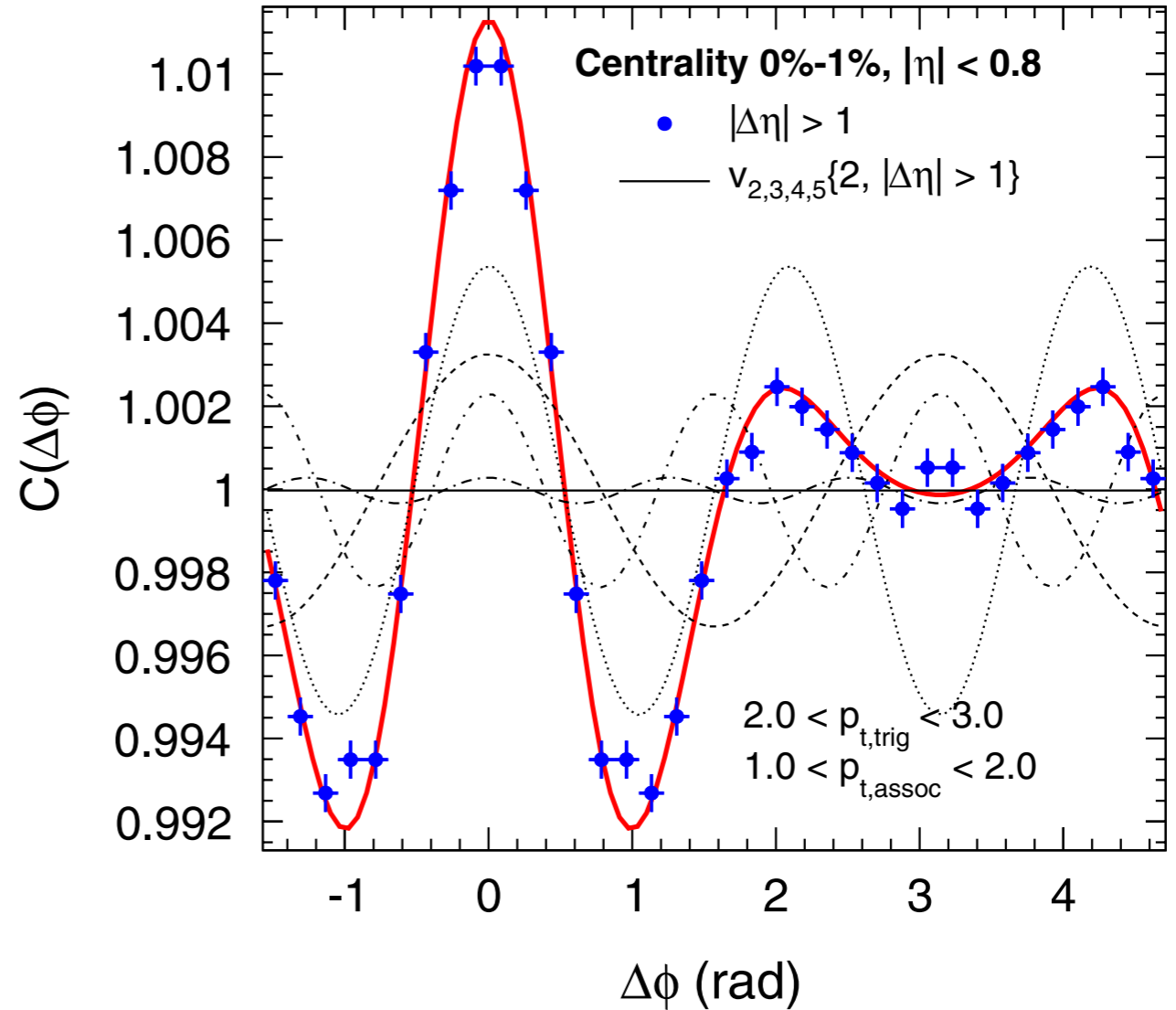
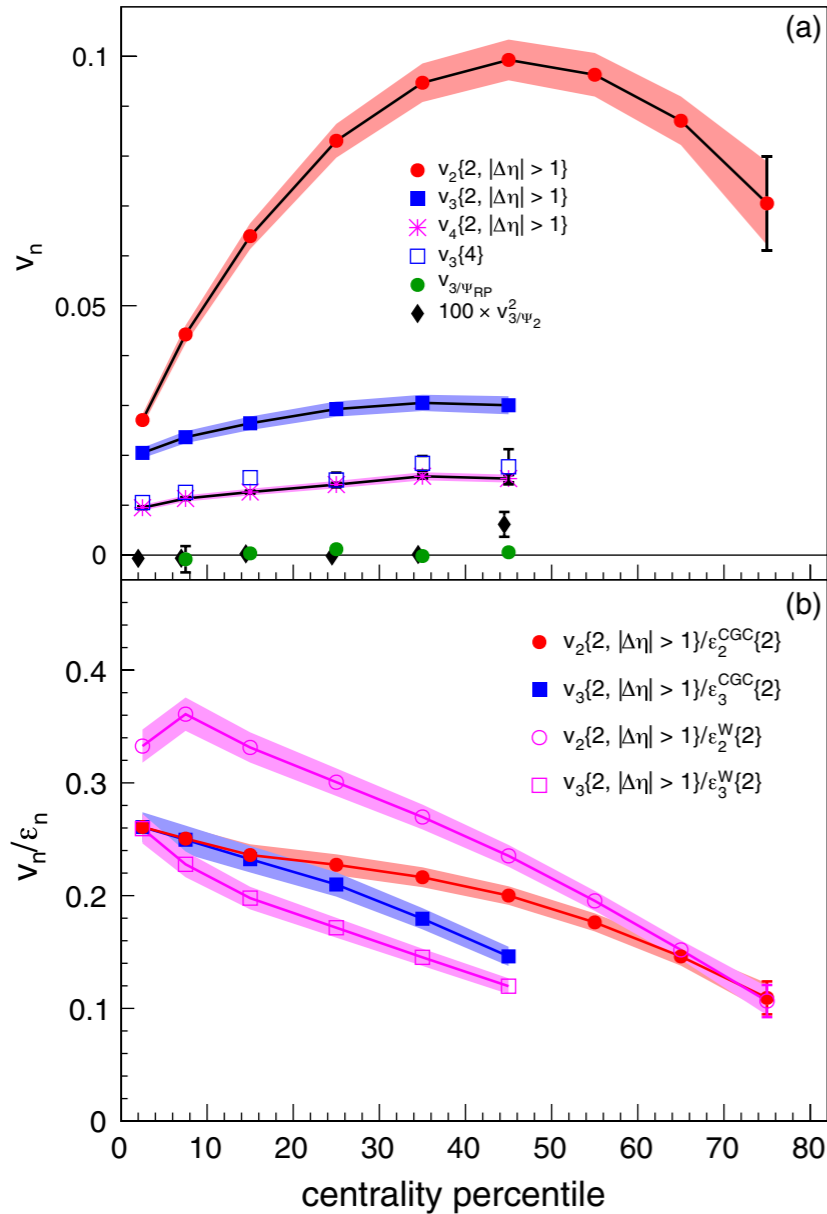
J.Y. Jia, S. Mohapatra, Eur. Phys. J. C (2013) 73:2510, 73:2558

L.X. Han, G.L. Ma, Y.G. Ma, et al., Phys. Rev. C 84 (2011) 064907



高阶流的测量

ALICE, Phys. Rev. Lett. 107 (2011) 032301



STAR: PRC-88-014904 (2013), PRL-116-112302 (2016);
PHINEX: PRC-93-051902(R) (2016), PRC-94-054910 (2016);
ATLAS: PRC-86-014907 (2012), EPJC-74-3157 (2014);
CMS: EPJC-72-2012 (2012), PLB-724-213 (2013).



集体流与初始几何不对称性

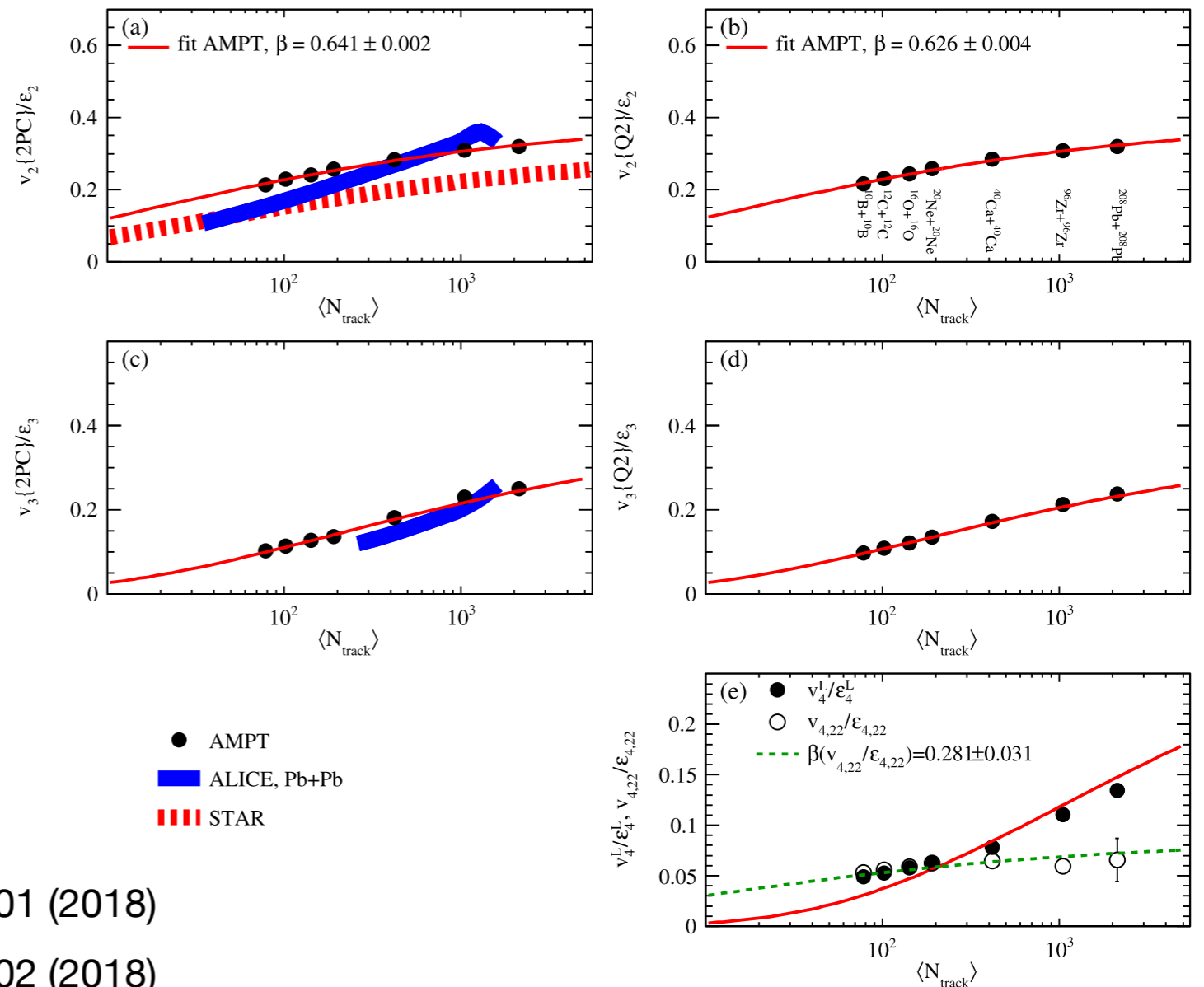
初始几何不对称向末态动量空间不对称的运输, 剪切粘滞系数, 流体力学

$$v_n^L/\varepsilon_n^L \propto \exp\left(-n^2 \beta \langle N_{track} \rangle^{-1/3}\right)$$

$$v_{n,ij}/\varepsilon_{n,ij} \propto \exp\left(-\left(i^2 + j^2\right)\beta \langle N_{track} \rangle^{-1/3}\right)$$

$$\mathcal{E}_n \equiv \varepsilon_n e^{in\Phi_n} \equiv -\frac{\langle r^n e^{in\phi_{Part}} \rangle}{\langle r^n \rangle}$$

$$V_n \equiv v_n e^{in\Psi_n} \equiv \{e^{in\phi}\}, \quad v_n = \langle |V_n|^2 \rangle^{1/2}$$



P. Liu and R. A. Lacey, Phys. Rev. C 98, 031901 (2018)

P. Liu and R. A. Lacey, Phys. Rev. C 98, 021902 (2018)

E. Shuryak and I. Zahed, Phys. Rev. C 88, 044915 (2013)

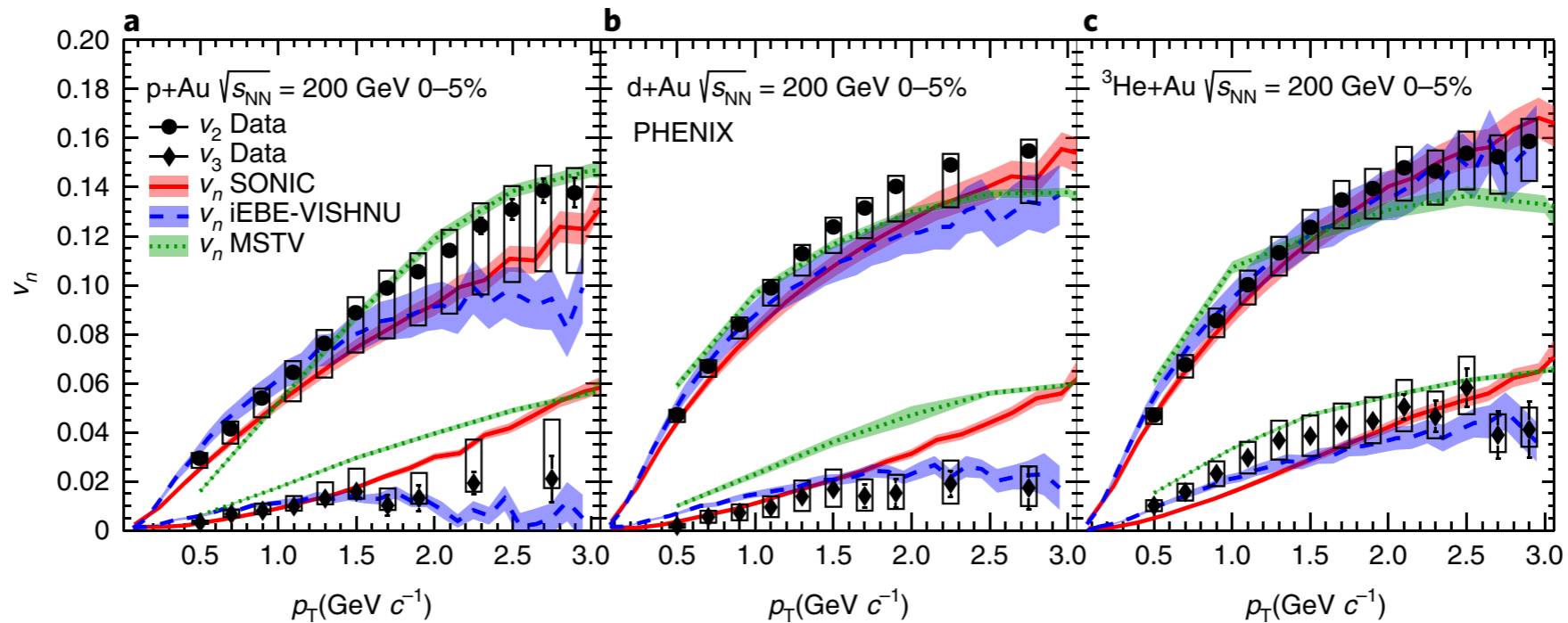
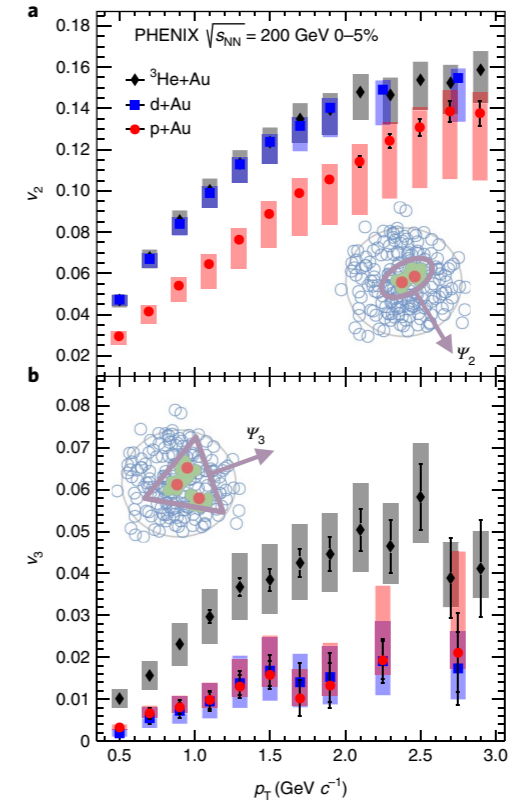
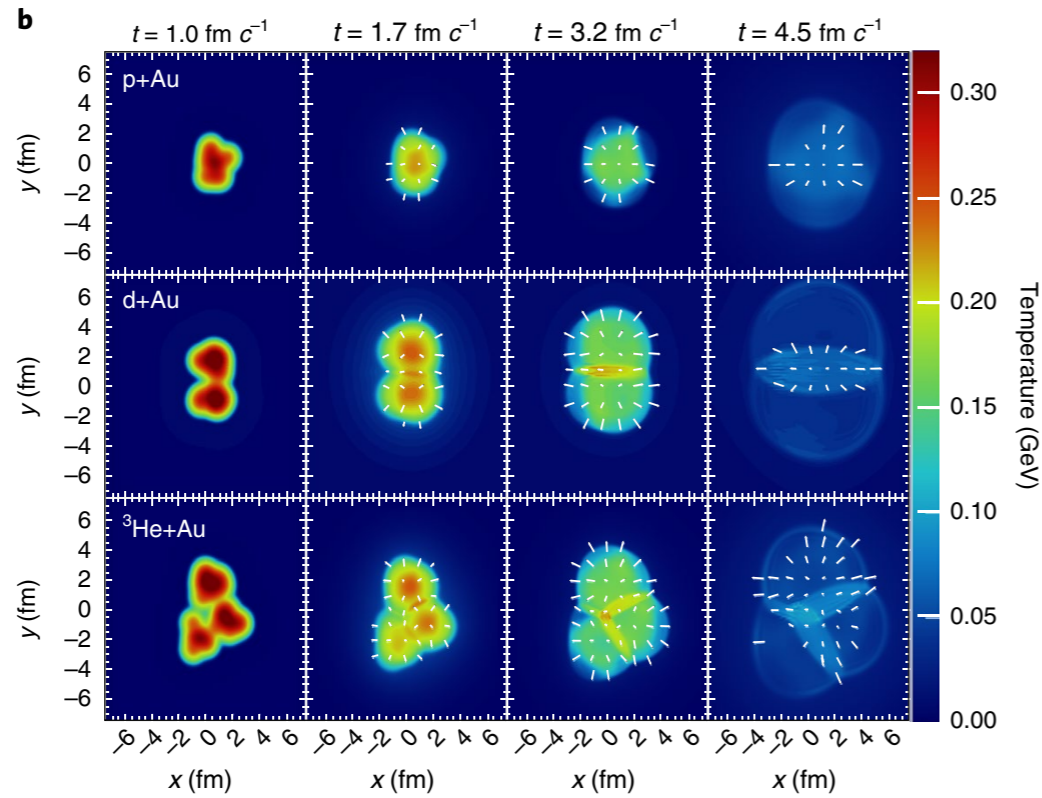
S. Acharya, D. Adamova, J. Adolfsson, et al., Phys. Lett. B 773, 68 (2017)

S. Zhang, Y. Ma, G. Ma, J. Chen, Q. Shou, W. He, and C. Zhong, Physics Letters B 804, 135366 (2020)



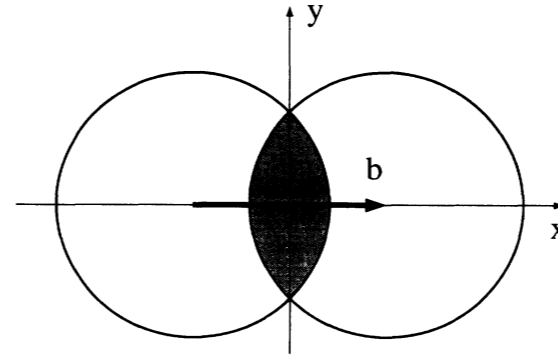
初始内秉几何结构对集体流的效应

PNENIX, Nat. Phys.15 (2019) 214; J. L. Nagle, et al., Phys. Rev. Lett. 113, 112301 (2014)

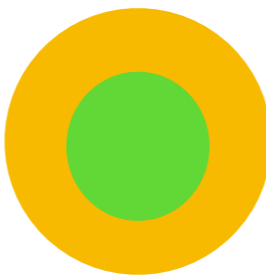


初始几何特性

- 非中心对撞几何不对称性

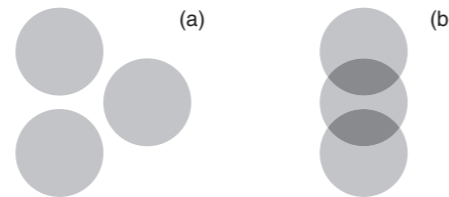


- 形变核 

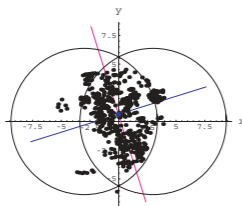
- 中子皮 (周边碰撞) 

Hao-jie Xu et al., PLB-819(2021)136453,
Hanlin Li et al., PRL-125(2020)222301

- **α -cluster**结构



- 涨落

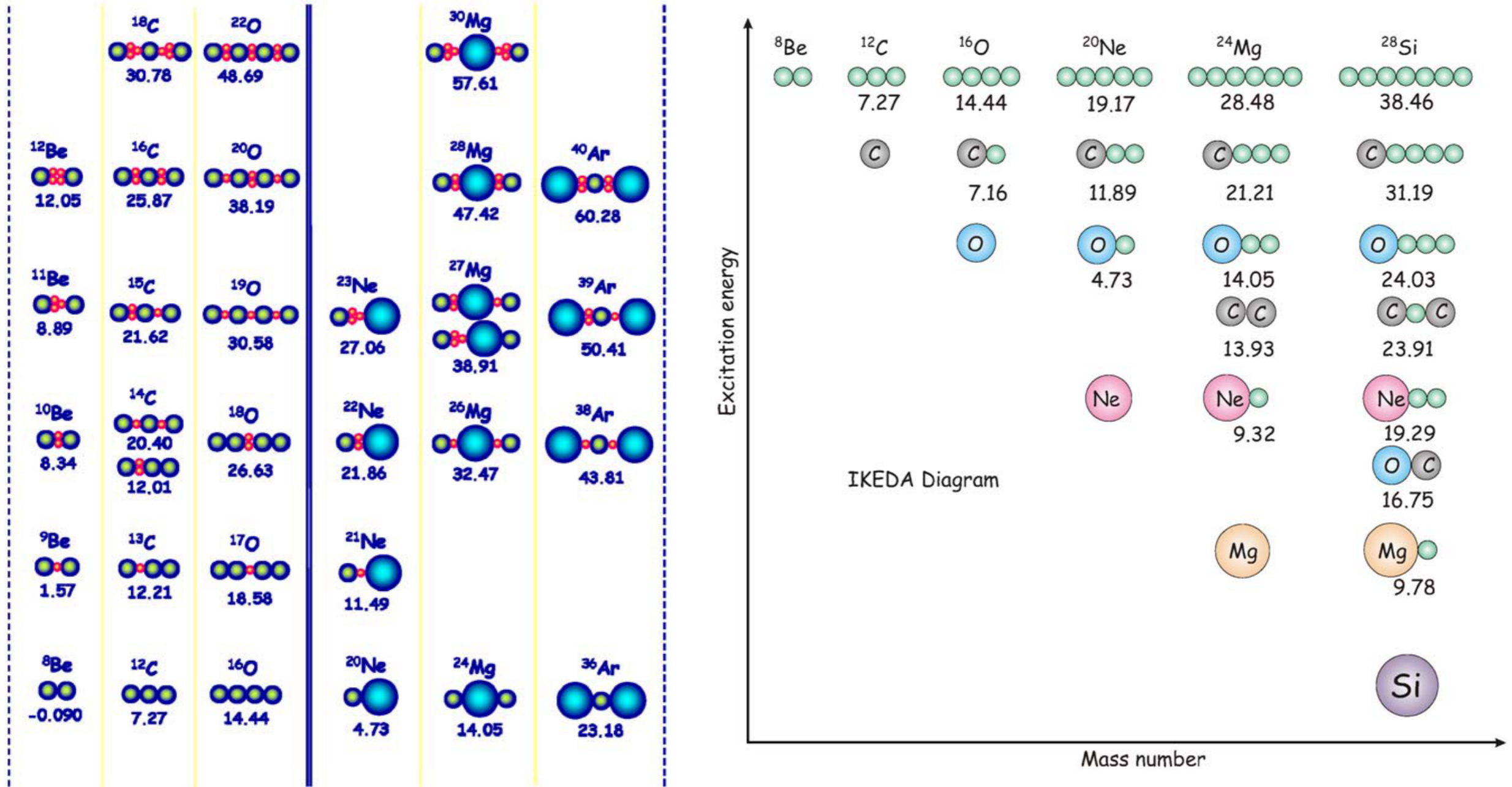




α -cluster结构核简介



α -cluster structure



G. Gamow, in Constitution of atomic nuclei and radioactivity (Clarendon Press Oxford, 1931)

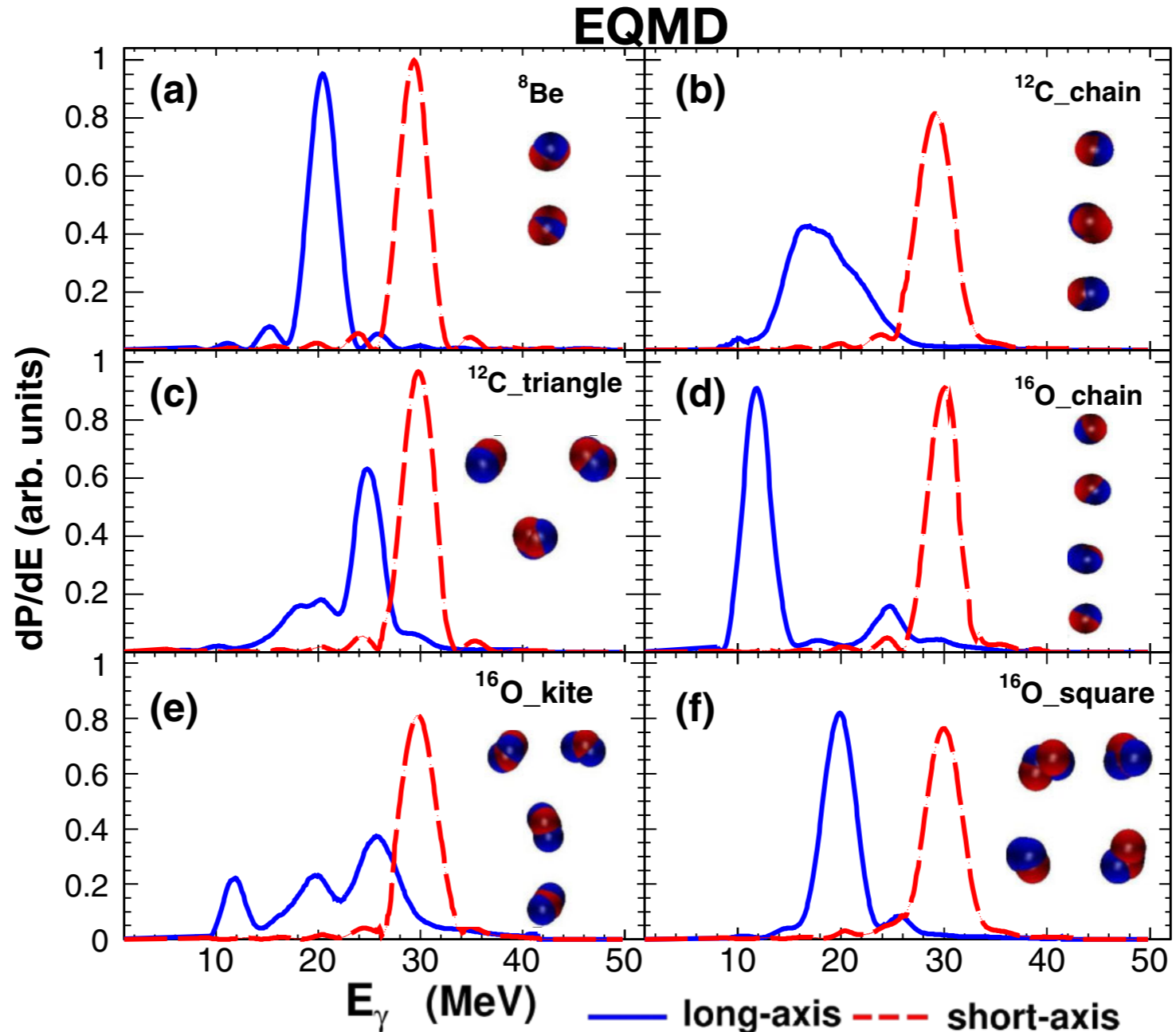
W. von Oertzen, M. Freer, and Y. Kanada-En'yo, Physics Reports 432, 43 (2006)

Martin Freer et al., Rev. Mod. Phys. 90, 035004 (2018)



α -cluster结构

W. B. He, Y. G. Ma et al. Phys. Rev. Lett. 113, 032506 (2014)



M. Chernykh et al., Phys. Rev. Lett. 98, 032501 (2007)

Y. Funaki, Eur. Phys. J. A 28, 259–263 (2006)

Y. Kanada-En'yo et al., PTEP 2012, 01A202 (2012)

D. J. Marín-Lámbarri et al., Phys. Rev. Lett. 113, 012502 (2014)



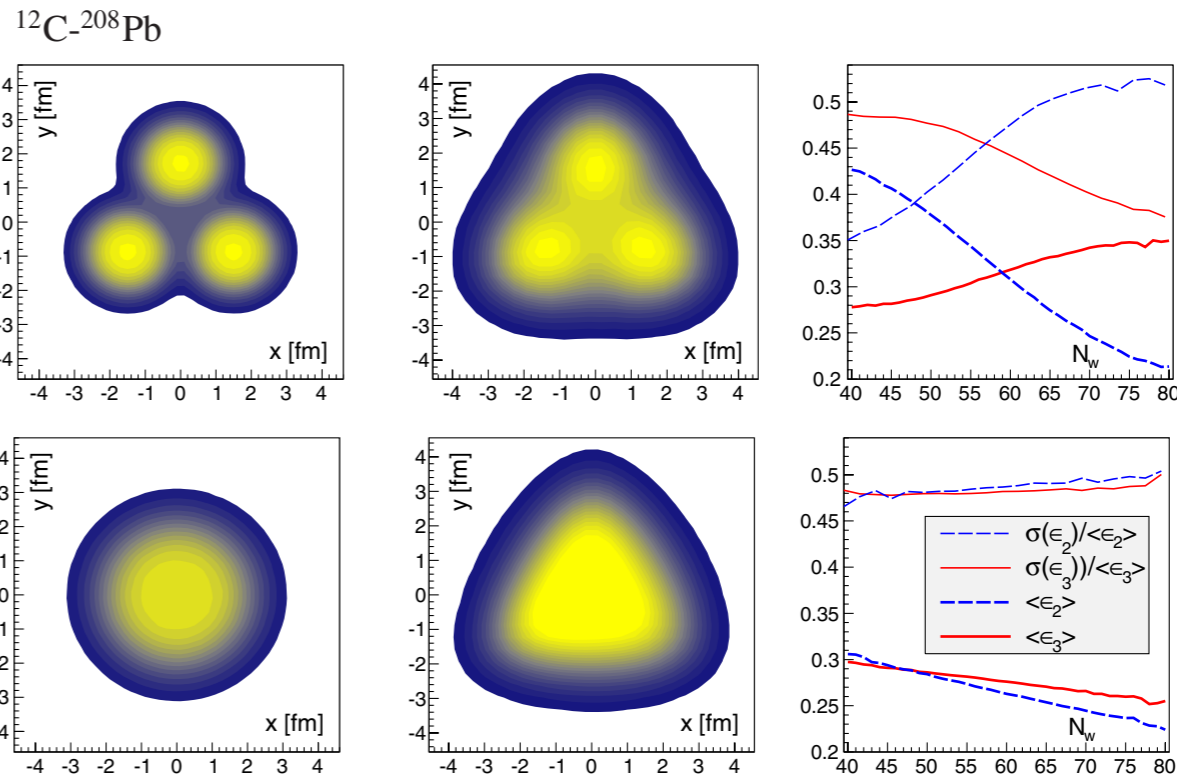
α -cluster结构在相对论重离子碰撞中的效应



α -cluster核与重核碰撞中的集体流(I)

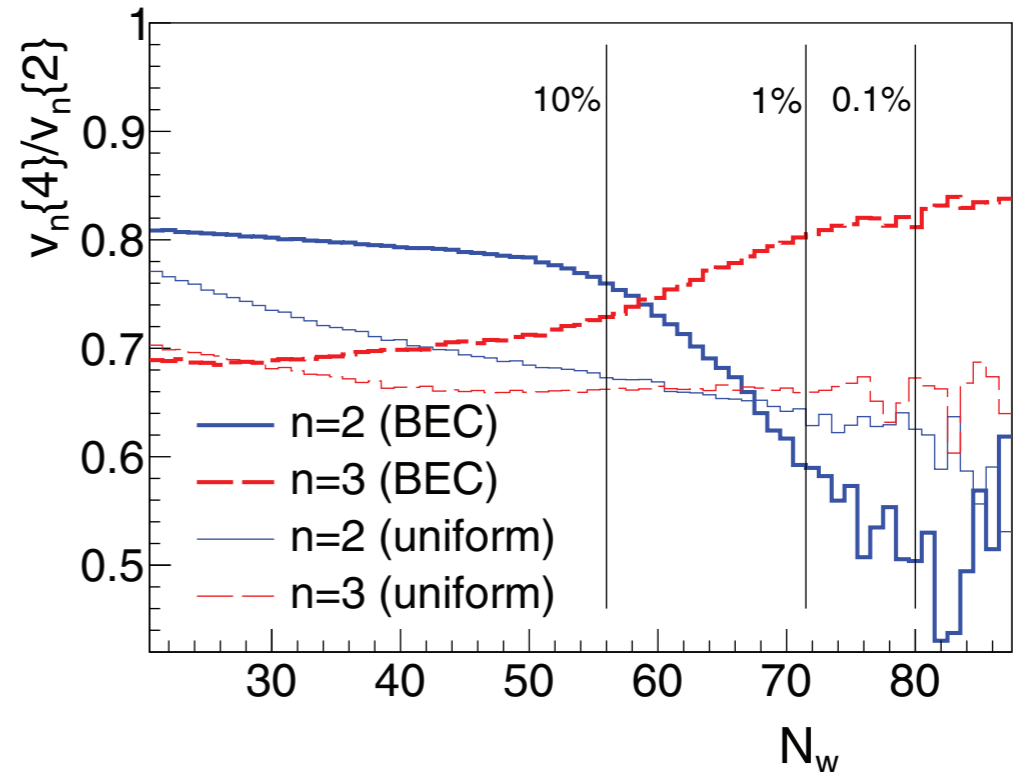
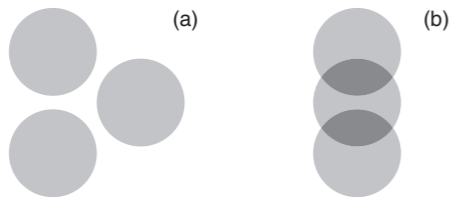


W. Broniowski, E. R. Arriola, PRL-112-112501



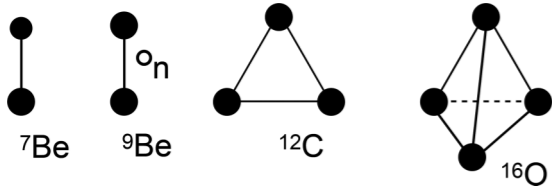
P. Bozek, W. Broniowski et al., PRC-90-064902

$$\frac{\epsilon_n\{4\}}{\epsilon_n\{2\}} \approx \frac{v_n\{4\}}{v_n\{2\}}$$





α -cluster核与重核碰撞中的集体流(II)



M. Rybczyński, M. Piotrowska, and W. Broniowski, Phys. Rev. C 97, 034912 (2018)

M. Rybczyński and W. Broniowski, Phys. Rev. C 100, 064912 (2019)

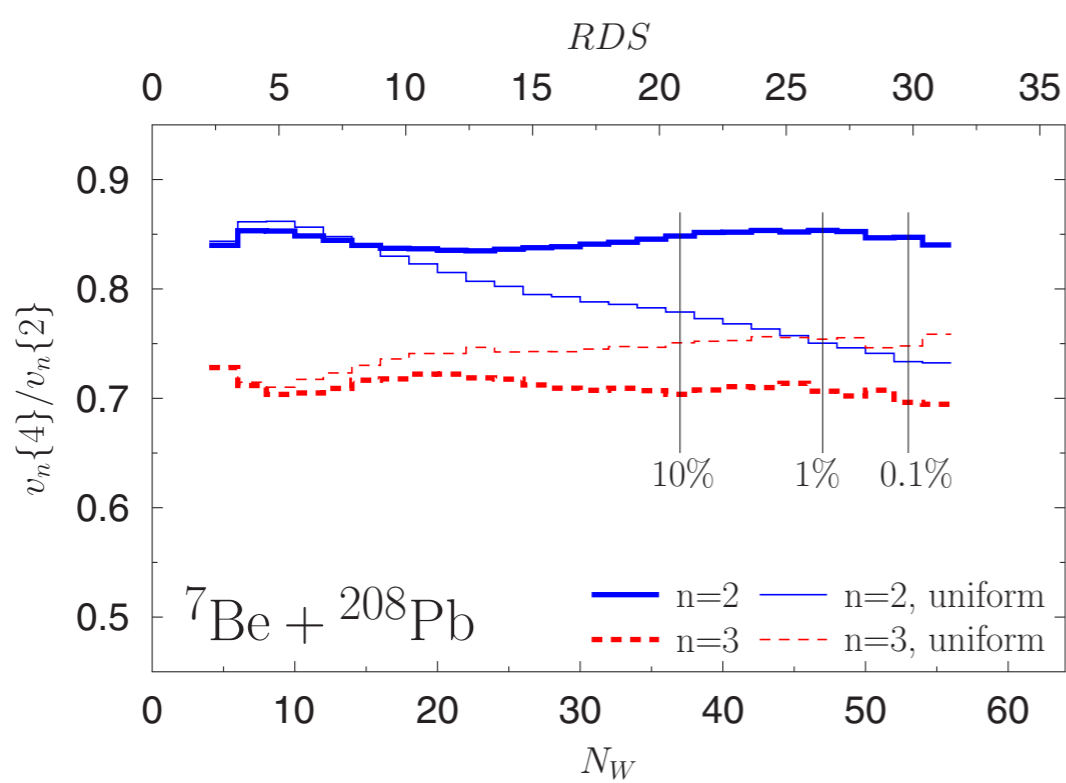


FIG. 4. Ratios of the four- to two-particle cumulants for ${}^7\text{Be} + {}^{208}\text{Pb}$ collisions, plotted as functions of the total number of the wounded nucleons. Clustered nuclei (thick lines) are compared with the case where the nucleons are distributed uniformly with the same one-body radial distributions (thin lines). The vertical lines indicate the multiplicity percentiles (centralities) corresponding to the indicated values of N_W . The upper horizontal axis shows the corresponding values of RDS of Eq. (4).

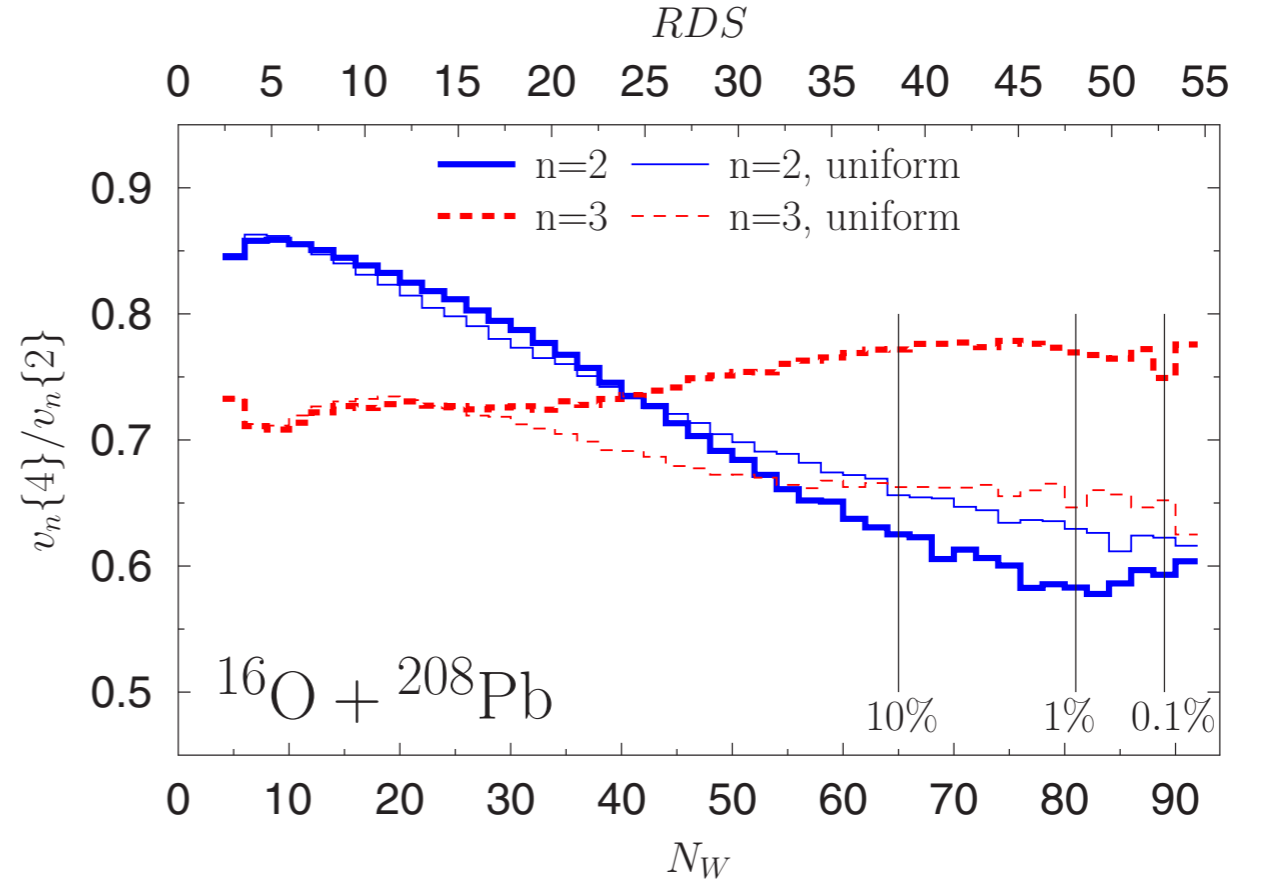
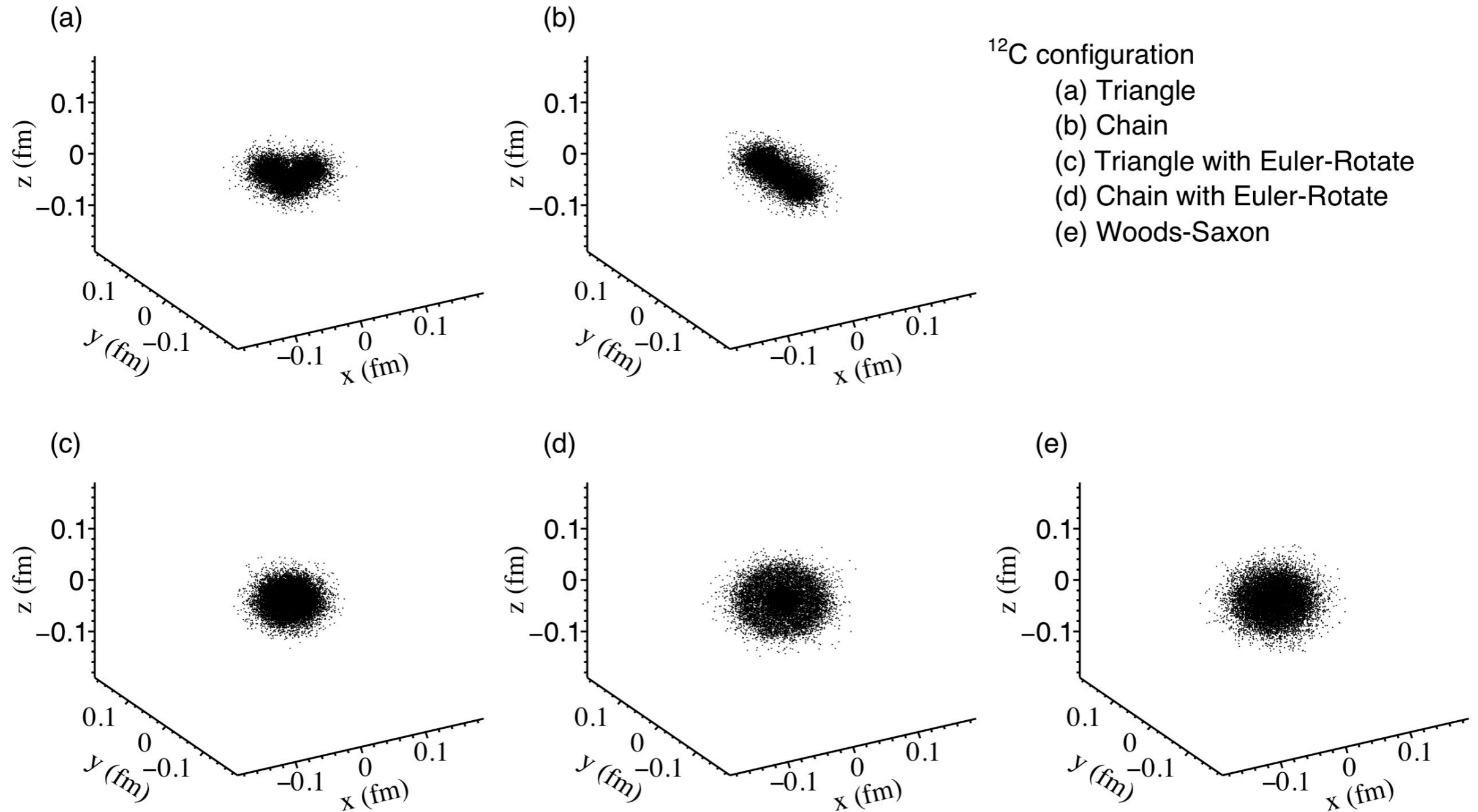


FIG. 7. The same as in Fig. 4 but for ${}^{16}\text{O} + {}^{208}\text{Pb}$ collisions.

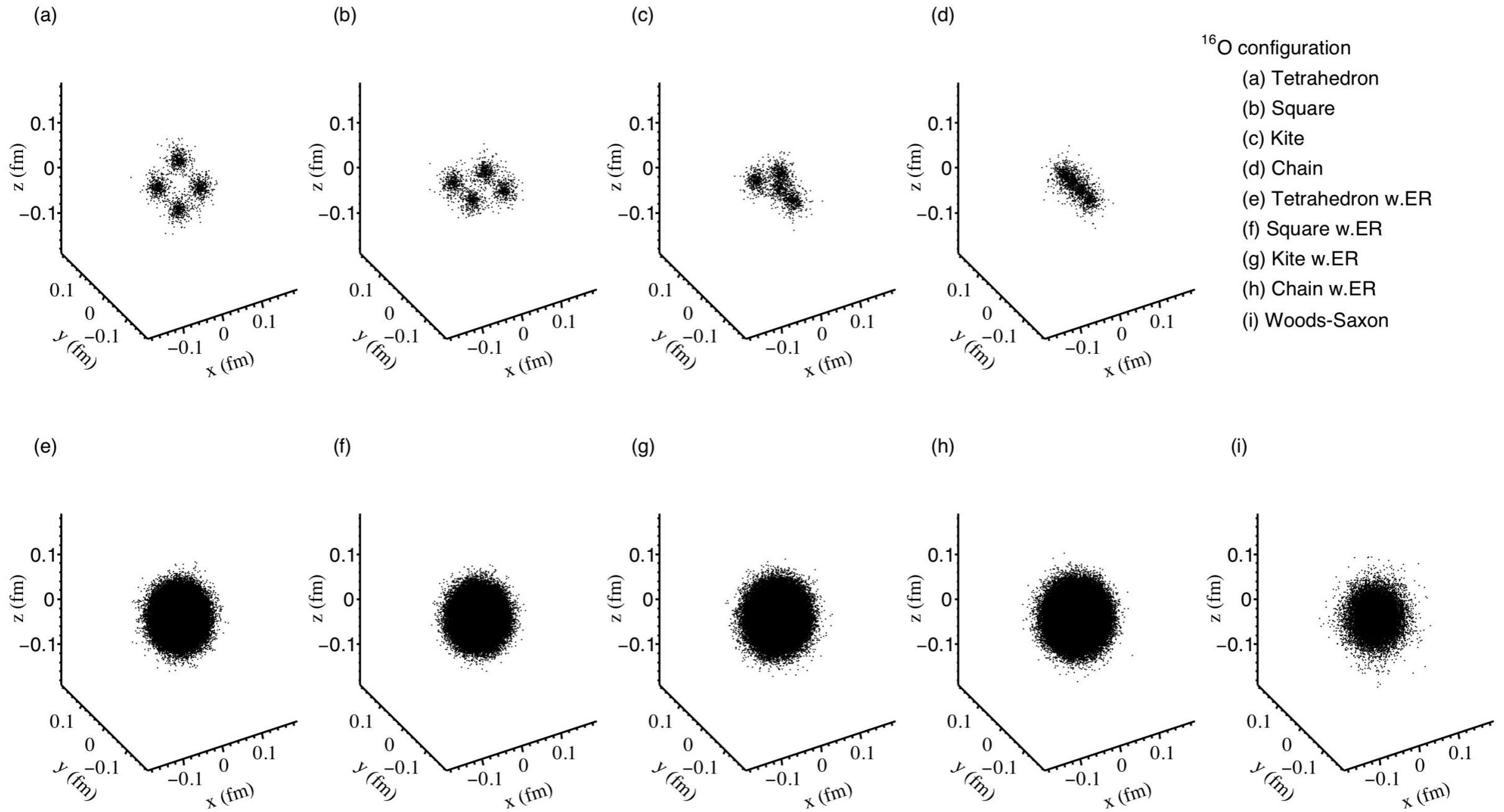


Initial nucleon distribution (^{12}C)





Initial nucleon distribution (^{16}O)

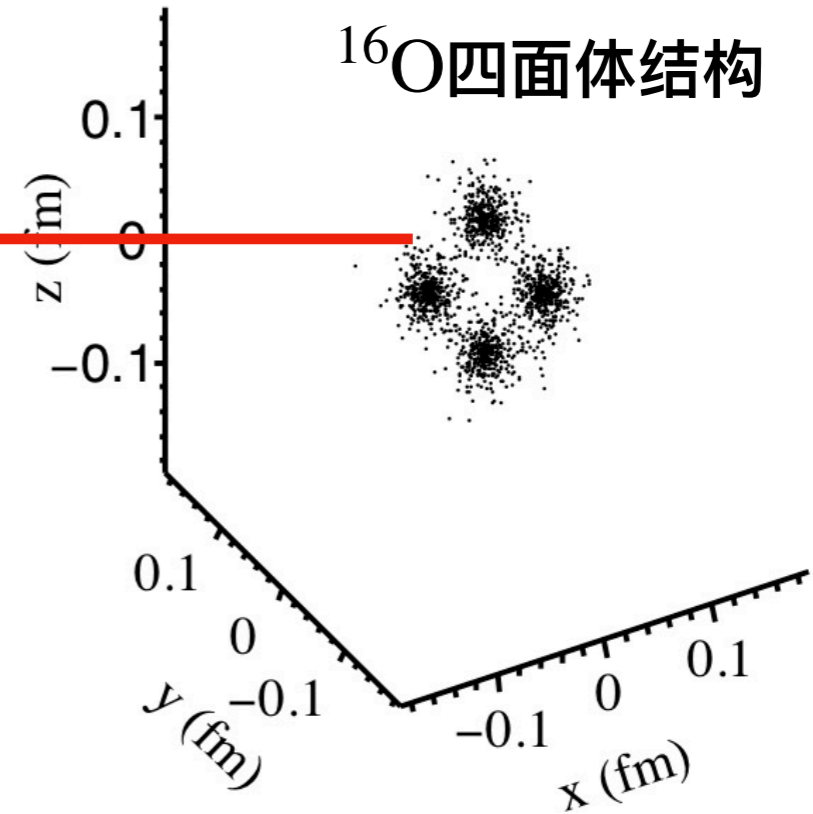
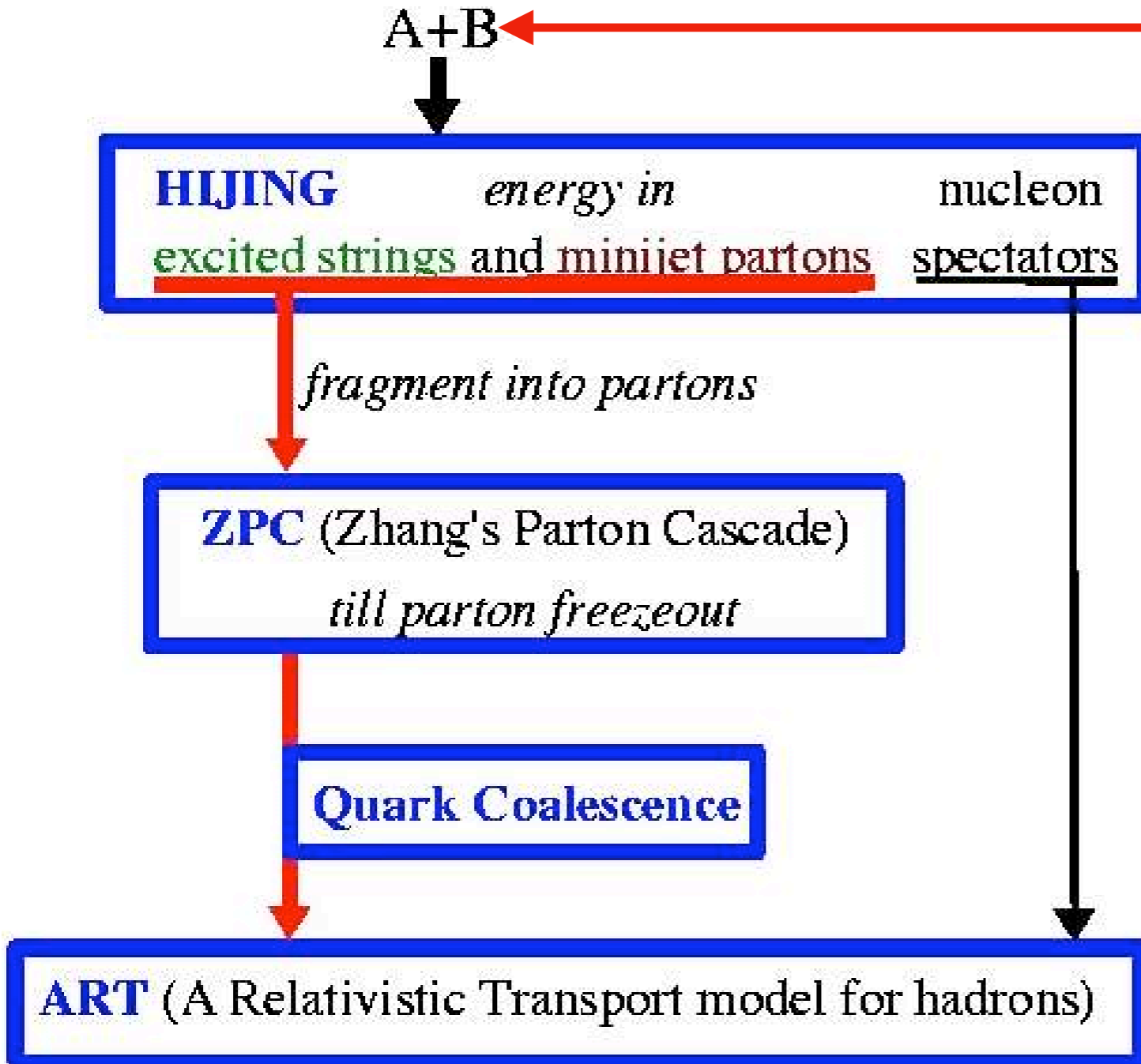




α -cluster核与重核碰撞中的集体流(III)

AMPT (a multi-phase transport model), Z. W. Lin, C. M. Ko, B. A. Li, S. Pal, PRC-72-064901(2005)

Structure of AMPT model with string melting



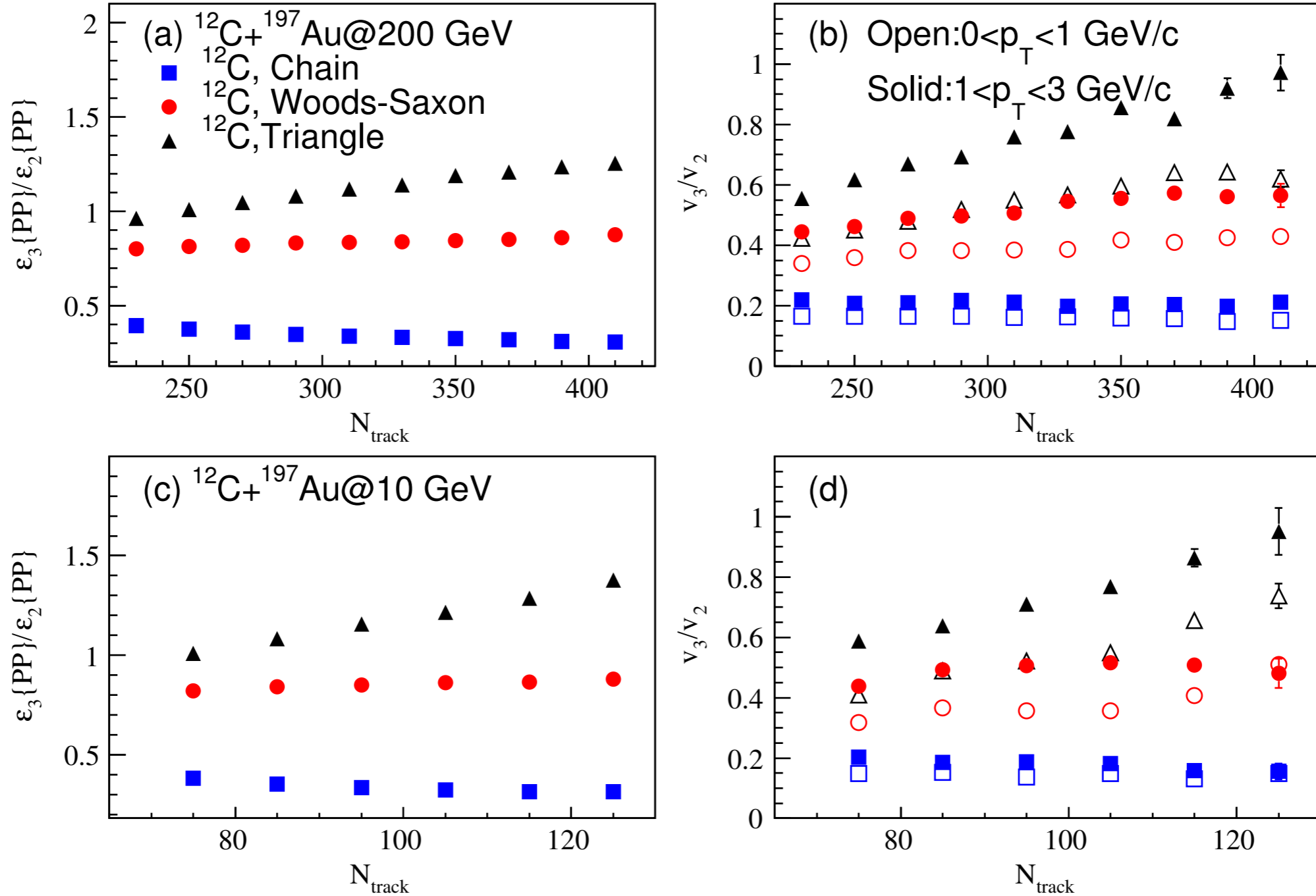
- (1) initial condition (HIJING);
- (2) parton cascade (ZPC);
- (3) hadronization;
- (4) hadronic rescattering (ART)

For high energy heavy ion collisions



α -cluster核与重核碰撞中的集体流(III)

S. Zhang, Y. G. Ma, et al., Phys. Rev. C 95, 064904 (2017); S. Zhang, Y.G. Ma et al., Eur. Phys. J. A (2018) 54

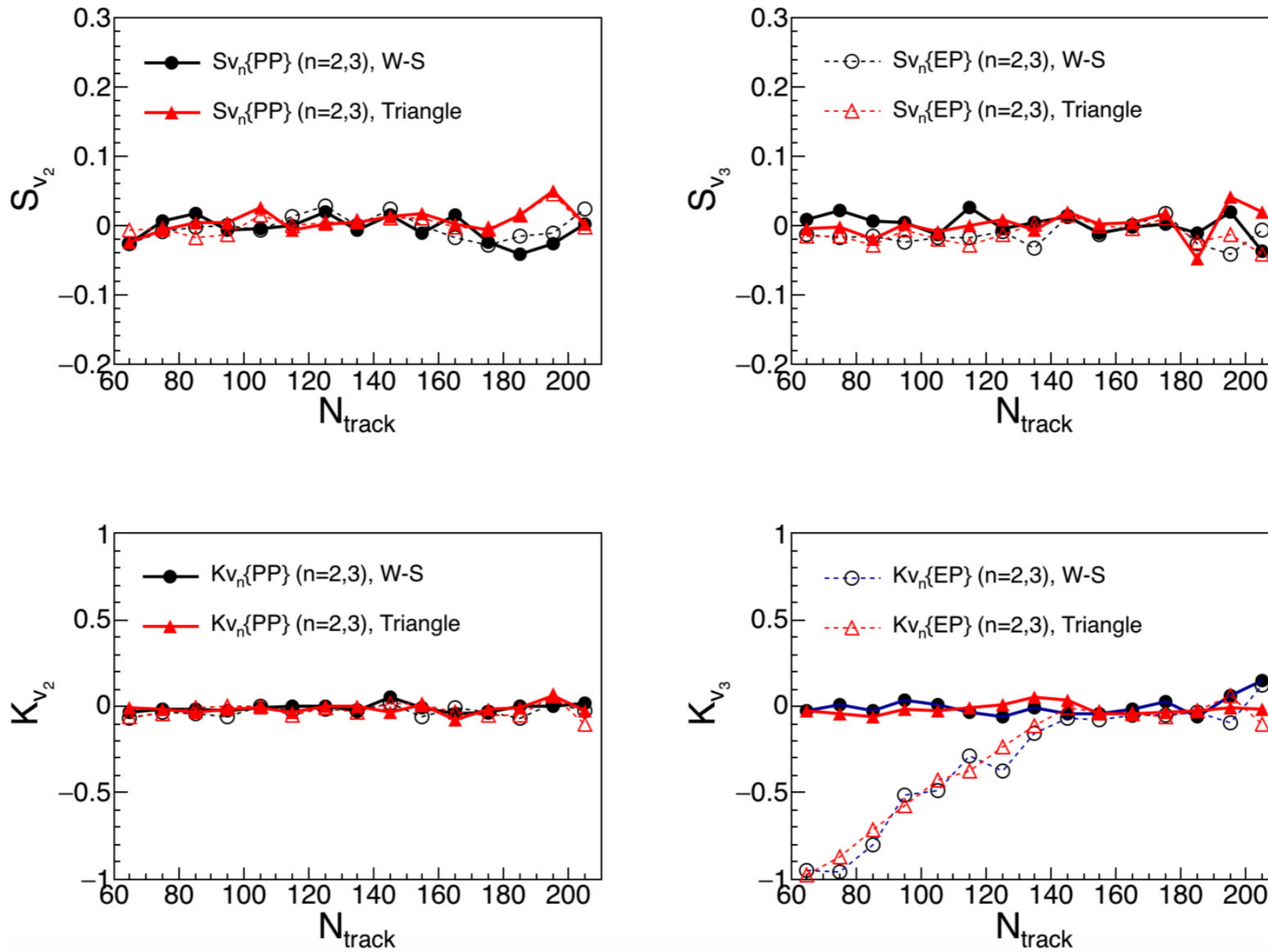


✓ The ratio keep flat tend with increasing of N_{track} for Woods-Saxon distribution and chain structure of ^{12}C

✓ The ratio increases with increasing of N_{track} for triangle structure.



$^{12}\text{C} + ^{197}\text{Au}$ 系统中集体流的涨落(I)



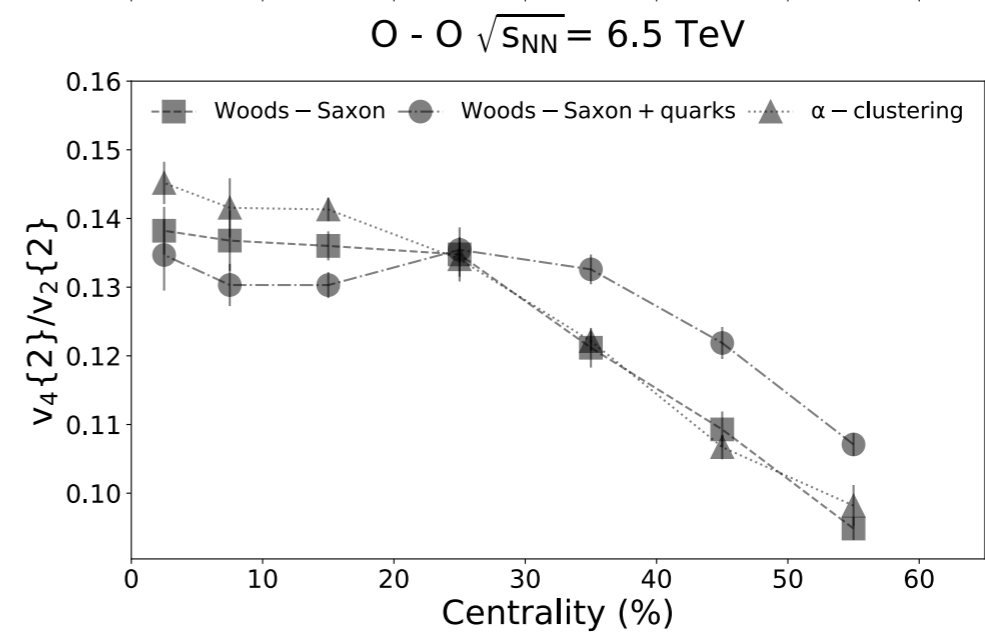
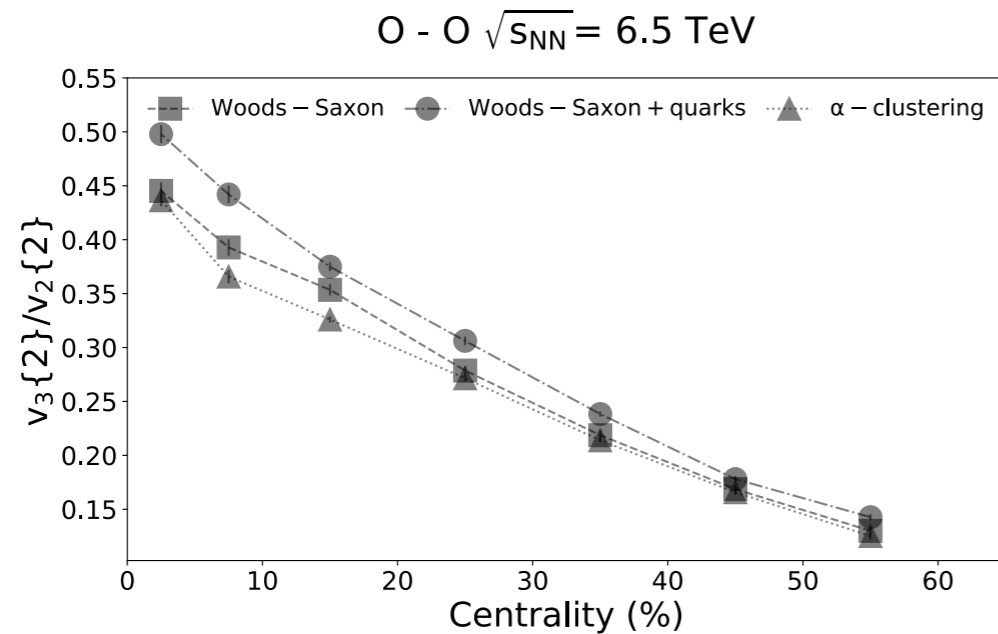
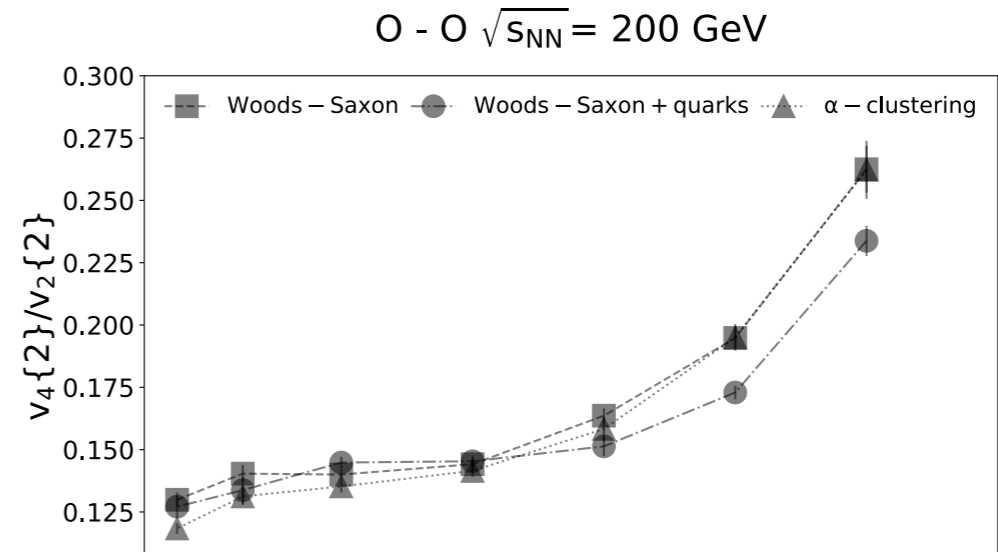
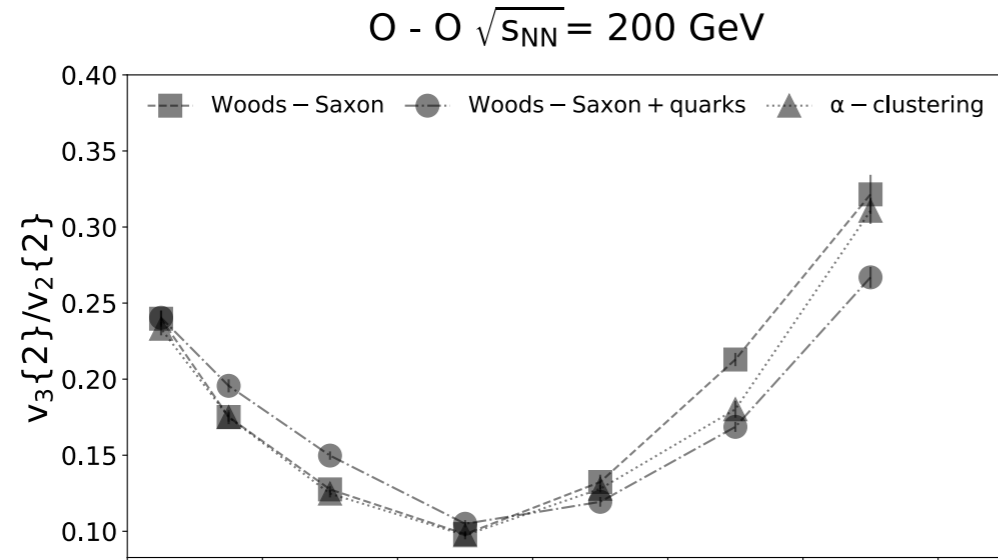
具有 α -cluster构型的情形，涨落的中心度依赖性明显不同于在WS情形

L. Ma, Y.G. Ma, S. Zhang, Phys. Rev. C **102**, 014910 (2020)



$^{12}\text{C} + ^{197}\text{Au}$ 系统中集体流的涨落(II)

N. Summerfield, B.-N. Lu, C. Plumberg, arXiv:2103.03345v1

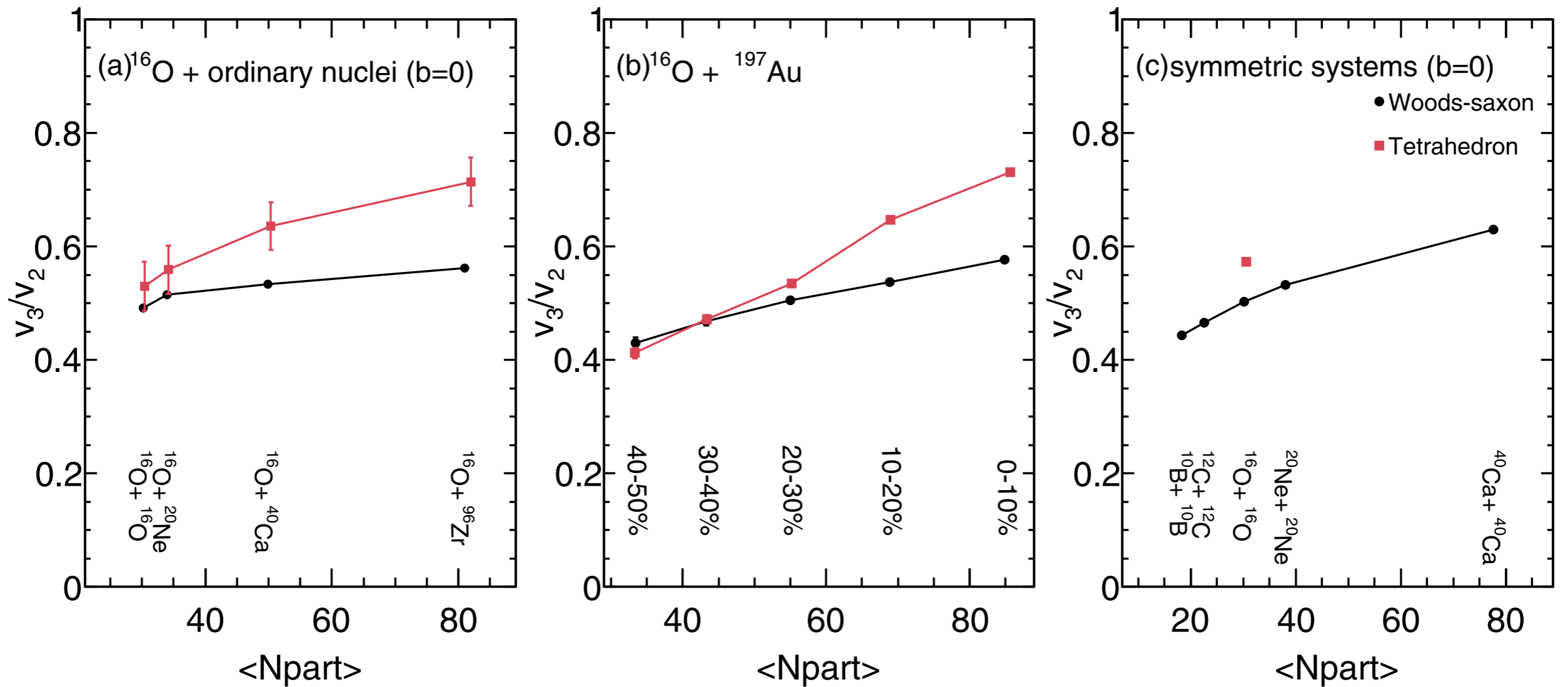


✓ iEBE-VISHNU package

✓ α -clustering suppresses $v_3\{2\}/v_2\{2\}$ and enhances $v_4\{2\}/v_2\{2\}$



利用系统扫描甄别 α -cluster结构



- ✓非对称系统扫描, v_3/v_2 两种构型具有明显的差别, WS构型非常平坦
- ✓ $^{16}\text{O} + ^{197}\text{Au}$ 中心度依赖, 高多重数下 v_3/v_2 的比, 两种构型具有明显的差别
- ✓对称系统扫描, 明显看到四面体构型的 $^{16}\text{O} + ^{16}\text{O}$ 系统系的 v_3/v_2 偏离系统学

Y.A. Li, S. Zhang, Y.G. Ma, Phys. Rev. C 102, 054907 (2020)

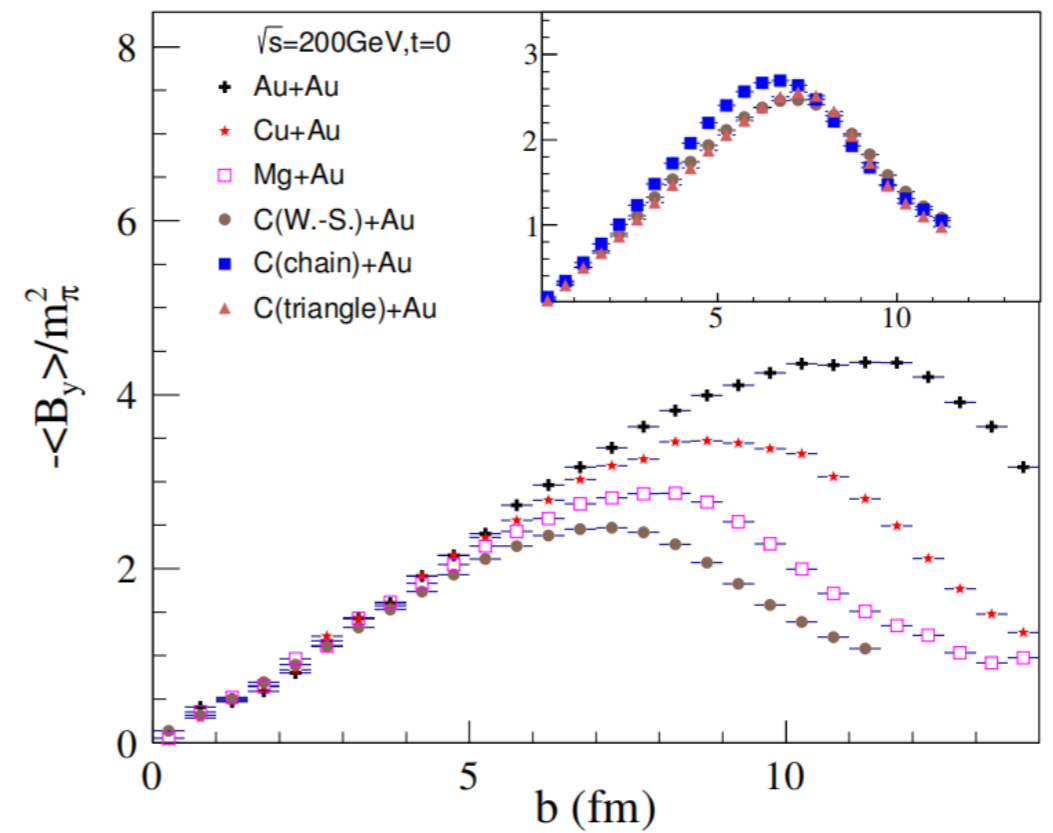
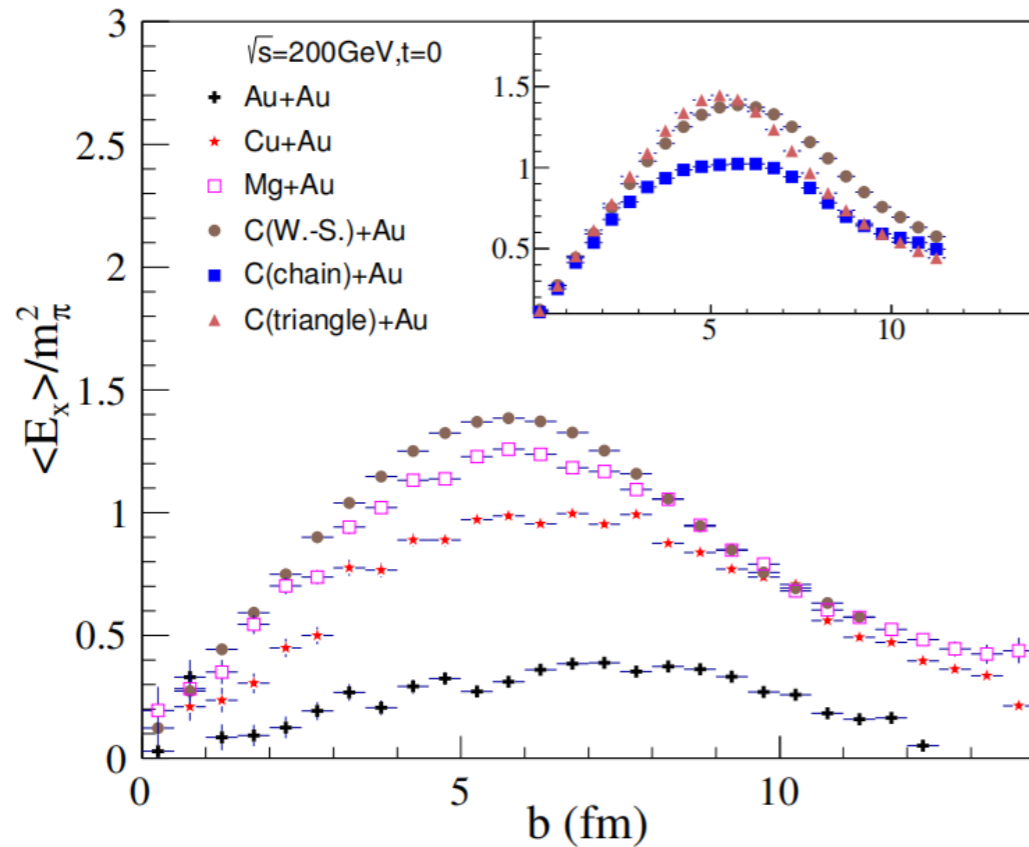
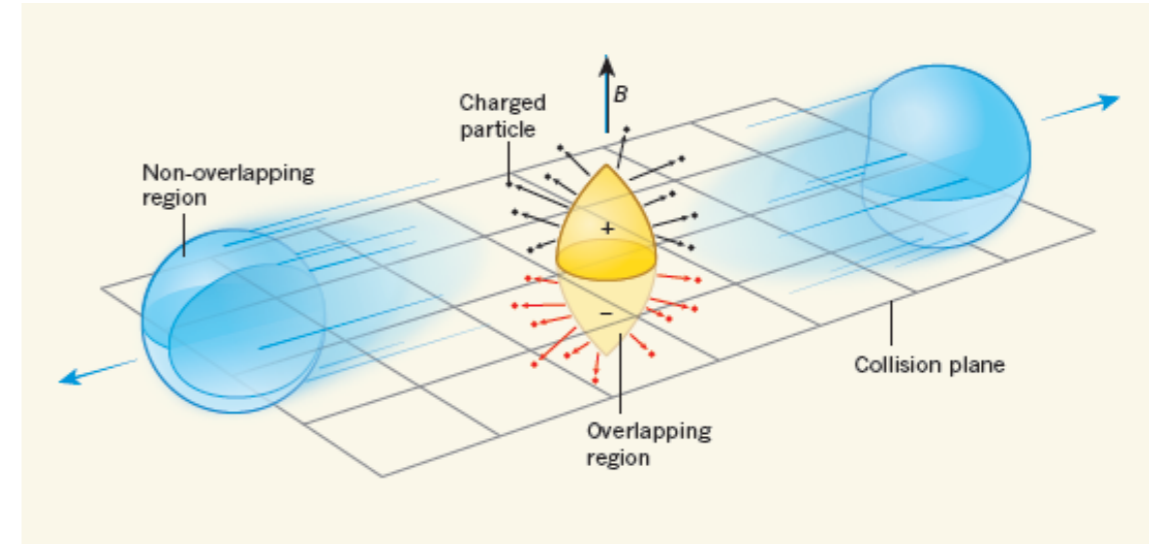
α -cluster结构核对电磁场影响

Li'enard-Wiechert potentials

Huang, (PRC) 85, 044907 (2012)

$$e\vec{E}(\vec{r}_i, t) = \frac{e^2}{4\pi} \sum_n Z_n \frac{1 - v_n^2}{(R_n - \vec{R}_n \cdot \vec{v}_n)^3} (\vec{R}_n - R_n v_n)$$

$$e\vec{B}(\vec{r}_i, t) = \frac{e^2}{4\pi} \sum_n Z_n \frac{1 - v_n^2}{(R_n - \vec{R}_n \cdot \vec{v}_n)^3} \vec{v}_n \times \vec{R}_n$$



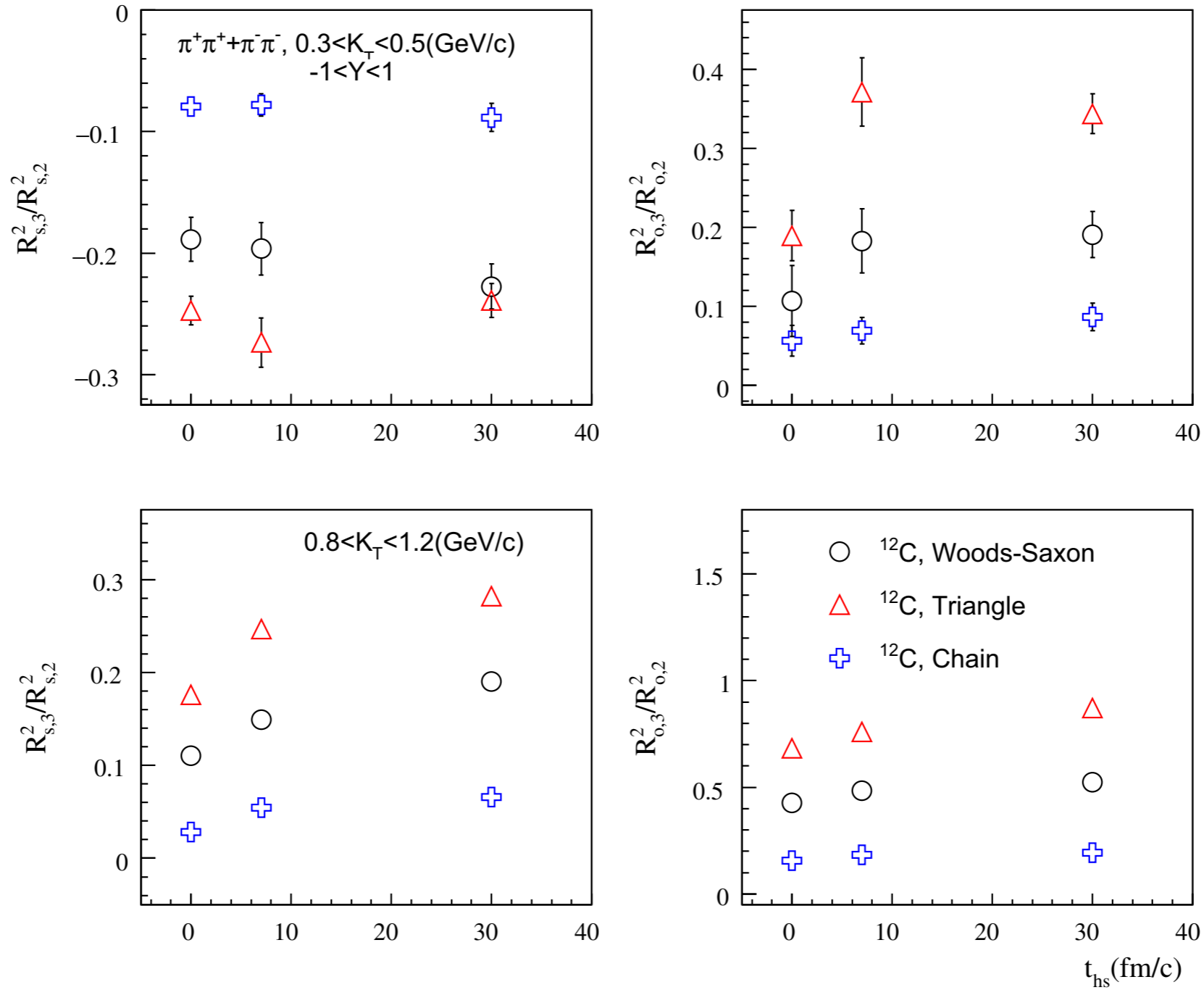
Y. L. Cheng (程艺琳), S. Zhang, Y. G. Ma, et al., Phys. Rev. C 99, 054906 (2019)

✓ α -cluster effect at semi-central collisions for chain structure



HBT关联半径

J.J. He, S. Zhang, Y.G. Ma, J.H. Chen, C. Zhong, Eur. Phys. J. A (2020) 56:52



α -cluster结构对HBT半径的比具有明显的效应



Forward-backward multiplicity correlations

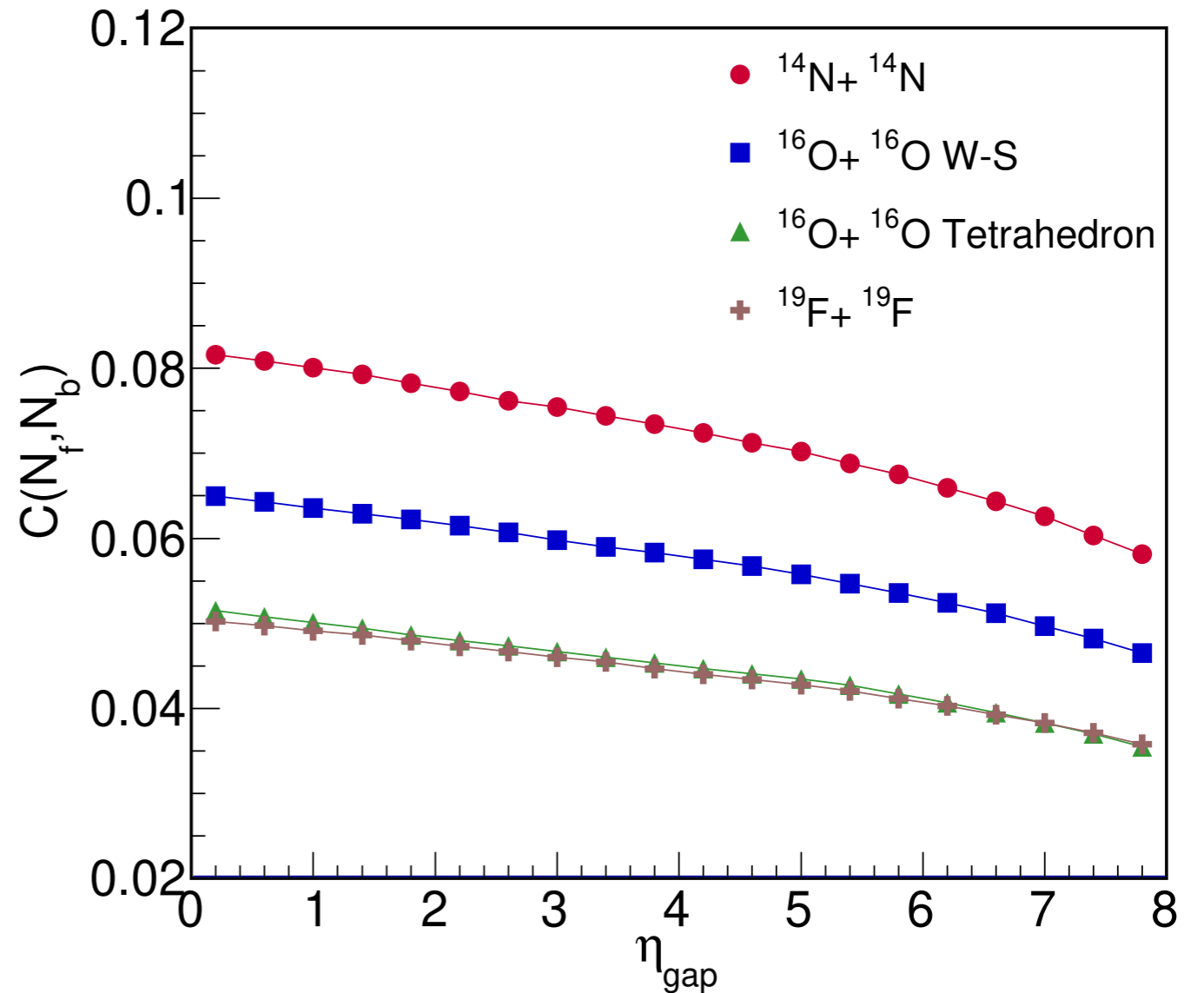
B. I. Abelev et al. (STAR Collaboration),
Phys. Rev. Lett. 103, 172301 (2009).

$$b_{corr} = \frac{\langle N_b N_f \rangle - \langle N_b \rangle \langle N_f \rangle}{\sqrt{\langle N_b^2 \rangle - \langle N_b \rangle^2} \sqrt{\langle N_f^2 \rangle - \langle N_f \rangle^2}} = \frac{D_{bf}^2}{D_{bb} D_{ff}}$$

M. Rohrmoser and W. Broniowski, Phys. Rev. C
101, 014907 (2020) ;

C. Pruneau, S. Gavin, and S. Voloshin, Phys. Rev.
C 66, 044904 (2002)

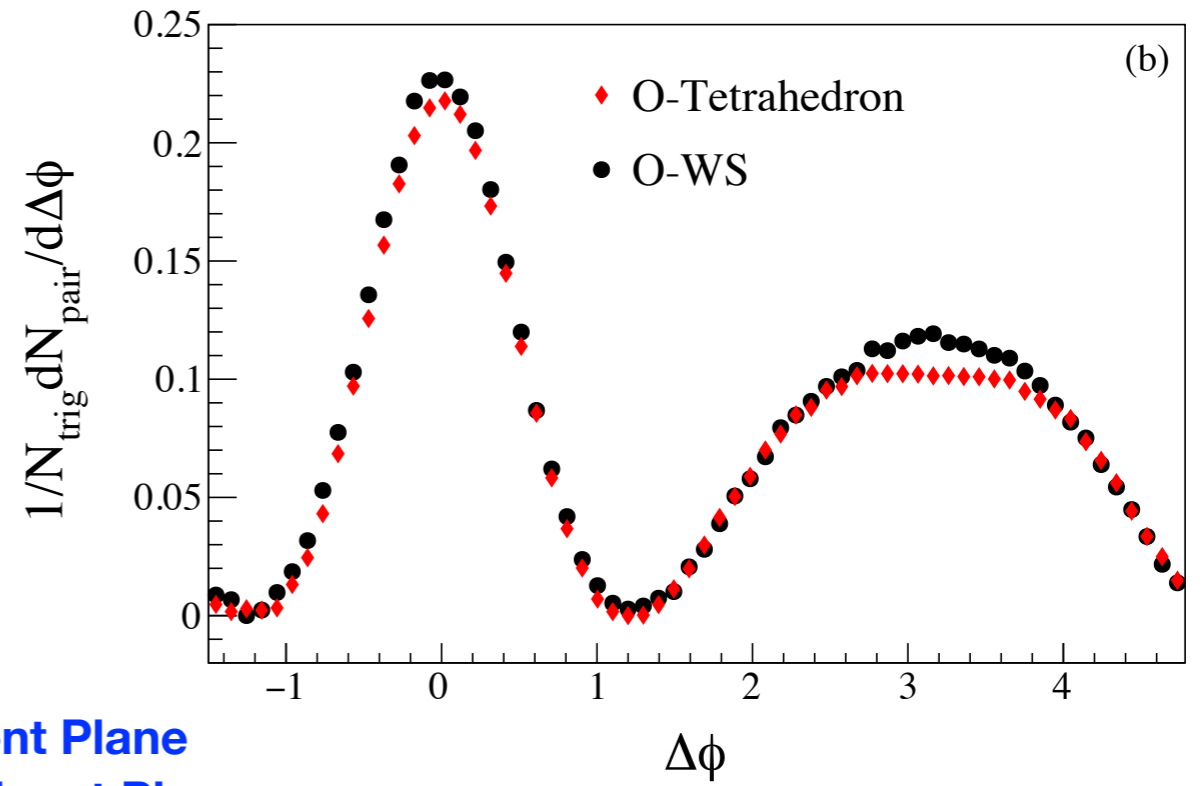
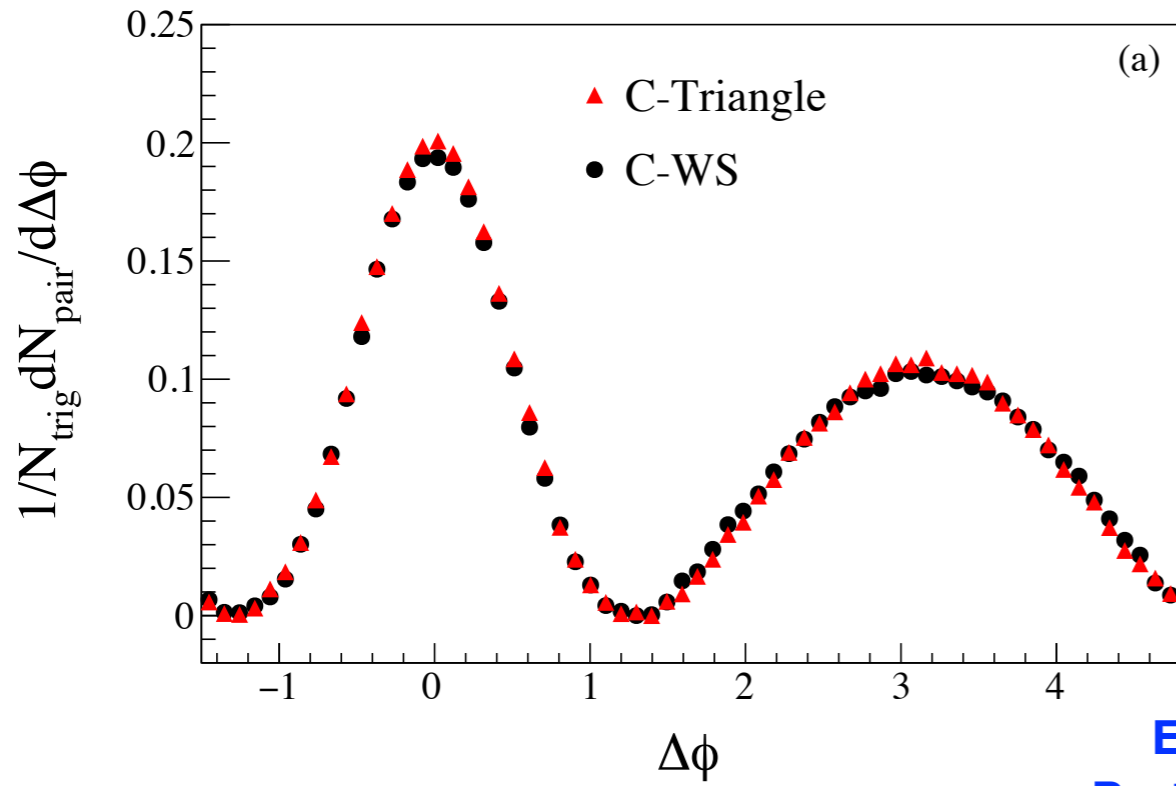
$$C(N_f, N_b) = \frac{\langle N_f N_b \rangle - \langle N_f \rangle \langle N_b \rangle}{\langle N_f \rangle \langle N_b \rangle}$$



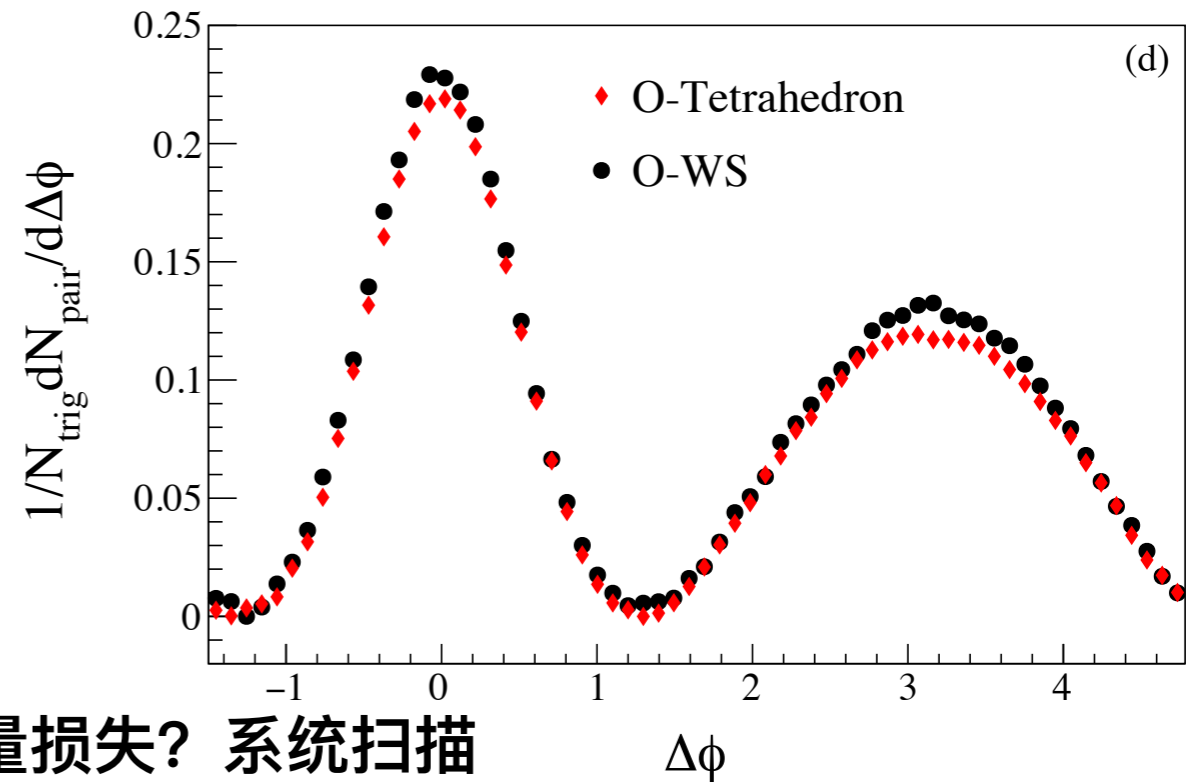
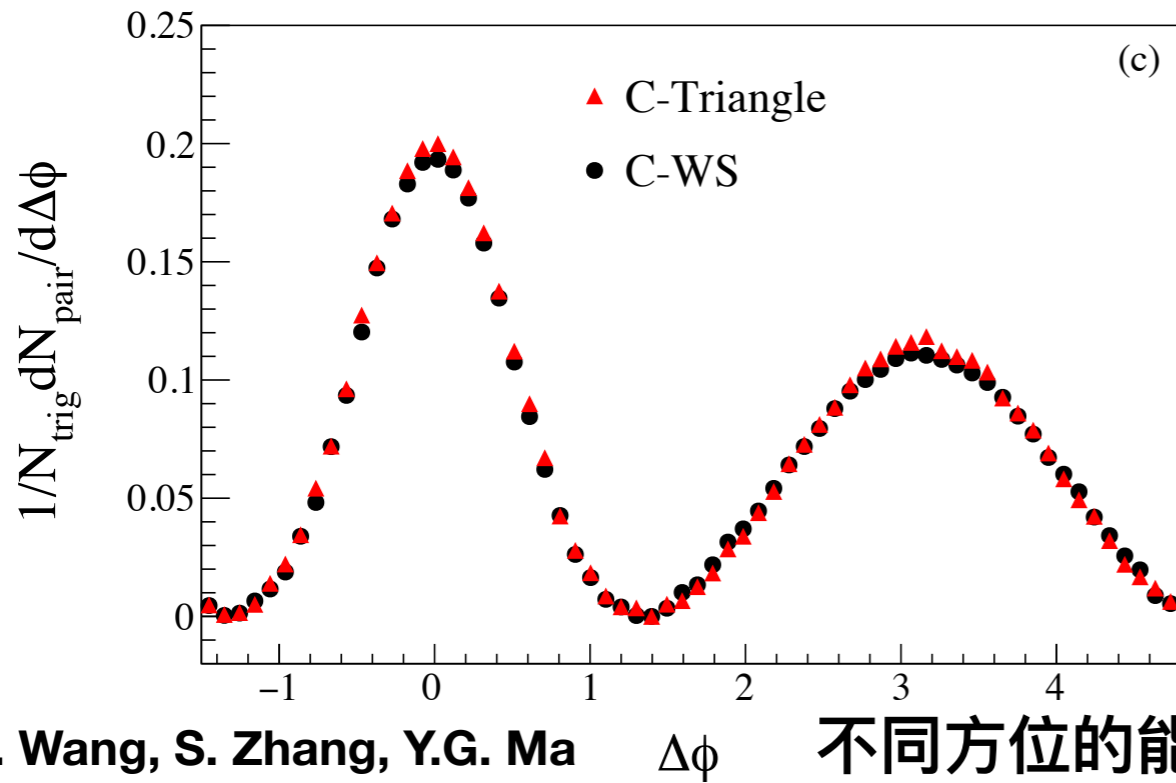
Y.A. Li, S. Zhang, Y.G. Ma, Submit to PRC



双强子方位角关联



Event Plane
Participant Plane



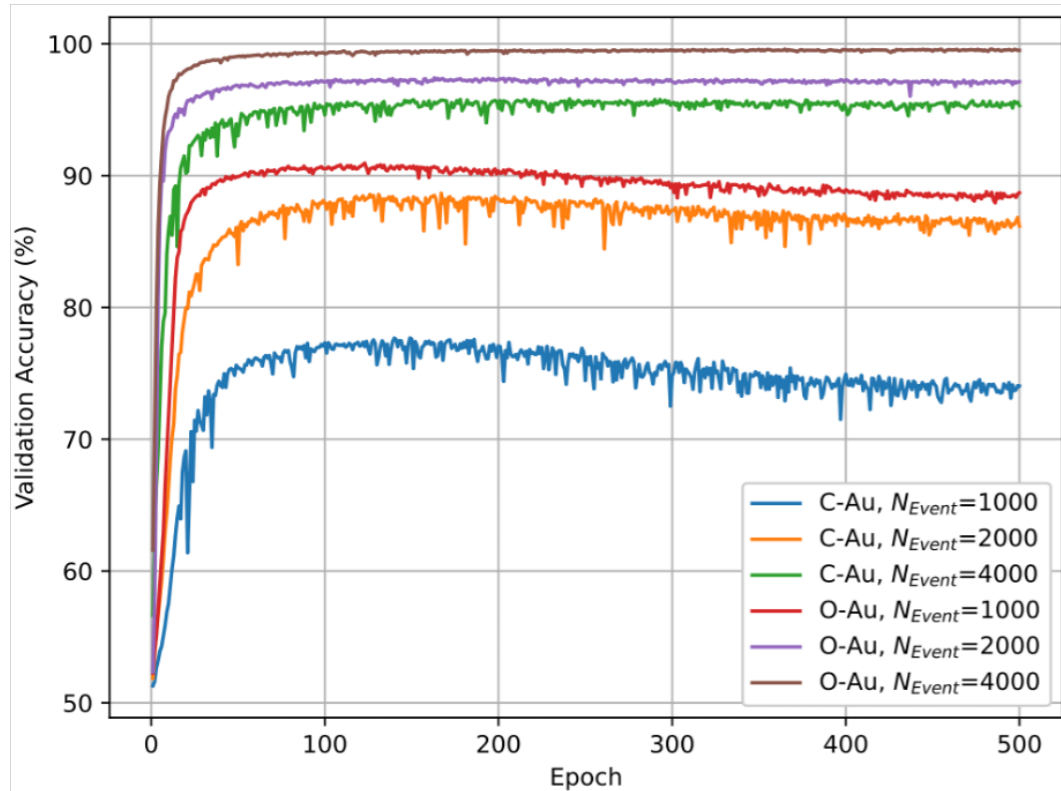
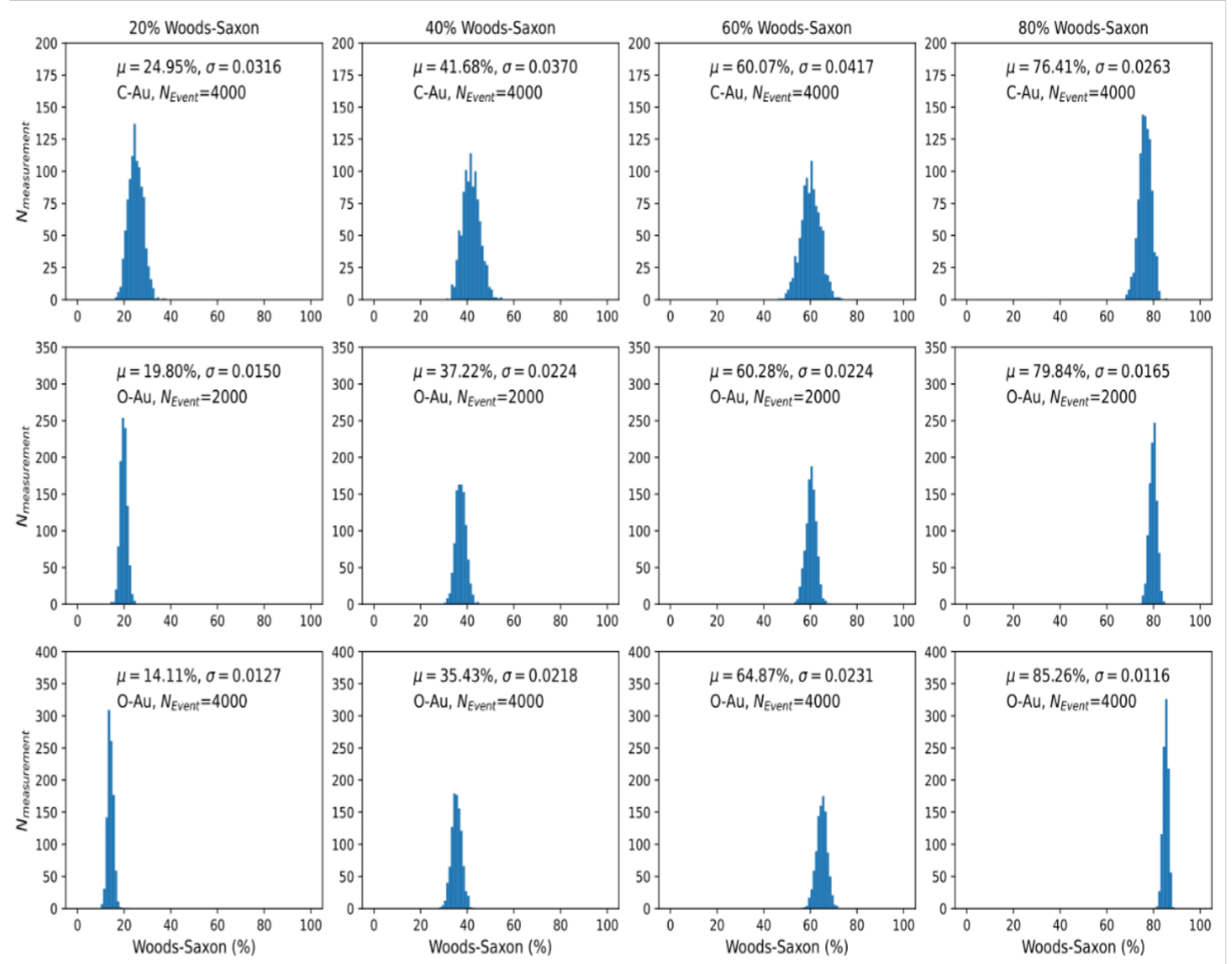
Y.Z. Wang, S. Zhang, Y.G. Ma

不同方位的能量损失? 系统扫描



神经网络识别初态结团结构

No.	Layer	Parameters
0	Input	$1 \times 64 \times 64$ tensor
1	Conv2D	6 kernels (3×3), BN, ReLU
2	MaxPool2D	2×2 kernel, stride 2
3	Conv2D	16 kernels (3×3), BN, ReLU
4	MaxPool2D	2×2 kernel, stride 2
5	Conv2D	32 kernels (3×3), BN, ReLU
6	MaxPool2D	2×2 kernel, stride 2
7	Conv2D	64 kernels (3×3), BN, ReLU
8	MaxPool2D	2×2 kernel, stride 2
9	Flatten	1024 neurons
10	BayesianFC	256 neurons, BN, ReLU
11	BayesianFC	64 neurons, BN, ReLU
12	BayesianFC+Softmax	2 outputs



- 对所有5000个样本预测的均值作为一次“测量”
- 1000次“测量”
- confidence threshold=0.999

J.J. He, W.B. He, Y.G. Ma, S. Zhang, Submit to PRC

S. H. Lim, et al., Phys. Rev. C **99**, 044904 (2019)

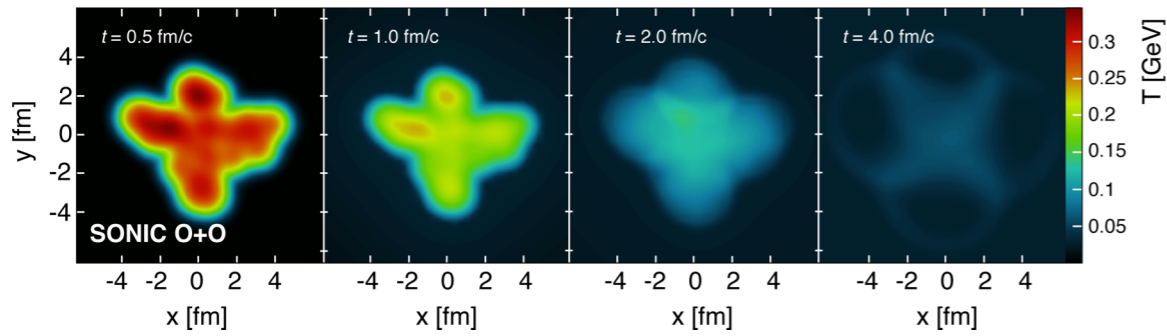


FIG. 3. An example of time evolution of a O+O event from SONIC; the color scale indicates the local temperature.

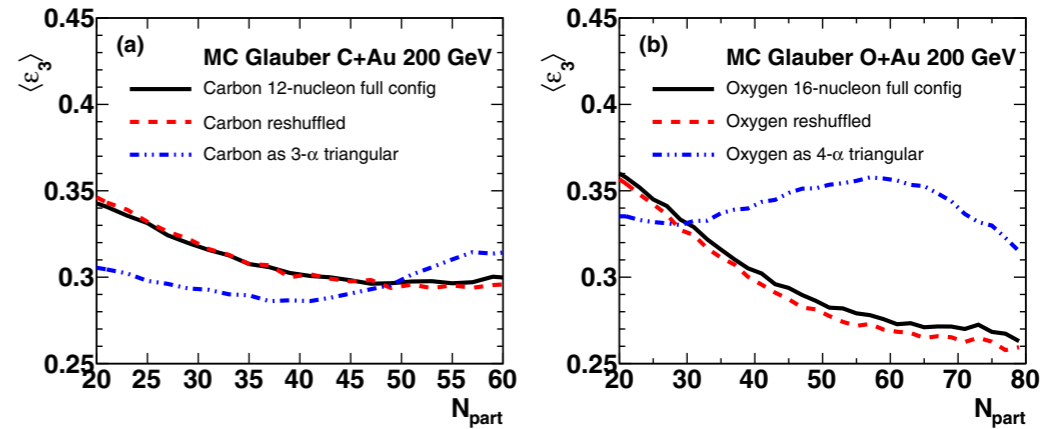


FIG. 12. Spatial triangularity (ϵ_3) is shown as a function of number of nucleon participants for C+Au (left) and O+Au (right) collisions at $\sqrt{s_{NN}} = 200$ GeV. Results are shown utilizing the full 12- and 16-nucleon configurations (black), the reshuffled nucleon configurations with no correlations (red), and with the toy geometry model involving simple triangles and tetrahedra (blue).

These results indicate that though there may be some α clustering in full configurations for carbon and oxygen, it is less than indicated in the simple toy geometry picture. This is not surprising as the toy model result is also seen to be reduced by additional spreading of the cluster geometry r_c and it is obvious that there would be event-by-event variations in the triangle configuration parameter L .



近些年部分（非特殊结构）小系统研究参考文献

- A. Huss, et al., Predicting parton energy loss in small collision systems, Phys. Rev. C **103**, 054903 (2021), OO collisions
- M. A. Braun and C. Pajares, Flow coefficients in O-O, Al-Al, and Cu-Cu collisions at 200 GeV in the fusing color string model, Phys. Rev. C **103**, 054902 (2021)
- B. Schenke, C. Shen, and P. Tribedy, Running the gamut of high energy nuclear collisions, Phys. Rev. C **102**, 044905 (2020), Pb + Pb, Xe + Xe, O + O (LHC); Au + Au, U + U, Ru + Ru, Zr + Zr, O + O (RHIC)
- R. Katz, System-size scan of D meson R_{AA} and v_n using PbPb, XeXe, ArAr, and OO collisions at energies available at the CERN Large Hadron Collider, Phys. Rev. C **102**, 041901(R) (2020)
- S. Huang, et al., Disentangling contributions to small-system collectivity via scans of light nucleus-nucleus collisions, Phys. Rev. C **101**, 021901(R) (2020)
- M. Sievert and J. Noronha-Hostler, CERN Large Hadron Collider system size scan predictions for PbPb, XeXe, ArAr, and OO with relativistic hydrodynamics, Phys. Rev. C **100**, 024904 (2019)
- M. Rybczynski and W. Broniowski, Glauber Monte Carlo predictions for ultrarelativistic collisions with ^{16}O , Phys. Rev. C **100**, 064912 (2019)
- J. L. Nagle and W. A. Zajc, Assessing saturation physics explanations of collectivity in small collision systems with the IP-JAZMA model, Phys. Rev. C **99**, 054908 (2019)



总结—— α -cluster结构效应

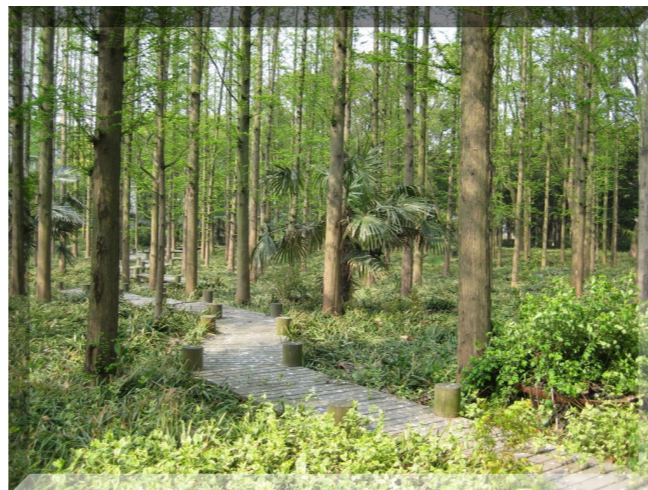
- 初始几何构型对集体流具有明显的影响
- 对称碰撞系统扫描建议作为探测手段之一
- 涨落和本征构型的影响在小系统中同时存在，高多重数中涨落影响变小
- 具有一定的模型依赖性，需要实验的检验，LHC或RHIC



相对论重离子碰撞中重 子相互作用

张松

复旦大学现代物理研究所





相互作用

Standard Model of Elementary Particles

three generations of matter (elementary fermions)			three generations of antimatter (elementary antifermions)			interactions / force carriers (elementary bosons)			
I	II	III	I	II	III				
mass $\approx 2.2 \text{ MeV}/c^2$ charge $\frac{2}{3}$ spin $\frac{1}{2}$ u up	mass $\approx 1.28 \text{ GeV}/c^2$ charge $\frac{2}{3}$ spin $\frac{1}{2}$ c charm	mass $\approx 173.1 \text{ GeV}/c^2$ charge $\frac{2}{3}$ spin $\frac{1}{2}$ t top	mass $\approx 2.2 \text{ MeV}/c^2$ charge $-\frac{2}{3}$ spin $\frac{1}{2}$ \bar{u} antiup	mass $\approx 1.28 \text{ GeV}/c^2$ charge $-\frac{2}{3}$ spin $\frac{1}{2}$ \bar{c} anticharm	mass $\approx 173.1 \text{ GeV}/c^2$ charge $-\frac{2}{3}$ spin $\frac{1}{2}$ \bar{t} antitop	0 0 1 g gluon	mass $\approx 124.97 \text{ GeV}/c^2$ 0 0 0 H higgs		
QUARKS	mass $\approx 4.7 \text{ MeV}/c^2$ charge $-\frac{1}{3}$ spin $\frac{1}{2}$ d down	mass $\approx 96 \text{ MeV}/c^2$ charge $-\frac{1}{3}$ spin $\frac{1}{2}$ s strange	mass $\approx 4.18 \text{ GeV}/c^2$ charge $-\frac{1}{3}$ spin $\frac{1}{2}$ b bottom	mass $\approx 4.7 \text{ MeV}/c^2$ charge $\frac{1}{3}$ spin $\frac{1}{2}$ \bar{d} antidown	mass $\approx 96 \text{ MeV}/c^2$ charge $\frac{1}{3}$ spin $\frac{1}{2}$ \bar{s} antistrange	mass $\approx 4.18 \text{ GeV}/c^2$ charge $\frac{1}{3}$ spin $\frac{1}{2}$ \bar{b} antibottom	0 0 1 γ photon	GAUGE BOSONS VECTOR BOSONS	SCALAR BOSONS
	mass $\approx 0.511 \text{ MeV}/c^2$ charge -1 spin $\frac{1}{2}$ e electron	mass $\approx 105.66 \text{ MeV}/c^2$ charge -1 spin $\frac{1}{2}$ μ muon	mass $\approx 1.7768 \text{ GeV}/c^2$ charge -1 spin $\frac{1}{2}$ τ tau	mass $\approx 0.511 \text{ MeV}/c^2$ charge 1 spin $\frac{1}{2}$ e^+ positron	mass $\approx 105.66 \text{ MeV}/c^2$ charge 1 spin $\frac{1}{2}$ $\bar{\mu}$ antimuon	mass $\approx 1.7768 \text{ GeV}/c^2$ charge 1 spin $\frac{1}{2}$ $\bar{\tau}$ antitau	mass $\approx 91.19 \text{ GeV}/c^2$ 0 1 1 Z Z^0 boson		
LEPTONS	mass $< 2.2 \text{ eV}/c^2$ 0 spin $\frac{1}{2}$ ν_e electron neutrino	mass $< 0.17 \text{ MeV}/c^2$ 0 spin $\frac{1}{2}$ ν_μ muon neutrino	mass $< 18.2 \text{ MeV}/c^2$ 0 spin $\frac{1}{2}$ ν_τ tau neutrino	mass $< 2.2 \text{ eV}/c^2$ 0 spin $\frac{1}{2}$ $\bar{\nu}_e$ electron antineutrino	mass $< 0.17 \text{ MeV}/c^2$ 0 spin $\frac{1}{2}$ $\bar{\nu}_\mu$ muon antineutrino	mass $< 18.2 \text{ MeV}/c^2$ 0 spin $\frac{1}{2}$ $\bar{\nu}_\tau$ tau antineutrino	mass $\approx 80.39 \text{ GeV}/c^2$ 1 1 1 W^+ W^+ boson	mass $\approx 80.39 \text{ GeV}/c^2$ -1 1 1 W^- W^- boson	

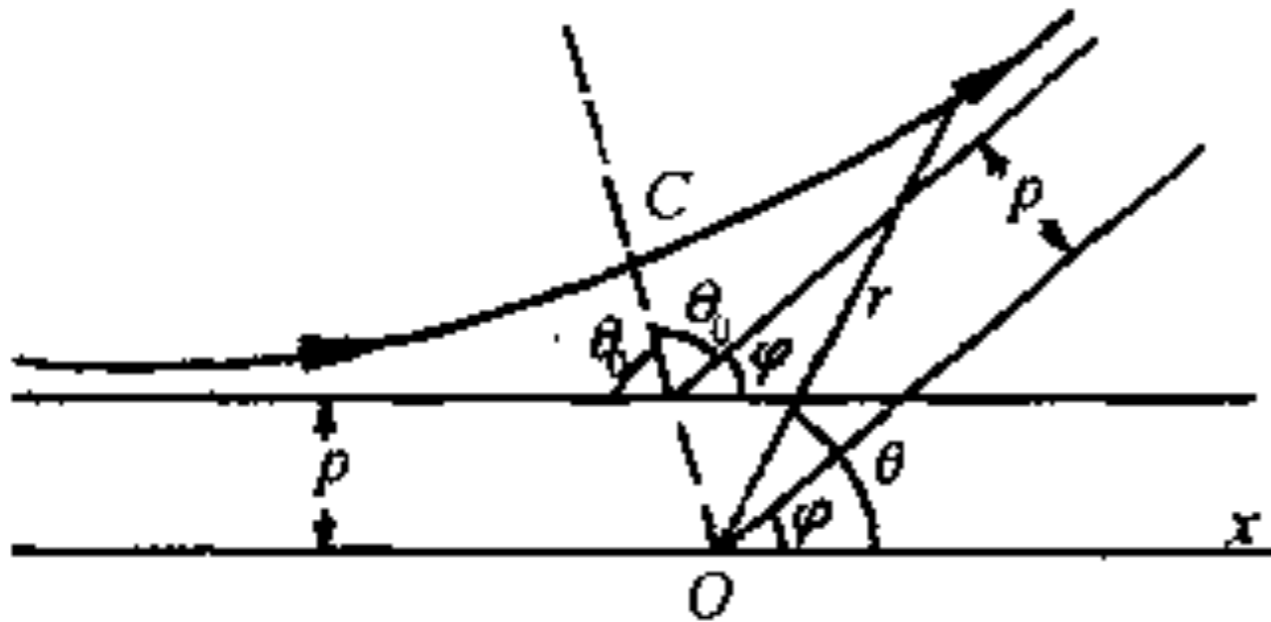
强相互作用, 电磁和弱相互作用、引力相互作用



强子及其相互作用

- 强子
 - ✓ 介子：两个组分夸克， π 介子、K介子
 - ✓ 中子：三个组分夸克，质子p、中子n、 Λ 超子
- 强子相互作用
 - ✓ 核物理研究中重点考虑：电弱相互作用、强相互作用
 - ✓ 例如：p-n, n-n, p- Λ
 - ✓ 意义：系统演化（寿命、尺寸），物质构成

经典散射

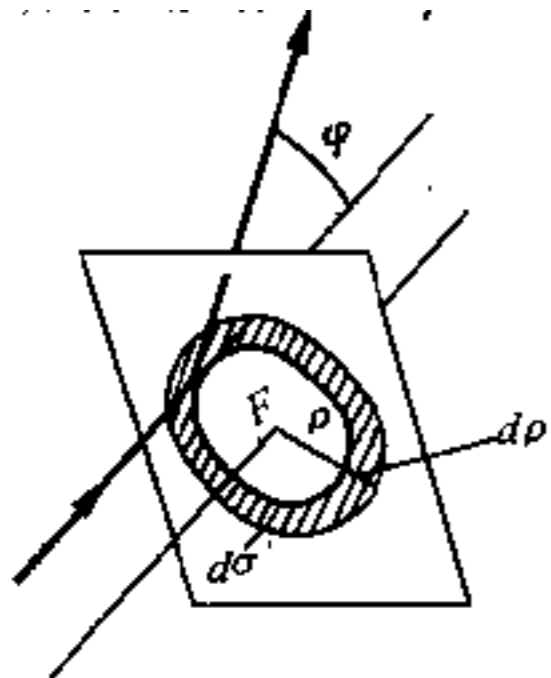


中心势场散射，O代表原子核（力心）的位置，质点轨道的对称轴是通过力心O及其最近距离点C的直线OC

质点 α 的能量方程

$$\frac{1}{2}m(\dot{r}^2 + r^2\dot{\theta}^2) + \frac{k'}{r} = E$$

质点 α 的瞄准距离 ρ 和质点 α 飞过力心后所发生的偏转角 φ 之间的关系： $\rho = \frac{k'}{mv_\infty^2} \text{ctg} \frac{\varphi}{2}$



n : 单位时间内通过垂直于粒子束的单位截面积的质点数

dN : 单位时间内在 φ 和 $\varphi + d\varphi$ 角度内所散射的质点数

显然 $d\sigma = \frac{dN}{n}$ 具有面积量纲，称为

散射截面

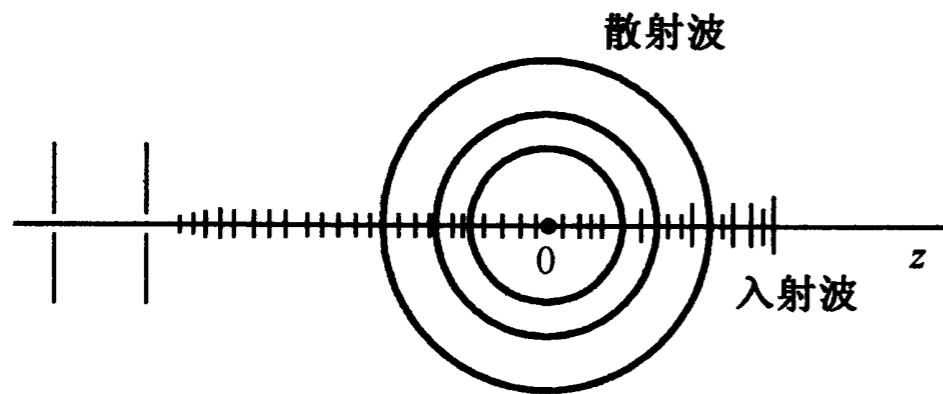
$$dN = 2\pi\rho d\rho \cdot n$$

$$d\sigma = 2\pi\rho d\rho$$

$$= -2\pi\rho(\varphi) \frac{d\rho(\varphi)}{d\varphi} d\varphi$$

$$= \frac{1}{4} \left(\frac{k'}{mv_\infty^2} \right)^2 \frac{2\pi \sin \varphi}{\sin^4 \left(\frac{\varphi}{2} \right)} d\varphi$$

量子散射



入射粒子波束可近似用平面波描述: $\psi_i = e^{ikz}$

波函数在 $z \rightarrow \infty$ 时的渐近行为: $\psi \xrightarrow{z \rightarrow \infty} \exp(ikz) + f(\theta) \frac{\exp(ikr)}{r}$

入射粒子流密度: $j_i = \hbar k / \mu$

散射粒子流密度: $j_s = \frac{\hbar k}{\mu} |f(\theta)|^2 / r^2$

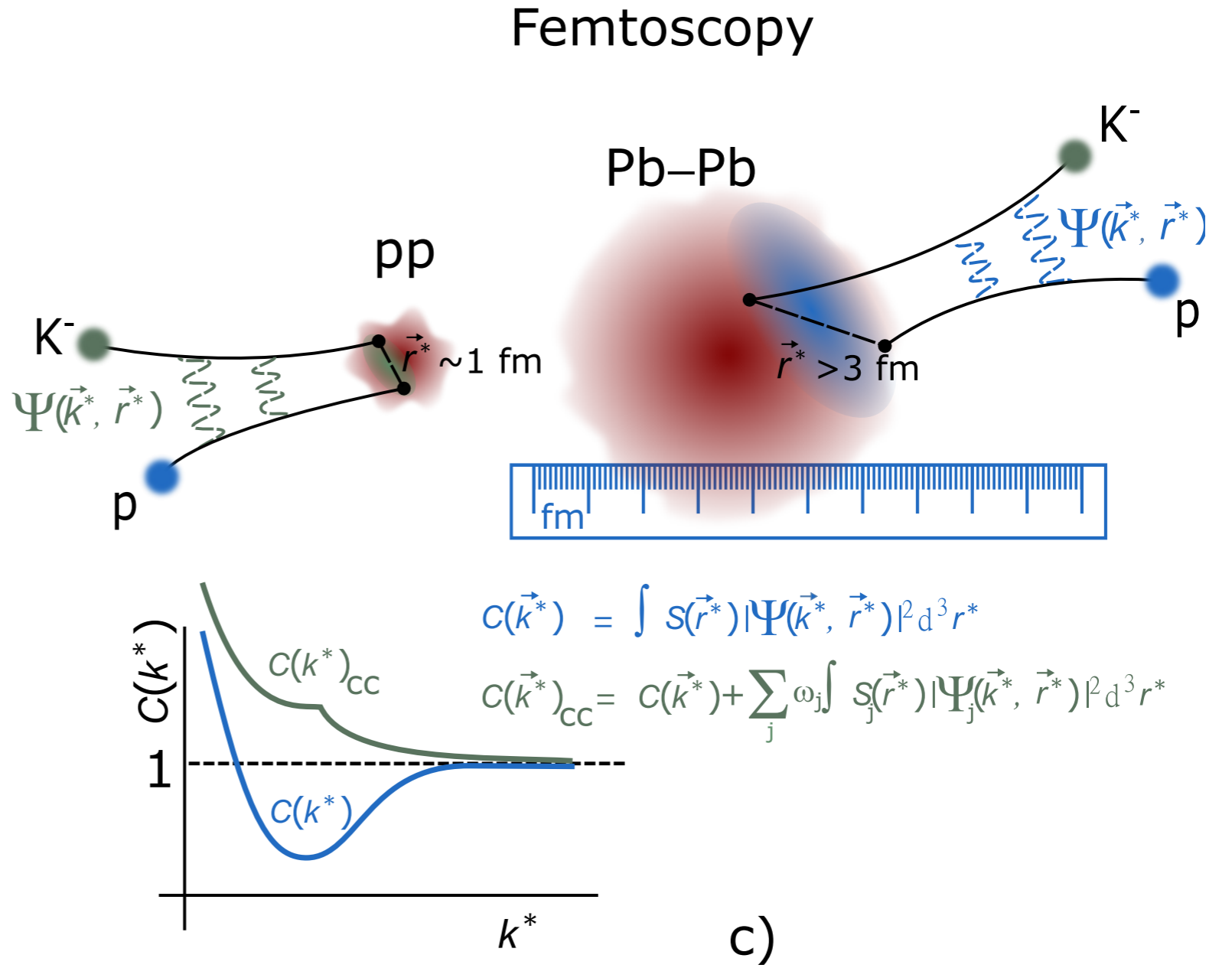
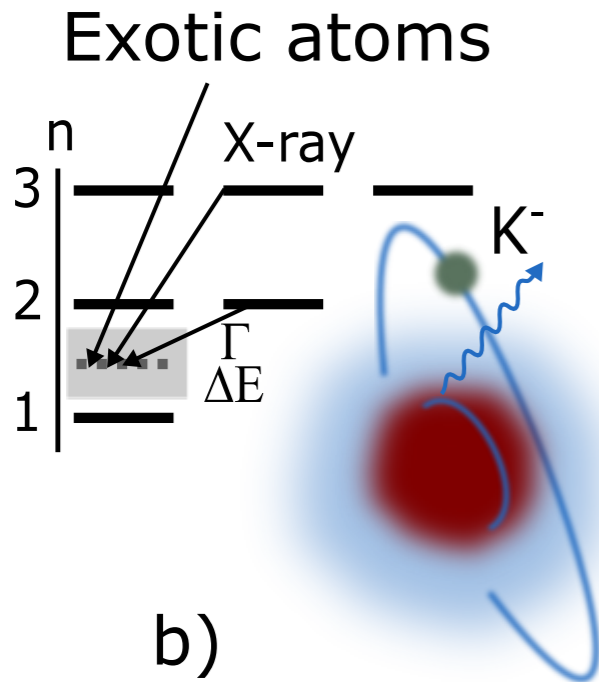
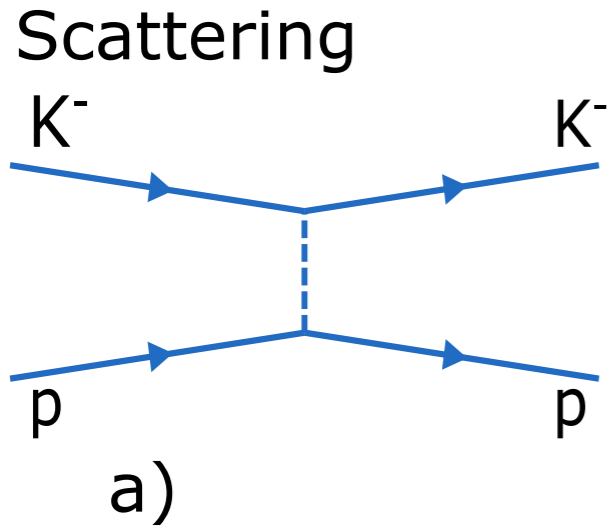
在 θ 方向的立体角元 $d\Omega$ 中单位时间的出射粒子数: $dn = j_s r^2 d\Omega = \frac{\hbar k}{\mu} |f(\theta)|^2 d\Omega$

按截面的定义有, **散射截面 (微分截面, 或角分布)**: $\sigma(\theta) = \frac{1}{j_s} \frac{dn}{d\Omega} = |f(\theta)|^2$

理论上, 散射波幅 $f(\theta)$ 可由 **Schrödinger** 方程求解

$$\left[-\frac{\hbar^2}{2\mu} \nabla^2 + V(r) \right] \psi = E\psi$$

相对论重离子碰撞中粒子末态散射





动量关联函数

- 粒子 a 动量 p_a , 粒子 b 动量 p_b
- 单粒子动量谱: dN^i/d^3p_i ($i = a, b$)
- 两粒子动量谱: $dN^{ab}/(d^2p_a d^3p_b)$

- 两粒子动量关联函数定义:

$$C^{ab}(\vec{P}, \vec{q}) = \frac{dN^{ab}/(d^3p_a d^3p_b)}{(dN^a/d^3p_a)(dN^b/d^3p_b)}$$

$$P \equiv p_a + p_b, \quad q^\mu = \frac{(p_a - p_b)^\mu}{2} - \frac{(p_a - p_b) \cdot P}{2P^2} P^\mu$$



动量关联函数 (续)

- 粒子在系统中的发射函数: $s(p, x)$
- 两粒子相互作用波函数: $\phi(\vec{q}, \vec{r})$

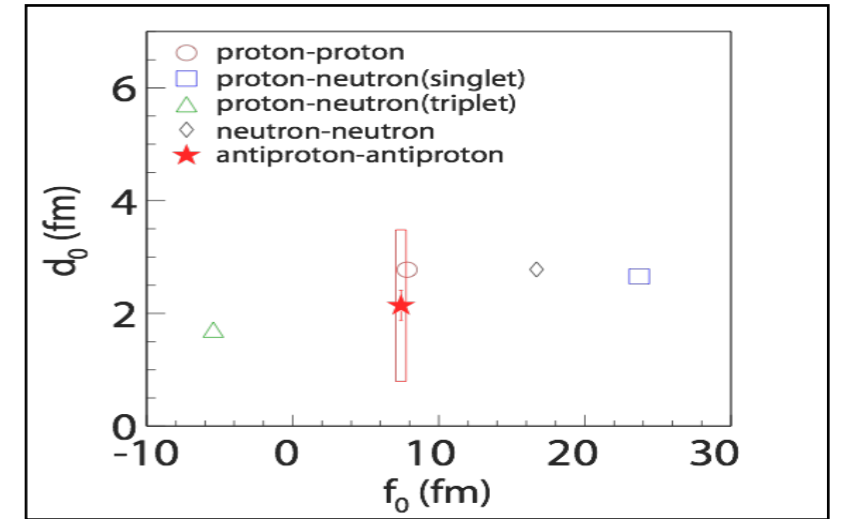
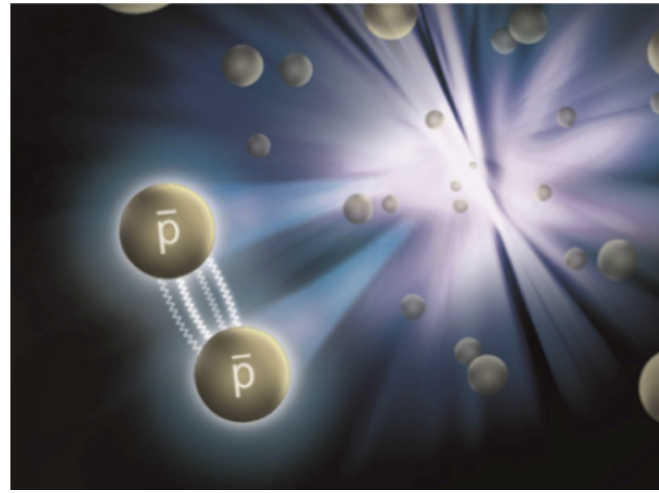
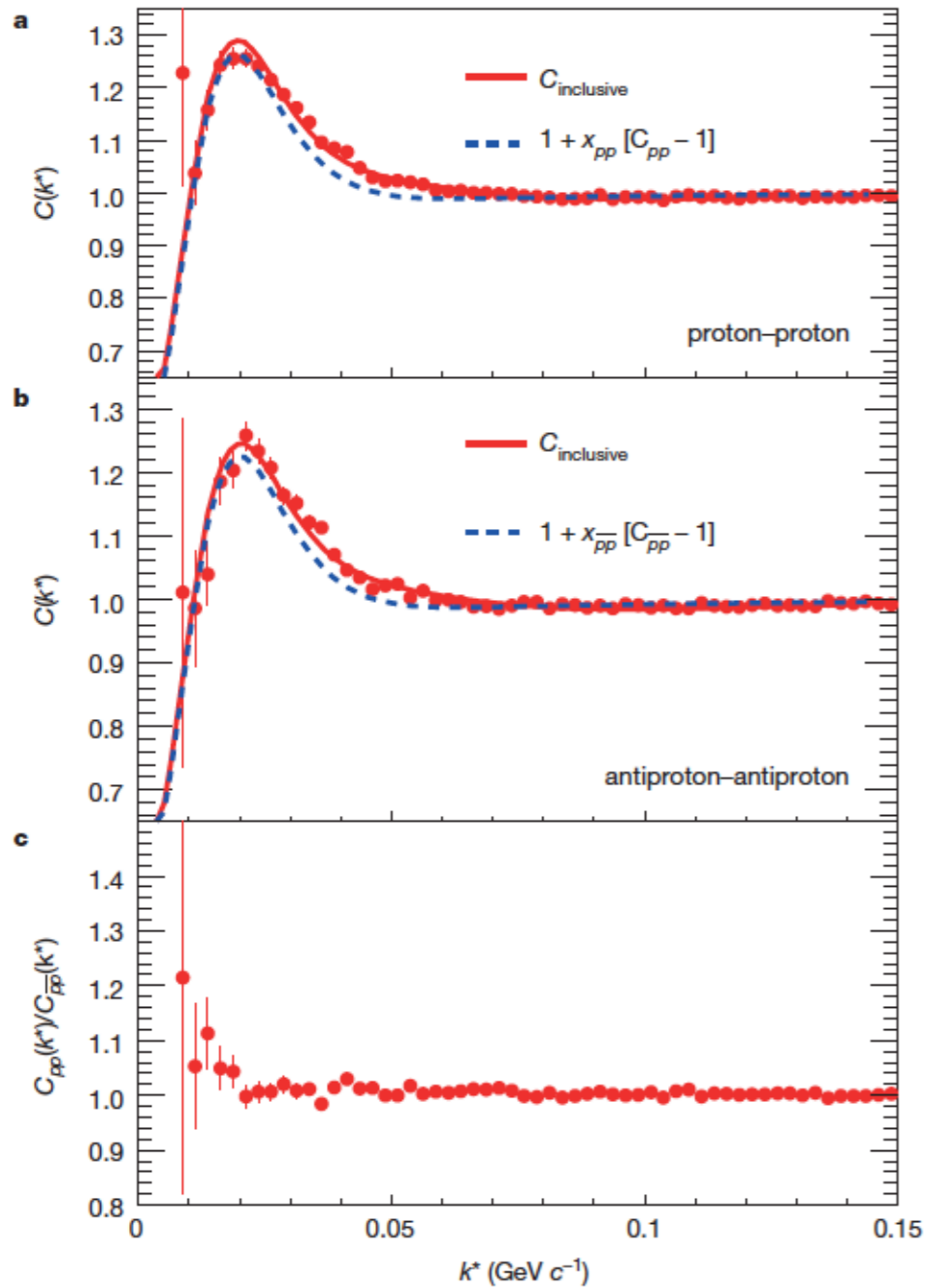
- 则关联函数可表示为:

$$C^{ab}(\vec{P}, \vec{q}) = \frac{\int d^4x_a d^4x_b s_a(p_a, x_a) s_b(p_b, x_b) |\phi(\vec{q}, \vec{r})|^2}{\int d^4x_a s_a(p_a, x_a) \int d^4x_b s_b(p_b, x_b)}$$

$$C^{ab}(\vec{P}, \vec{q}) = \int d^3r' \mathcal{S}_p(\vec{r}') [|\phi(\vec{q}, \vec{r}')| - 1]^2$$

$$\mathcal{S}(\vec{r}') \equiv \frac{\int d^4x_a d^4x_b s_a(p_a, x_a) s_b(p_b, x_b) \delta(\vec{r}' - \vec{x}'_a + \vec{x}'_b)}{\int d^4x_a d^4x_b s_a(p_a, x_a) s_b(p_b, x_b)}$$

RHIC-STAR反质子-反质子关联



LL分析模型

$$w(\mathbf{k}^*, \mathbf{r}^*) = |\psi_{-\mathbf{k}^*}^{S(+)}(\mathbf{r}^*) + (-1)^S \psi_{\mathbf{k}^*}^{S(+)}(\mathbf{r}^*)|^2 / 2$$

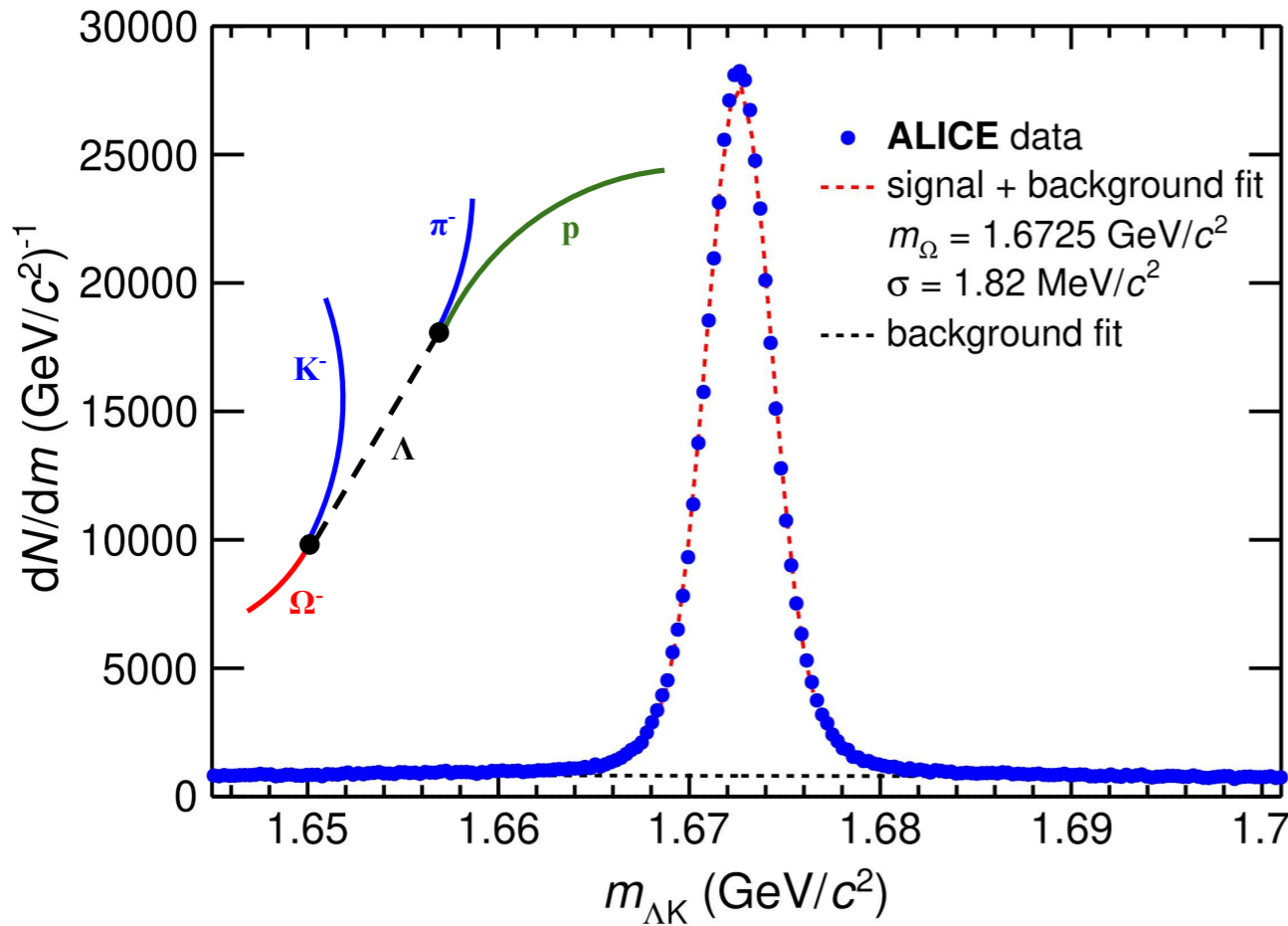
$$\psi_{-\mathbf{k}^*}^{S(+)}(\mathbf{r}^*) = e^{i\delta_c} \sqrt{A_c(\eta)} \left[e^{-i\mathbf{k}^* \cdot \mathbf{r}^*} F(-i\eta, 1, i\xi) + f_c(k^*) \frac{\tilde{G}(\rho, \eta)}{r^*} \right]$$

$$f_c(k^*) = \left[\frac{1}{f_0} + \frac{1}{2} d_0 k^{*2} - \frac{2}{a_c} h(\eta) - i k^* A_c(\eta) \right]^{-1}$$

Nature 527, 325 (2015)

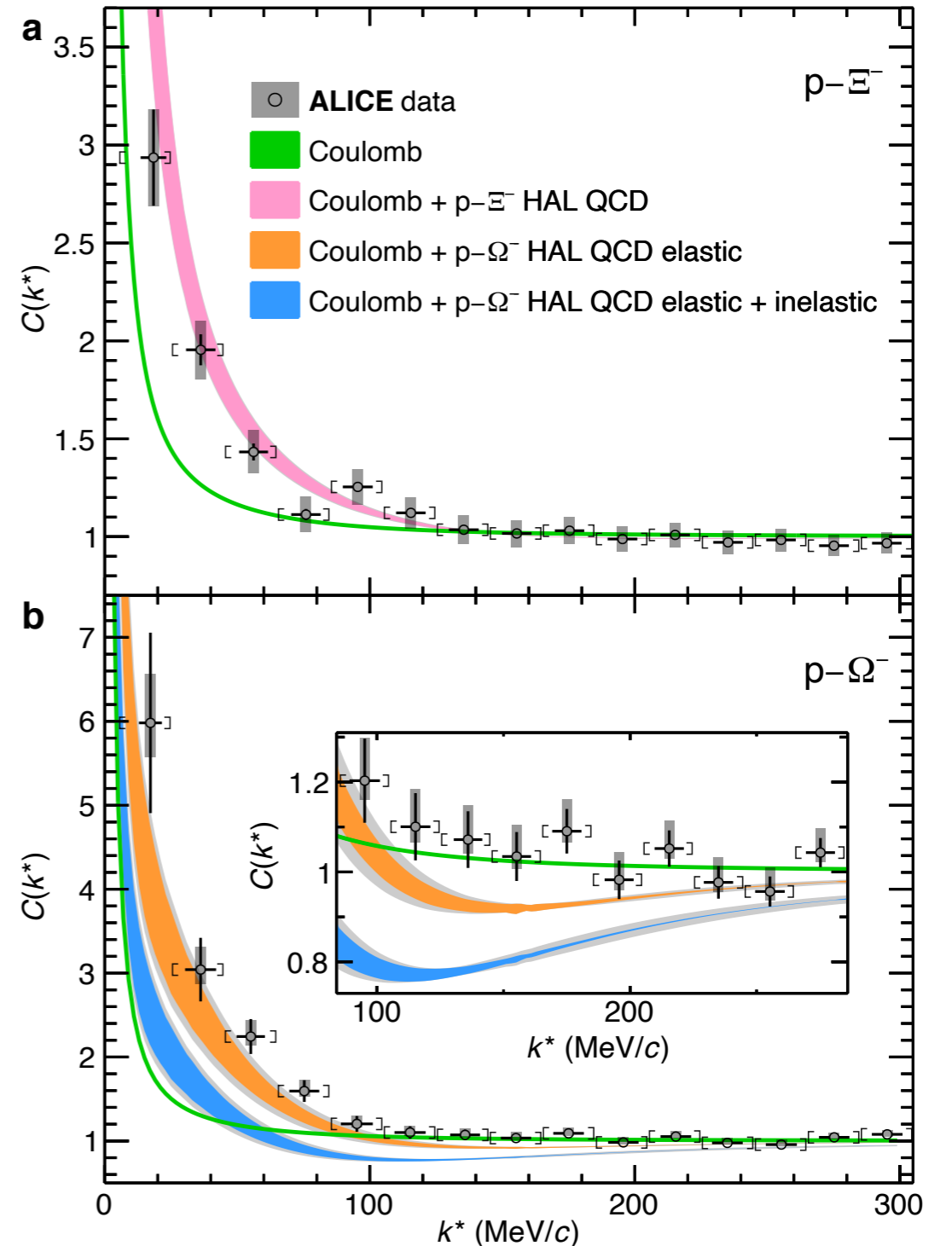


CERN-ALICE 强子相互作用测量



ALICE, Nature, 588 (2020) 232

- ✓高精度测量 $p - \Omega$ 相互作用
- ✓首次进行 $p - \Xi$ 相互作用测量





定态薛定谔方程

$$H\phi(\vec{r}) \equiv \left[-\frac{\hbar^2}{2m}\nabla^2 + V(r) \right] \phi(\vec{r}) = E\phi(\vec{r})$$

$V(r)$: 两体中心势能, 与两体距离有关的函数

通过一定的物理边界条件求解上述方程可以得到束缚态能级等信息, 波函数 $\phi(\vec{r})$ 具有概率意义, $|\phi(\vec{r})|^2$ 表征了在 \vec{r} 处发现粒子的概率密度

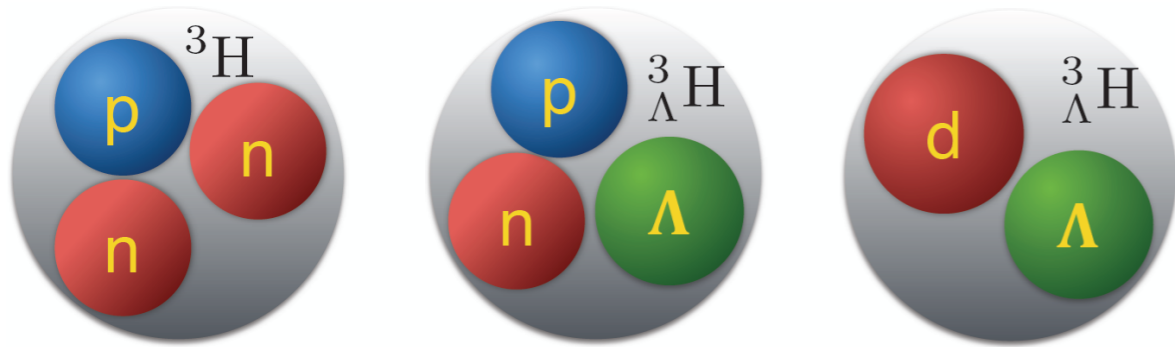
显然, 物质的构成与其组分粒子的相互作用有关, 一定的相互作用决定了形成物质的质量、所处的状态。



相对论重离子碰撞中束缚态物质的观测

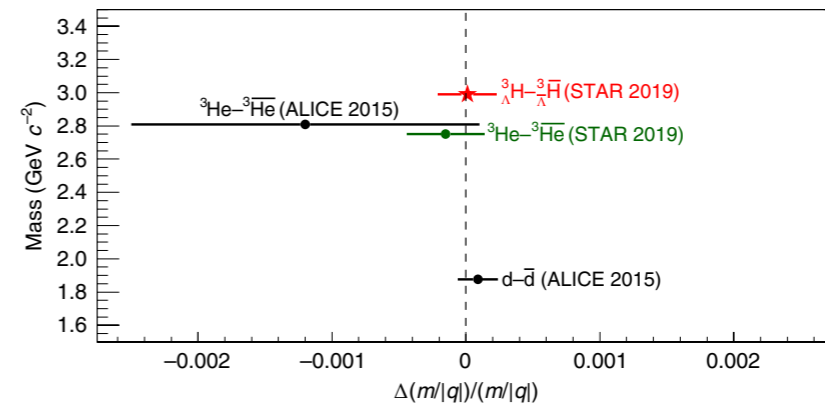
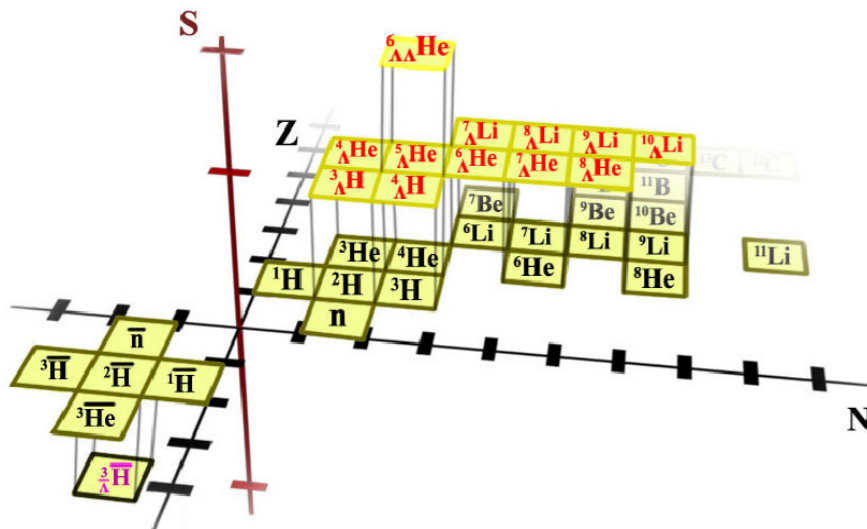
- RHIC-STAR对 (反) 超核的测量
- ALICE对轻核、超核的测量
- 双重子态、多奇异性超核的预言举例

RHIC-STAR对 (反) 超核的测量



超核：含有超子的原子核，是研究超子-核子相互作用的实验载体，其信息是研究致密中子星等物质构成的重要内容。

首个反超核：2010年，STAR, *Science* 328, 58
 在目前的实验精度：反超核和超核表现出一样的物理性质



STAR, *Nature Phys.*, 16 (2020) 409

✓在含有奇异性系统下对CPT原理的实验检验

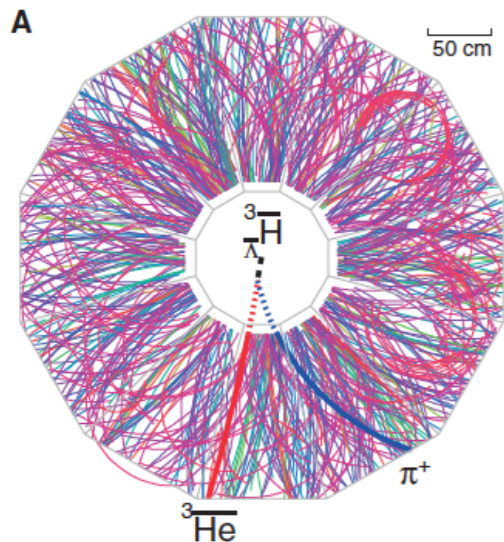
正反超氦核的质量差

$$\frac{\Delta m}{m} = \frac{m_{\Lambda}^3\text{H} - m_{\Lambda}^3\bar{\text{H}}}{m} = (0.1 \pm 2.0(\text{stat.}) \pm 1.0(\text{syst.})) \times 10^{-4}$$

超氦核的束缚能

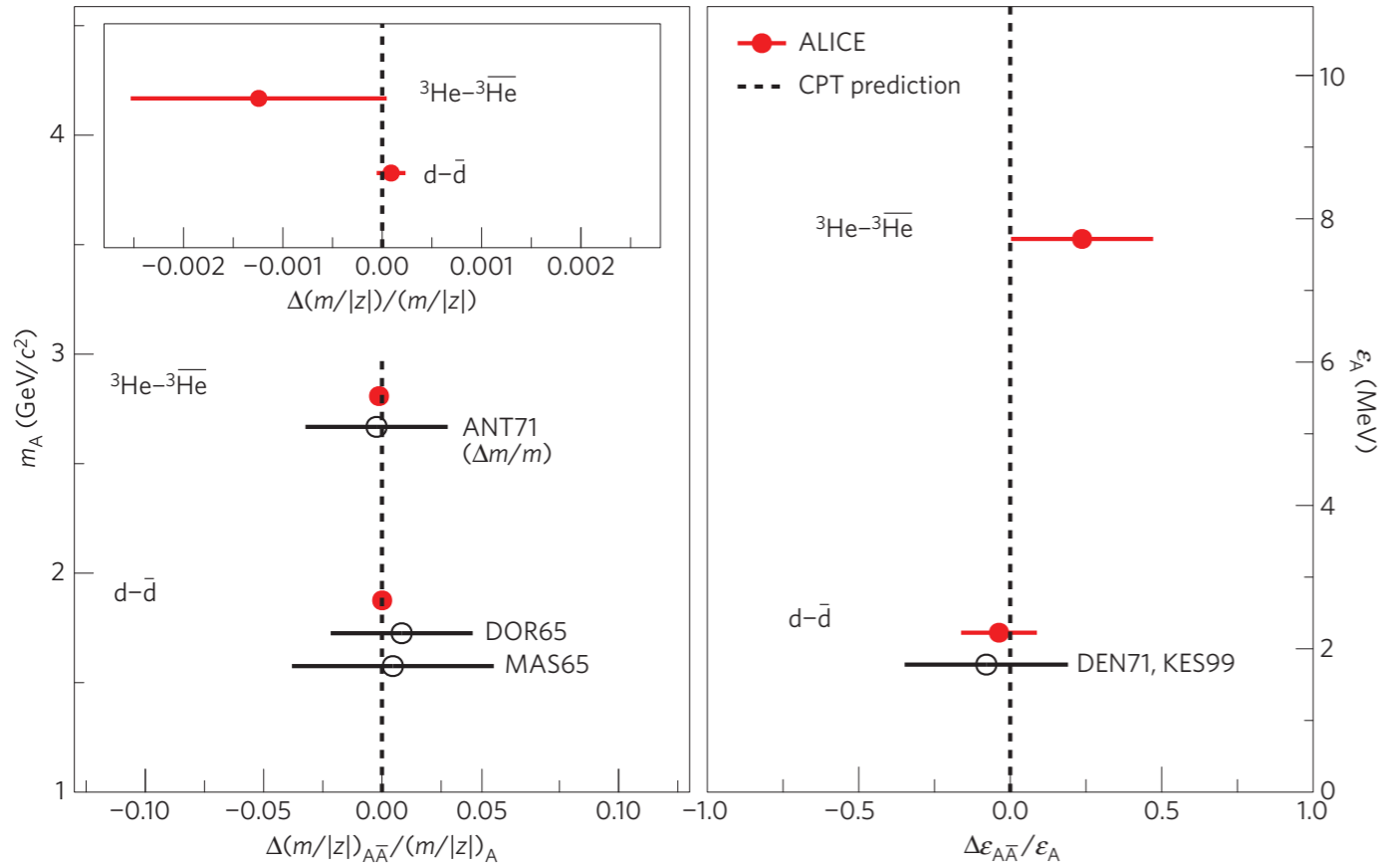
$$B_{\Lambda} = 0.41 \pm 0.12(\text{stat.}) \pm 0.11(\text{syst.}) \text{ MeV}$$

✓进一步对超子-核子相互作用提供了实验数据，约束模型参数

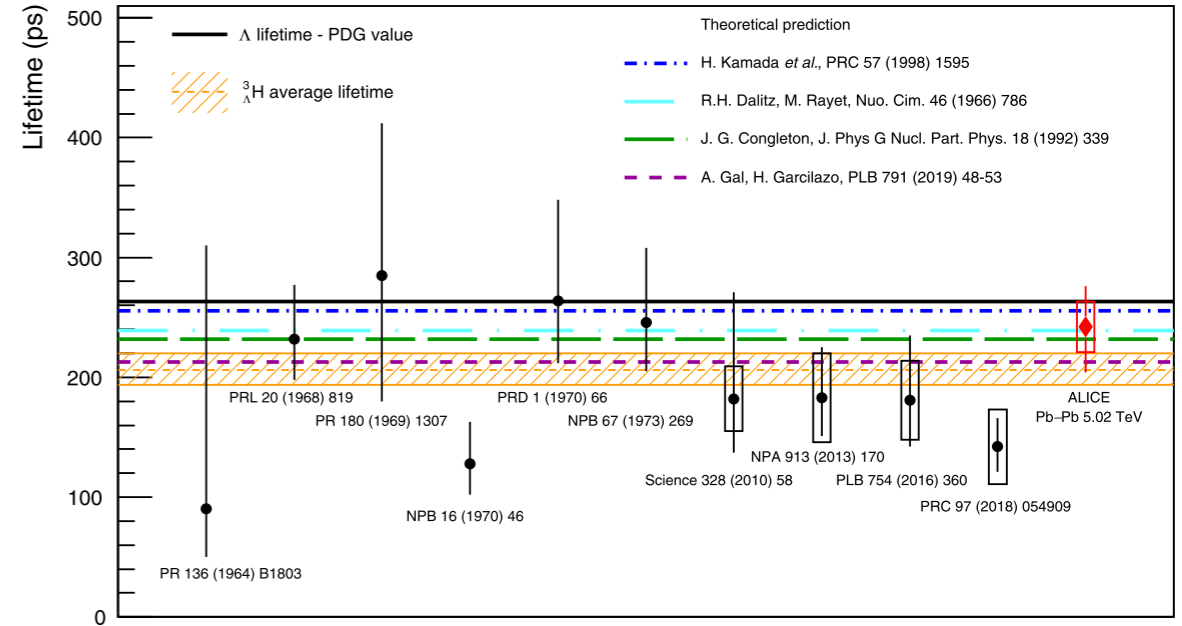




CERN-ALICE轻核、超核测量



ALICE, Nature Phys., 11 (2015) 811



ALICE, Physics Letters B 797 (2019) 134905

- ✓精确测量轻核、超核正反物质质量差
- ✓CPT联合反演
- ✓反物质和粒子相互作用平台

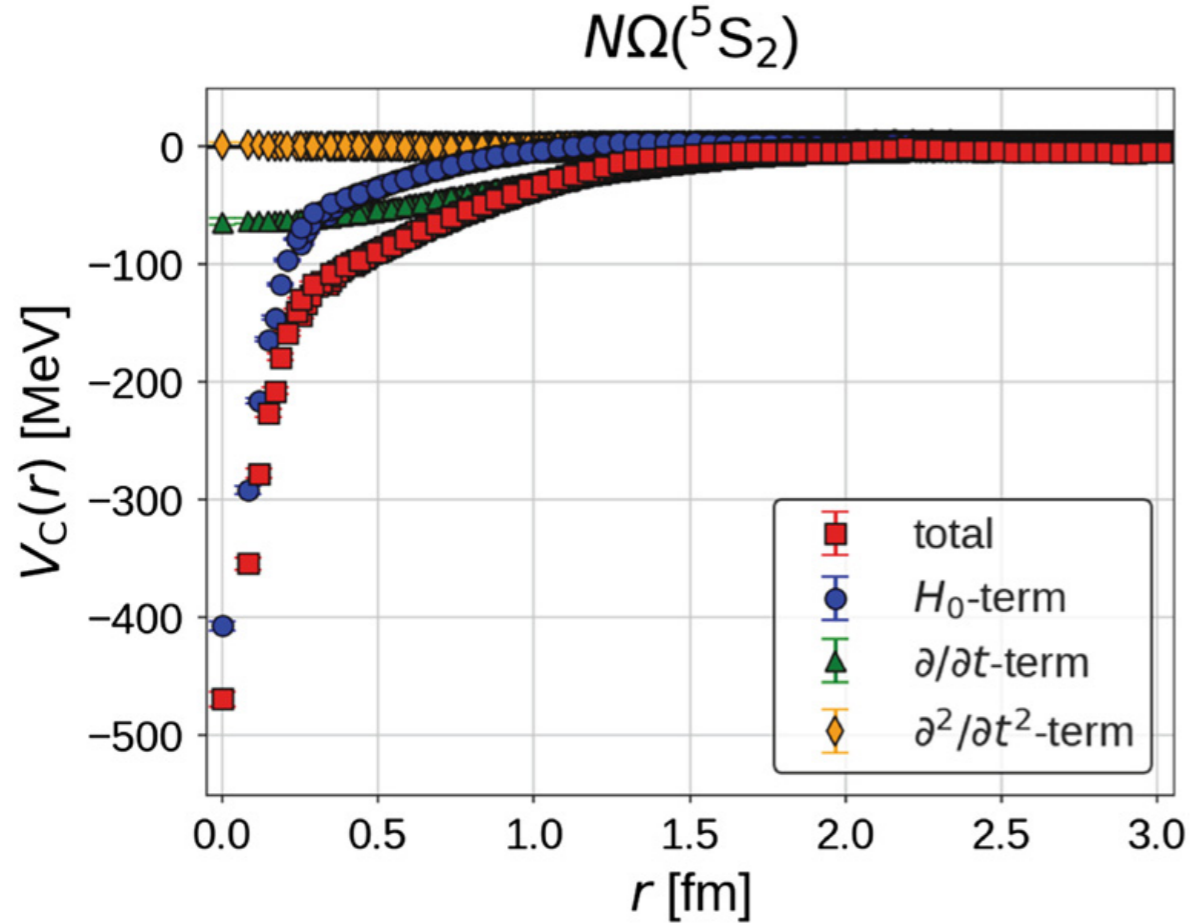
- ✓超核寿命、束缚能等参数与超子-核子相互作用密切相关
- ✓更高精度的测量，对理论模型的限制 (鉴别)



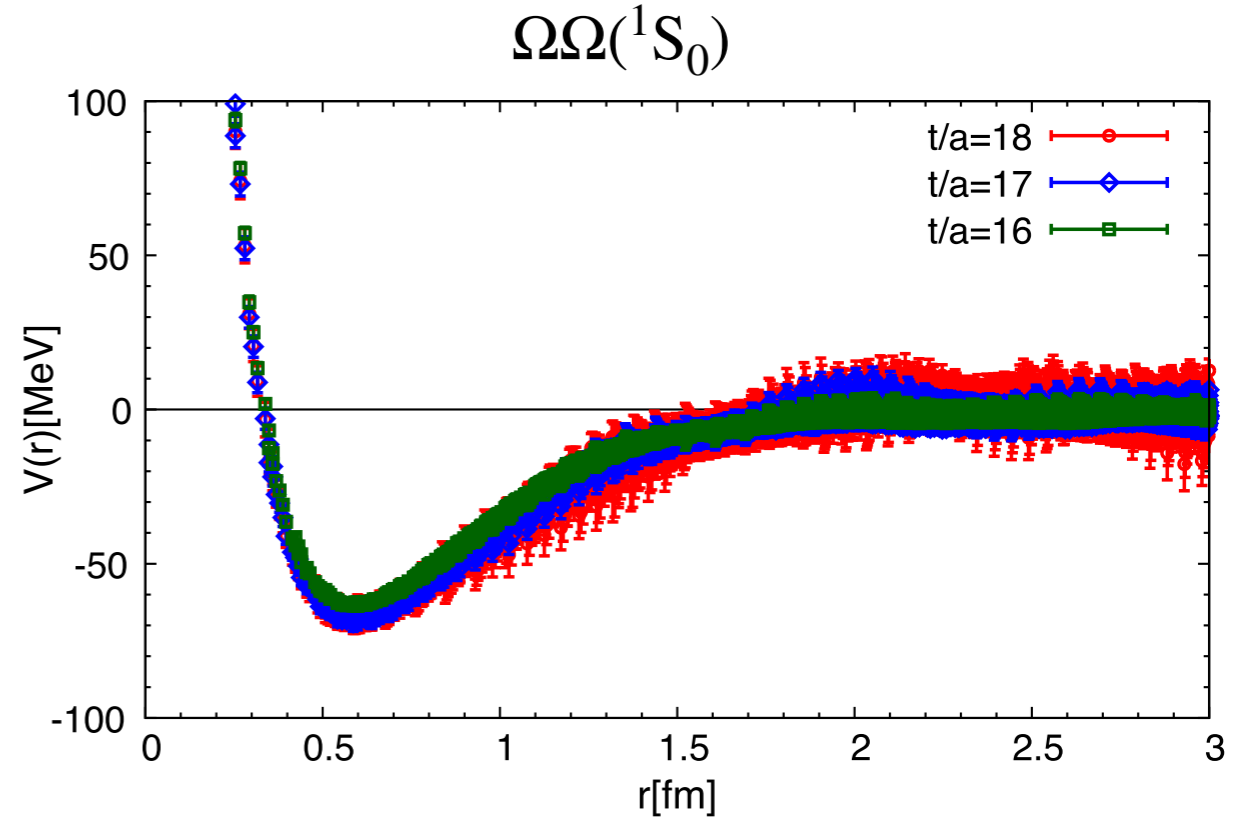
格点量子色动力学 $N - \Omega$, $\Omega - \Omega$ 相互作用

T. Iritani et al., Physics Letters B 792 (2019) 284–289

S. Gongyo et al. , PHYSICAL REVIEW LETTERS 120 (2018) 212001



$$V_{N\Omega}(r) = b_1 e^{-b_2 r^2} + b_3 \left(1 - e^{-b_4 r^2}\right) \left(\frac{e^{-m_\pi r}}{r}\right)^2$$



$$V_{\Omega\Omega}(r) = \sum_{i=1}^3 C_i e^{-(r/d_i)^2}$$



$N\Omega$, $\Omega\Omega$ 双重子态预言

组合模型

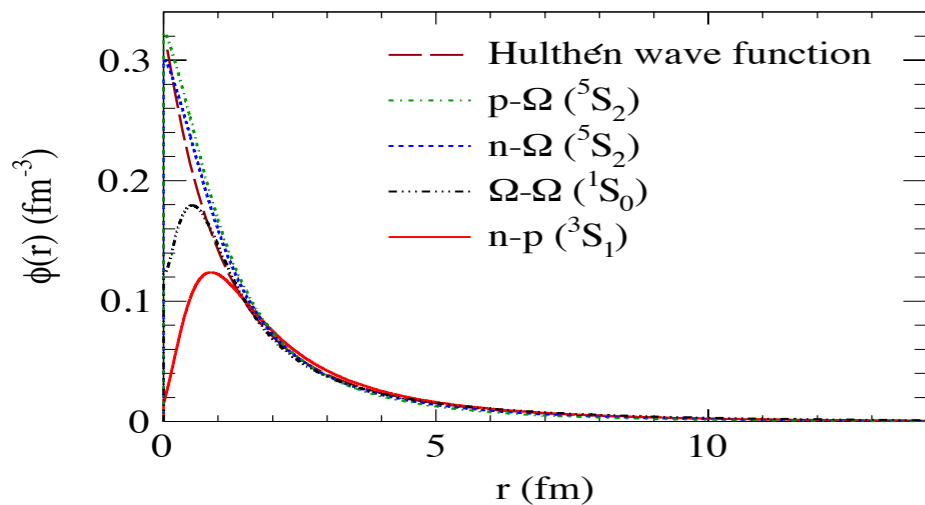
$$N_{2b} = g_2 \int \left(d^4x_1 S_1(x_1, p_1) \frac{d^3p_1}{E_1} \right) \times \left(d^4x_2 S_2(x_2, p_2) \frac{d^3p_2}{E_2} \right) \times \rho_2^W(x_1, x_2; p_1, p_2)$$

Wigner密度函数

$$\rho_2^W(\vec{r}, \vec{q}) = \int \phi\left(\vec{r} + \frac{\vec{R}}{2}\right) \phi^*\left(\vec{r} - \frac{\vec{R}}{2}\right) \times \exp(-i\vec{q} \cdot \vec{R}) d\vec{R}$$

相对波函数

$$H\phi(\vec{r}) \equiv \left[-\frac{\hbar^2}{2m} \nabla^2 + V(r) \right] \phi(\vec{r}) = E\phi(\vec{r})$$



	this work	value/Reference
E_d (MeV)	2.23	2.2307 [55]
$E_{p\Omega}$ (MeV)	2.26	2.46 [8]
$E_{n\Omega}$ (MeV)	1.38	1.54 [8]
$E_{\Omega\Omega}$ (MeV)	0.6	0.7 [16]

S. Zhang, Y.G. Ma, *Physics Letters B*, 811 (2020) 135867

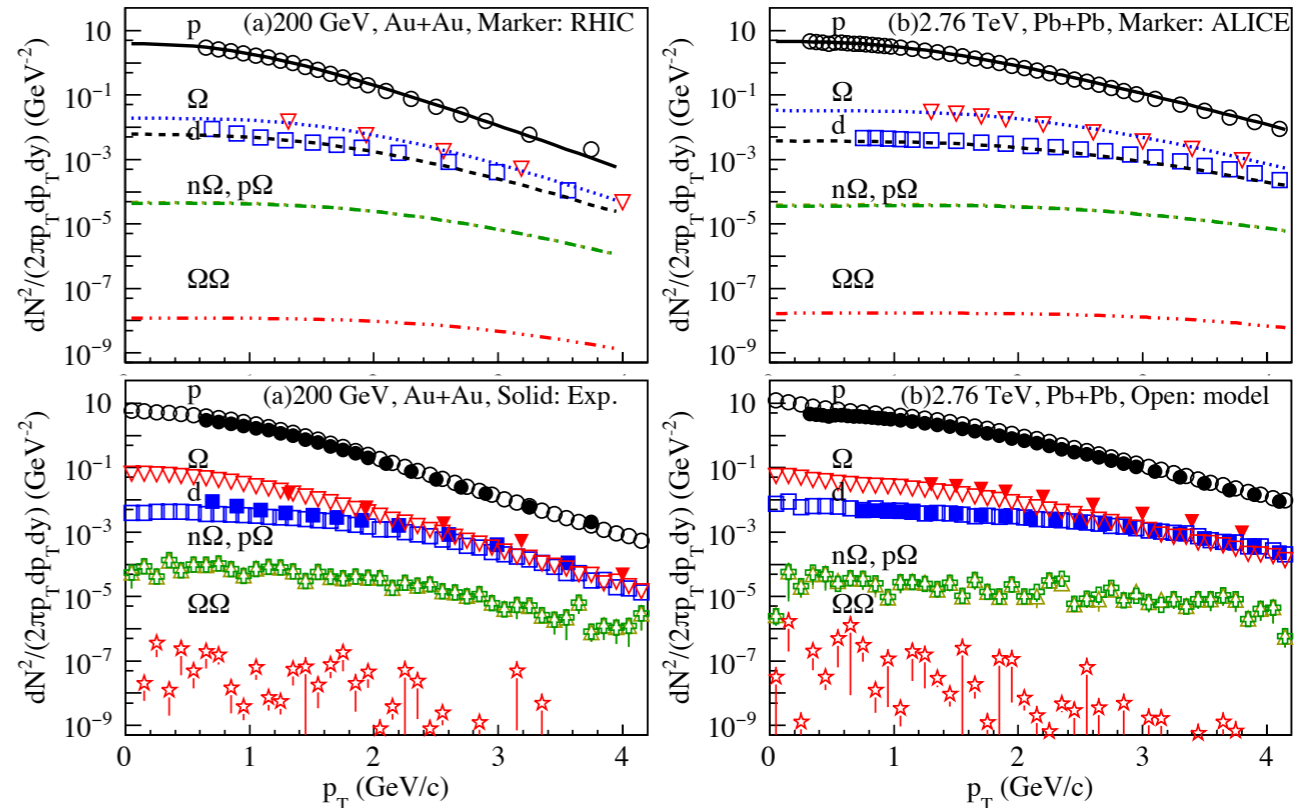


TABLE III: dN/dy of $p\Omega$, $n\Omega$, $\Omega\Omega$ at mid-rapidity.

	$p\Omega$	$n\Omega$	$\Omega\Omega$
200 GeV			
BLWC	7.51×10^{-4}	7.39×10^{-4}	0.31×10^{-6}
AMPTC	9.5×10^{-4}	9.5×10^{-4}	0.81×10^{-6}
	$\pm 7.9 \times 10^{-5}$	$\pm 7.9 \times 10^{-5}$	$\pm 1.1 \times 10^{-6}$
2.76 TeV			
BLWC	1.31×10^{-3}	1.27×10^{-3}	0.79×10^{-6}
AMPTC	1.11×10^{-3}	1.10×10^{-3}	1.1×10^{-6}
	$\pm 8.57 \times 10^{-5}$	$\pm 8.57 \times 10^{-5}$	$\pm 1.3 \times 10^{-6}$

- ✓ 在组合模型中引入LQCD超子-核子相互作用势
- ✓ 对 $N\Omega$ 和 $\Omega\Omega$ 双重子态在RHIC和LHC能区的相对论重离子碰撞中的产额和动量谱给出了预言



总结与展望

- 强子相互作用观测量：动量关联，束缚态本征参数测量
- 相对论重离子碰撞：目前超子-核子相互作用的最佳平台
- 基本对称性的检验
- 测量分析中充分考虑可靠模型提出的相互作用
- 双重子态或多奇异性超核的寻找



复旦大学博士后计划：国家博新计划，国家引进计划、上海市超级博士后，学校超级博士后，学校资助全职博士后；

ALICE&STAR实验物理：马余刚，张松，寿齐焯，陈金辉

Email: song_zhang@fudan.edu.cn